Improving the Performance of Lithium-Oxygen Batteries by Controlling the Contained Water

March 2017

WU SHICHAO

Improving the Performance of Lithium-Oxygen Batteries by Controlling the Contained Water

Graduate School of Systems and Information Engineering

University of Tsukuba

March 2017

WU SHICHAO

ABSTRACT

Lithium–oxygen batteries have attracted extensive interests due to their high theoretical energy densities (3500 Wh kg^{-1}). Although much effort has been devoted in promoting their performance for decades, there are still many challenges towards practical application such as the high charge potential, low round-trip efficiency and cycling instability over long time. In the state-of-the-art lithium–oxygen batteries, the charge potentials are as high as 3.5 V that are higher by 0.70 V than the discharge potentials. In order to further reduce the charge potential, we firstly report a reaction mechanism at an oxygen cathode, ruthenium and manganese dioxide nanoparticles supported on carbon black Super P by applying a trace amount of water in DMSO-based electrolytes to catalyze the cathode reactions of lithium–oxygen batteries during discharge and charge. The discharge products are converted to LiOH instead of Li_2O_2. In this case, the charge overpotential is significantly reduced to 0.21 V, and this results in a small discharge/charge potential gap of 0.32 V and superior cycling stability of 200 cycles. The overall reaction scheme will alleviate side reactions involving carbon and electrolytes, and shed light on the construction of practical, rechargeable lithium–oxygen cells.

Because the very high volatility of DMSO solvent makes it impractical in the future open Li-air battery system, we further employ the tetraglyme (G4) solvent-based electrolyte with much lower volatility in Li-O_2 battery and investigate the influence of water concentration in electrolyte on the discharge-charge ability. The discharge products change from the mixture of Li_2O_2 and LiOH with toroid-like morphology in original electrolyte to LiOH with large sheet morphology in electrolyte with additional 4600 ppm of H_2O. The charge potential gradually decreases as the H_2O concentration increases. Especially, with 4600 ppm of H_2O in electrolyte, the low charge potentials of around 3.2 V, corresponding to overpotentials of 0.24 V, is achieved and this results in improved rate capability and cycling performance.

Actually, in practical application of Li-air battery, H_2O exists as moisture in

ambient air not directly in electrolyte and its quantity is unlimited. Therefore, moisture in air is an another major obstacle for realizing practical lithium-air batteries. Based on the proposed mechanism, we integrate a hydrophobic ionic liquid (IL)-based electrolyte and a cathode composed of electrolytic manganese dioxide and ruthenium oxide supported on Super P (carbon black) to construct a promising system for Li-O_2 battery that can be sustained in humid atmosphere (RH: 51%). A high discharge potential of 2.94 V and low charge potential of 3.34 V for 218 cycles are achieved. The outstanding performance is attributed to the synergistic effect of the unique hydrophobic IL-based electrolyte and the composite cathode. This is the first time that such excellent performance is achieved in humid O_2 atmosphere and these results are believed to facilitate the realization of practical lithium-air batteries.

With moisture in air for operating Li-air battery, severe safety problems from the dramatic exothermal reactions with lithium metal anode will be resulted and it also can deteriorate the battery with poor charge ability as well as short cycle life. Then, we design a super-hydrophobic solid-state electrolyte (SHSSE) incorporated nano-fumed SiO_2 with hydrophobic ionic liquid-based electrolyte and construct a safe and long-life Li-O_2 battery with Li metal anode in humid atmosphere. The battery can run for 150 discharge-charge cycles with low charge potential through the water "catalysis". The unique super-hydrophobic performance (contact angles > 150 ^{o}) and the strong ability blocking the H_2O permeation are realized. Thus, the corrosion of Li metal anode by H_2O crossover is efficiently suppressed. The SHSSE also shows high electrochemical stability, ionic conductivity and strong thermal tolerance. These superiorities endow the Li-O_2 battery with good cycling stability and reliable safety even in humid atmosphere. Our results indicate an appealing strategy to break the bottleneck of the related Li metal anode issues caused by H_2O crossover, enable the merit of H_2O assisting for battery performance improvement, and facilitate the operation of practical Li-air battery.

TABLE OF CONTENTS

LIST OF FIGURES

LIST OF TABLES

LIST OF SCHEMES

Chapter 1. General Introduction

1.1 Urgent demand for energy storage medium with high power

Conventional energy resources such as oil, coal and natural gas have been widely used for thousands of years to provide energy for industry, electric generation, automobile and cooking, etc. As the world population increases rapidly in the previous years, the requirement for energy is exploding and the conventional energy resources are being depleted. Accordingly, recent years, the development of renewable energy resources has attracted extensive attention all over the world.[1] The most popular resources include wind, solar and ocean energy, etc. This is because these resources from nature are inexhaustible and environmental friendly. However, they are not constant but remittent depending on the natural environment like weather and temperature. It is nearly impossible to provide stable energy for energy clients from them. One of the alternative solution is to storage these energy by energy storage mediums and to release the stored energy whenever necessary. Among these energy storage mediums, batteries are considered as an attractive selection due to their high reversibility during discharge and charge processes and favorable portability.[2] These unique properties make them become the prime electric sources in mobile phones, notebook computers, electric vehicles and so on.

The most popular batteries include lead-acid (Pb-acid) battery invented in the year of about 1859, dry (Zn-Mn) battery from 1887, nickel-cadmium (Ni-Cd) battery from 1899, nickel-metal hydride (Ni-MH) battery from 1976 and lithium ion (Li-ion) battery from 1991. Their ability for storing electric (energy density) increases from about 40 Wh kg^{-1} for Pb-acid battery to as high as about 200 Wh kg^{-1} for Li-ion battery, as shown in Fig. 1.1.[3] Due to the much higher energy density, long cycle life, no memory effect, fast charged and low self-discharge, Li-ion battery has captured the major market in the field of mobile phones, digital camera, notebook computers and electric vehicles.

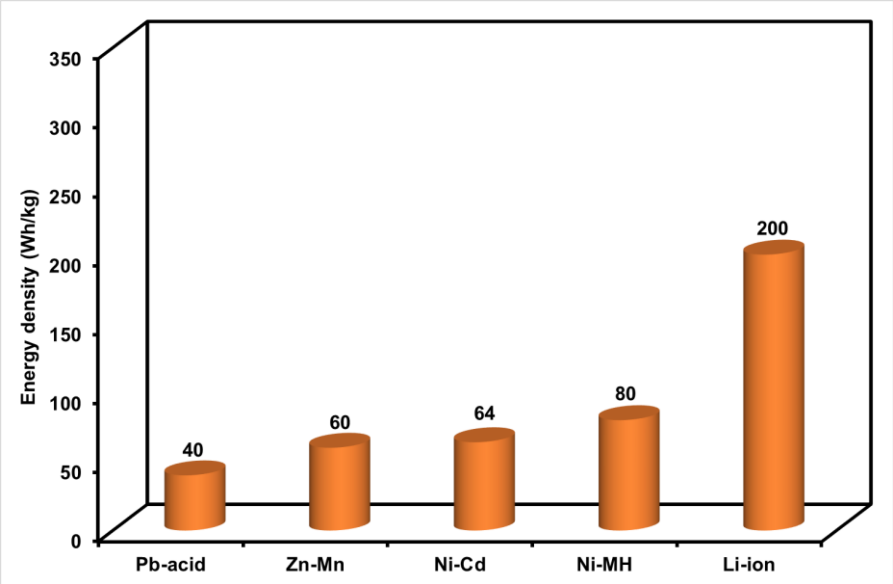

Fig. 1.1 Energy densities of the selected popular batteries.[3]

1.1.1 Li-ion battery has almost reached the limitation of energy density

Although Li-ion battery has been widely used, it has to face severe challenges at present. It already cannot meet the requirement for high capacity and energy density battery for long-term use of smart mobile devices. For example, the smart mobile phones can sustain only about one-day use, for note computers, only 4 to 8 hours, for electric vehicles, only 200 to 500 kilometer. Therefore, developing Li-ion battery with higher energy density is extremely urgent. Fig. 1.2 presents the technical solutions to improve the energy density of Li-ion battery in the short-term development.[4]

TIME →		2011	2012 - 2016	2015 - 2020
Batteries	Type	Li-ion battery (4.2 V)	Li-ion battery (4.4 V)	Li-ion battery (Si anode)
	Energy density	150 Wh kg^{-1}	160-250 Wh kg^{-1}	300 Wh kg^{-1}

Fig. 1.2 The development of Li-ion battery towards high energy density in the short-term.[4]

The cathode and the anode are the two key components for Li-ion batteries. The property of each material has a great influence on the improvement of energy density. However, the cathode materials employed face several problems, restricting the promotion of capacity. $LiCoO_2$, as the cathode material which is firstly commercially employed and still occupies a portion of market at present, has low specific capacity of 145 mAh g^{-1}, which is a crucial problem for developing Li-ion battery with high capacity. Li(Ni, Mn, Co)O_2 that is steadily expanding its market has low calendar density which result in that it is unwise choice for cathode of Li-ion battery with high capacity. Even the high voltage $LiCoO_2$ and Li(Ni, Mn, Co)O_2, that can sustain being charged to 4.4V, only reaches a specific capacity of 167-180 mAh g^{-1} and about 160-250 Wh kg^{-1} can be expected.

Improving the anode is another alternative choice for development of Li-ion battery. Si materials are considered as the next generation anode material because they can exhibit high theoretical specific capacity of 4200mAh g^{-1}, three or more times than current graphite material. However, large volume change during lithiation/delithiation process makes the electrochemical active particles crack and lose the electrical contact, which result in fast decline of reversible capacity. It has been suggested that carbon-compositing may be an effective way to improve the cycling performance. But the compositing anode materials commercially used at present with Si no more than 10% is limited for enhancing the capacity of Li-ion battery. In this case, the energy density can be improved to about 300 Wh kg^{-1}.

Until now, no promising cathode and anode materials have been explored to design Li-ion battery with enough high capacity to meet the strict requirement for expected endurance time of mobile devices and EVs. Developing innovative battery technology admits of no delay. Fig. 1.3 shows the widely accepted roadmap of battery technology for next generation.[4] In the mid-term development, lithium sulfur battery, lithium polymer battery, lithium solid battery and 5 Volt Li-ion battery can be expected. In the long-term development, lithium air battery shows the potential as an ultimate energy

Fig. 1.3 The development of new battery chemical system beyond Li-ion battery towards high energy density in the middle-term and long-term.[4]

storage battery. Its theoretical energy density can be 3500 Wh kg^{-1}.

1.2 Lithium air battery

1.2.1 Brief introduction of lithium air battery

Lithium air (Li-air) battery has four typical chemical architectures as shown in Fig. 1.4.[3] Non-aqueous Li-air battery was introduced by Abraham and Jiang and the electrolyte is based on non-aqueous solvent and organic lithium salt.[5] Aqueous Li-air battery was developed by Polyplus and the electrolyte is based on H_2O solvent and inorganic lithium salt.[6] The lithium metal anode is protected by a film preventing H_2O penetration. The hybrid Li-air battery with an aqueous electrolyte immersing the cathode and a non-aqueous electrolyte immersing the anode was designed by Polyplus, Wang and Zhou.[7] The all-solid-state battery with a solid electrolyte was reported by Kumar.[8]

Non-aqueous Li-air battery seems to be firstly developed in the term of mass production and application due to the simple structure similar to that of Li-ion battery, except for the substitutions of lithium transition metal oxide by porous catalyst cathode and graphite anode by lithium metal. In addition, non-aqueous Li-air battery

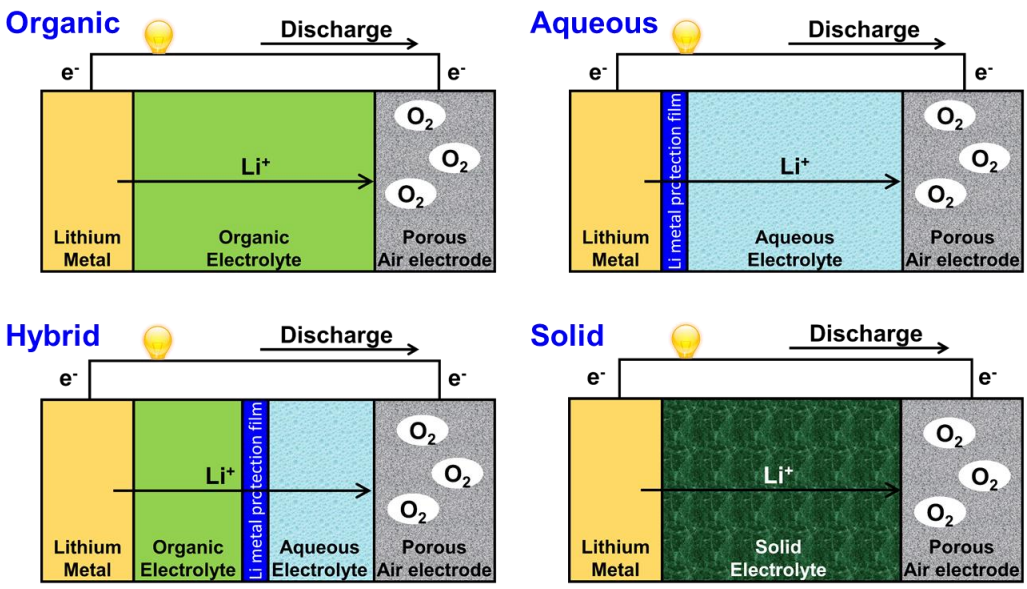

Fig. 1.4 Four typical battery architectures of reported Li-air battery.[3]

exhibits better rechargeable capability. Most researches about non-aqueous Li-air battery focus on the non-aqueous electrolyte and developing high catalytic efficiency cathode with large surface area and suitable pore structure holding enough reaction products Li_2O_2 and preventing the pore blocked.

1.2.2 Operation mechanism of non-aqueous Li-air battery

Generally, non-aqueous lithium-air battery is composed of a lithium metal anode, a separator, an electrolyte and a cathode.[9] The Li metal anode is considered as the most promising candidate to ensure the attracting superiority of Li-air battery with paramount energy density, because it has much high specific capacity (3860 mAh g^{-1}). The schematic illustration of the operation mechanism during discharge and charge is shown in Fig.1.5. When the battery is discharged, lithium ions (Li^+) extract from Li metal anode and go through separator to cathode in electrolyte. On cathode, Li^+ reacts with oxygen in air to produce Li_2O_2 as the discharge product. The theoretical potential is about 2.96 volt. During charging, Li_2O_2 is decomposed to release oxygen gas and

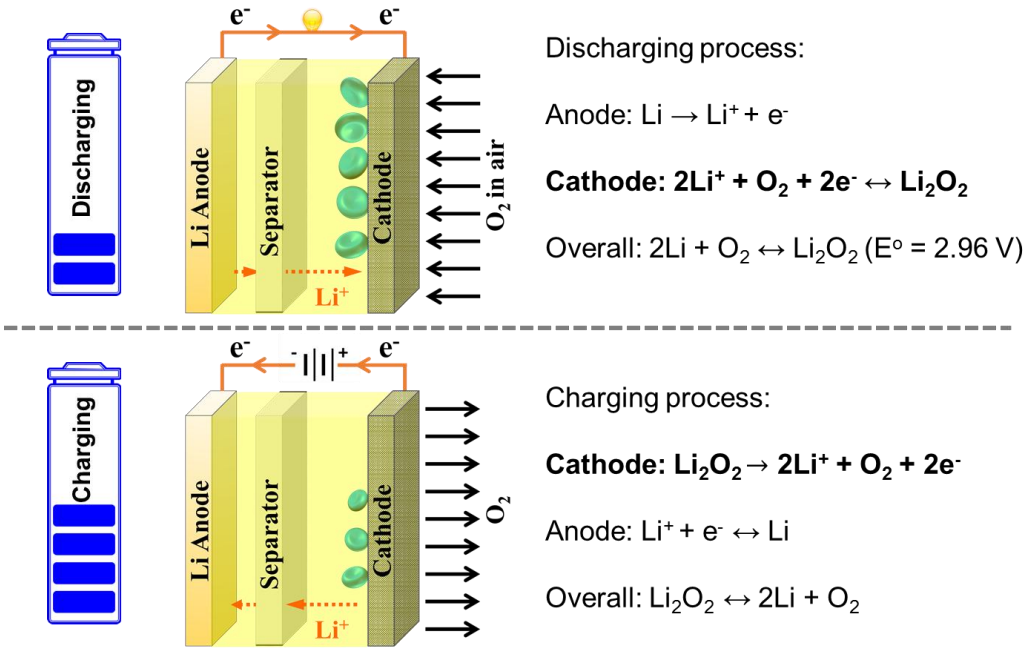

Fig. 1.5. A schematic illustration of operation mechanism of non-aqueous Li-air battery.

generate Li^+. Li^+ returns to lithium anode through electrolyte. As the conductivity of the discharge products Li_2O_2 is poor, carbon-based materials have been considered as the optimal selection for air cathode because their particularly superior conductivity can buffer the poor electron conductivity of Li_2O_2 and then improve the discharge-charge performance.[10-11] They also show other advantages such as low cost and the high specific area, light weight, which ensure the high specific capacity and energy density of Li-air batteries.

1.3 Critical problems of non-aqueous Li-air battery

The performance improvement and the practical application of non-aqueous Li-air battery is mainly retarded by the high charge potential as well as the resultant low Coulombic Efficiency and the contaminations in air especially moisture.

1.3.1 High charge potential related problems and proposed strategies

Li_2O_2 is generally considered as the ideal discharge products in non-aqueous Li-air battery.[12-14] Actually, during discharging process, the formation of Li_2O_2 is resulted through several steps.[15-18] At the beginning of discharge, O_2 in air is firstly reduced to generate superoxide (O_2^-). Some O_2^- absorbed on the surface of cathode is further electrochemically reduced to Li_2O_2. Other O_2^- diffuses in the electrolyte away from cathode and disproportionate to Li_2O_2 and O_2 ($2LiO_2 \rightarrow Li_2O_2 + O_2$). Either Li_2O_2 is produced through a two-step electrochemical reduction or through one-step electrochemical reduction and one-step chemical disproportionation, the formation of O_2^- is an inevitable step. Since the intermediate O_2^- is a supernucleophile, O_2^- readily attacks the organic electrolyte and carbon-based cathode, resulting in the formation of byproducts (Fig. 1.7, lithium carbonate and lithium carboxylates etc.).[19-20] Consequently, the accumulation of byproducts during discharging blocks O_2 evolution from Li_2O_2-electrolyte interface, thereby raising a severe polarization during charge.[21] On the other hand, because of the insulation nature of Li_2O_2, electrochemically oxidizing the Li_2O_2 particles at the surface of cathode inevitably leads to high polarization. Both of the byproducts from O_2^- attack and the insulate Li_2O_2 will result in the high charge overpotential. Additionally, the high charge potential, generally above 4.20 V (Fig. 1.6), can induce the decomposition of organic electrolyte and carbon cathode, producing large amounts of byproduct (Fig. 1.7) and

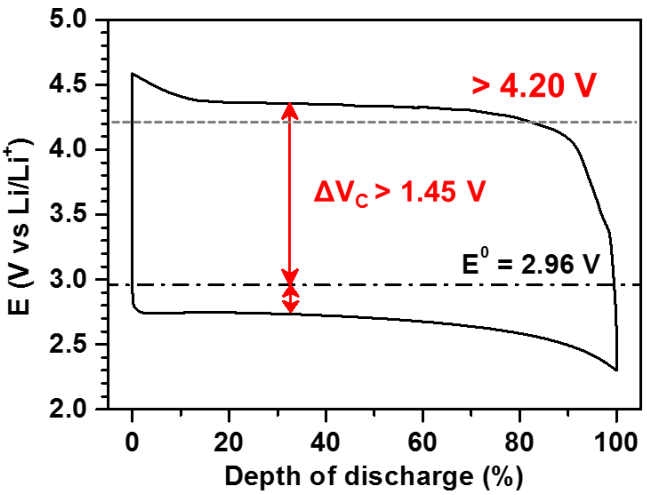

Fig. 1.6 A typical discharge-charge profile of non-aqueous Li-O_2 battery with carbon cathode.

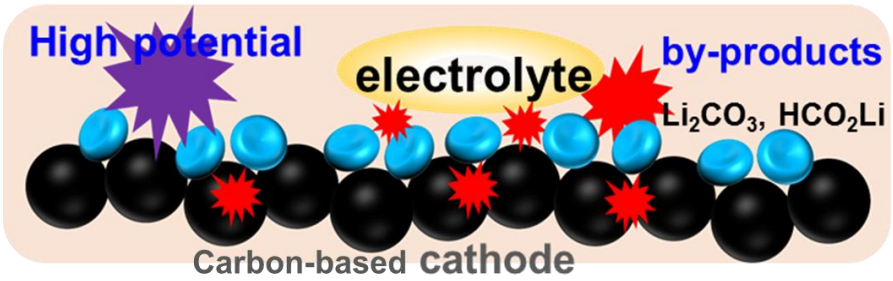

Fig. 1.7 The side reactions resulted from the high charge potential and overstrong oxidation ability of intermediate O_2^- and Li_2O_2.

further exacerbating the charge ability. Finally, the pores on cathode are gradually clogged by these irreversible byproducts during cycles and the Li-air battery fails. Therefore, in order to extend the cycle life, lowing the charge potential is extremely necessary.

One of the strategies to reduce the charge potential is designing high-efficient cathode by integrating catalysts towards oxygen reduction reaction (ORR) during discharge and oxygen evolution reaction (OER) during charge. Noble metals and oxides (Pt, Au, Ru and RuO_2 etc.), transition metals and oxides (Co_3O_4, MnO_2, TiC, TiN, and $NiCo_2O_4$ etc.) are extensively attempted. Table 1.1 lists part of reported results about using catalysts to improve the performance of non-aqueous Li-air battery. In this way, the charge potential can be reduced to ~3.5 V, but it is hard to break through this limit. The introduction of these metal compounds with heavy molecular weight is inevitably subjected to the significantly decreased energy density.

Table 1.1. Reported results about performance improvement of non-aqueous Li-air battery with catalysts in cathode.

Cathode materials	Voltage (V)	Specific Capacity (mAh/g)	Cycle life		Ref.
			Capacity	Cycle No.	
40 wt% Au/C	~4	1500	/	/	[22]
40 wt% Pt/C	~3.8	750	/	/	[22]

PtAu/C	~3.6	1300	/	/	[23]
Pt/MnO_2	~3.5	150-250	250	20	[24]
Nanoporous Au	~3.5	~330	320	100	[25]
$RuO_2 \cdot 0.64H_2O$/rGO	~3.6	>5000	5000	30	[26]
Ru/ITO	~3.6	2.5 mAh cm^{-2}	1.8 mAh cm^{-2}	50	[27]
RuO_2/CNT	~3.5	1800	1000	20	[28]
RuO_2/CNF	~3.6	20600	1000	300	[29]
$Pd/Al_2O_3/C$	~3.3	>1000	500	10	[30]
α-MnO_2	>4.0	2300	~2000	10	[31]
MoN/NGS	~4.0	1490	1100	9	[32]
Pd/MnO_2	~3.6	550	300	15	[33]
$CoMn_2O_4$/GNS	~4.0	3000	/	7	[34]
Fe/N/C	~3.6	/	450	50	[35]
TiN/C	~3.8	6000	/	/	[36]
Co_3O_4/Carbon Sphere	~4.0	7000	1000	20	[37]
Co_3O_4/HGPC	~3.55	1600	500	50	[38]
Mo_2C/CNT	3.25-3.4	/	500	100	[39]
$La_{0.75}Sr_{0.25}MnO_3$/KB	~3.9	~10000	1000	130	[40]
$La_{0.5}Ce_{0.5}Fe_{0.5}Ni_{0.5}O_3$/GNS	~3.8	~1700	1100	100	[41]
Pyrochlore	~3.8	7000-11000	8000	4	[42]

Another promising strategy to reduce the charge potential is employing soluble redox mediator (RM) in the electrolyte.[43] In the presence of redox mediator in electrolyte, during charge, the redox mediator is easily oxidized to produce RM^+. The RM^+ can further oxidize the Li_2O_2 through a chemical reaction to generate Li^+ and O_2. At the same time, RM^+ is reduced to RM again. Thus form a circle until all the Li_2O_2 is decomposed. In Table 1.2, the reported RMs are summarized. In this way, the

charge potential depends on the RM and the value can be reduced to about 3.5 V. However, practical mediators are very limited.

Although the charge potential can be largely reduced by using catalyst in cathode or redox mediator in electrolyte to about 3.5 V, it is still lacking to further achieve an available low charge potential for practical application of non-aqueous Li-air battery with high Coulombic efficiency, high reversibility and stable cycling performance. Exploring new reaction mechanisms to significantly improve the performance is essential and urgently necessary.

Table 1.2. Reported results about charge potential reduction of non-aqueous Li-air battery with RM in electrolyte.

Redox mediator	Voltage (V)	Specific Capacity (mAh/g)	Cycle life		Ref.
			Capacity	Cycle No.	
Tetrathiafulvalene (TTF)	~3.5	/	300	100	[44-46]
2,2,6,6-Tetramethylpiperidinyloxyl (TEMPO)	~3.6	7500	500	50	[47-48]
Lithium nitrate ($LiNO_3$)	~3.6	6000	1000	50	[49-50]
Iron phthalocyanine (FePc)	~3.6	3600	1000	135	[51]
1-methyl-2-azaadamantane-N-oxyl (1-Me-AZADO)	~3.7	5000	/	/	[52]
Lithium iodine (LiI)	~3.5	/	1000	900	[53]
Lithium bromine (LiBr)	~3.5	/	0.52 mAh cm^{-2}	30	[54-55]

Cesium iodide (CsI)	~3.6	/	1500	125	[56]
Cobalt bis(terpyridine) ($Co(Terp)_2$)	~3.45	6000	1000	/	[57]
Tris[4-(diethylamino)-phenyl]amine (TDPA)	~3.4	/	500	100	[58]

1.3.2 Moisture in air/H_2O in electrolyte related problems

The ultimate goal of developing Li-air battery is to realize the application of Li-air battery operated in ambient air. However, most of the present research on Li-air battery is conducted in pure O_2 atmosphere. This is because in ambient air, the thermodynamic instability of ideal discharge products Li_2O_2 can initiate undesired reactions with the air component, especially with the inherent moisture and these byproducts generally further result in poor rechargeability. Only limited publications have attempted to develop a Li-O_2 battery that works in humid atmosphere, which is an inevitable step for the realization of practical Li-air battery.

The reaction between Li_2O_2 and H_2O was reported to produce LiOH and H_2O_2 ($Li_2O_2 + 2H_2O \rightarrow 2LiOH + H_2O_2$).[59] The produced LiOH was supposed to coat the porous cathode surface and form a film which can block further catalytic activity. Surprisingly, Aetukuri N. B. demonstrated that the discharge products on cathode were detected to only Li_2O_2 even when 4000 ppm of H_2O was intentionally added in electrolyte and no LiOH was detected.[60] They also found that in the presence of H_2O in electrolyte, the discharge capacity was obviously increased and the size of Li_2O_2 particles increased. They attempted to explain these phenomena and though that the enhanced solubility of the intermediate LiO_2 in electrolyte with high Gutman donor number (DN) or acceptor number (AN) activated a mechanism where O_2^- acted as a redox mediator for the electrochemical growth of Li_2O_2 that was not limited by the charge transport of Li_2O_2. The reason that no LiOH was detected was still unclear in

the article. Although the discharge capacity can be significantly improved in the H_2O-containing electrolyte, this will introduce some undesired results. H_2O may result in the severe corrosion of Li metal anode and the battery safety may become poor.[61] During charge, the potential for decomposing Li_2O_2 particles with larger size was predicted to be much higher than those batteries in the absence of H_2O in electrolyte. Also, Schwenke K. U. et al. presented the enhancement of discharge capacity and the growth of larger Li_2O_2 particles due to the H_2O addition.[62] The important function of proton that can solubilize Li_2O_2 much more efficient than H_2O and should be more eligible than H_2O to prevent surface passivation was indicated. However, the charge potential in this H_2O-containing electrolyte is still much higher.

In the humid atmosphere, Meini S. et al. showed a more than 5-fold increase of the discharge capacity in a water-vapor Li-O_2 battery.[63] Similarly, Guo et al. found that the discharge capacity of a Li-O_2 battery in a relative humidity (RH) of 15% was enhanced by nearly two times compared to that in dry O_2 atmosphere.[64] Once more, the high charge potential as well as the poor cycling stability were demonstrated.

1.4 Target and outline of this dissertation

1.4.1 Motivation of this research

High charge potential induced low Coulombic efficiency, side reactions of electrolyte decomposition, corrosion of carbon-based cathode and the short cycle life have been a great challenge for realization of practical Li-O_2 battery. And, moisture in air is another major obstacle. It is complete in both respects if we can explore a way to use H_2O as redox mediator to reduce the charge potential. Considering the difficulty of oxidizing Li_2O_2 products at low charge potential, we suppose to convert Li_2O_2 to LiOH products through the reaction between Li_2O_2 and H_2O ($Li_2O_2 + 2H_2O \rightarrow 2LiOH + H_2O_2$) because LiOH is easier to be decomposed in the presence of strong catalysts. Since the LiOH products were not detected even when large amount of H_2O

was added into the electrolyte in previous publications, we think there should be a balance between the solid Li_2O_2 and H_2O, LiOH, H_2O_2 in the electrolyte, that prevents the continuous conversion from Li_2O_2 to LiOH on cathode. In view of the catalytic decomposition of MnO_2 towards H_2O_2, the balance can be break when MnO_2 is introduced in cathode and the conversion from Li_2O_2 to LiOH can be completed. Once the LiOH is realized as the discharge products, the charge potential can be reduced by incorporating a catalyst like Ru or RuO_2 for LiOH decomposition. In this case, the side reactions resulted from the high charge potential can be efficiently avoided and long cycle life may be achieved.

1.4.2 Targets of this research

The targets of this study on reduction of charge potential in Li-O_2 battery are as follows:

- To reduce the charge potential (< 3.5 V) and to break the limitation reported by a novel H_2O-involved mechanism.
- To reveal the detailed function of H_2O in electrolyte in several kinds of commonly used electrolytes.
- To realize a Li-O_2 battery with low charge potential and long cycle life in humid atmosphere.
- To design a quasi-solid electrolyte that block H_2O permeation and protect Li metal anode from H_2O attack and to achieve the high performance Li-O_2 battery.

1.4.3 Outline of this thesis

There are six chapters in this dissertation.

Chapter 1 is the background of this research work. It mainly includes the limitation

of the current Li-ion batteries, the necessity of developing Li-air battery with ultrahigh energy density, a brief introduction of Li-air battery, the critical problems and reported results. The research motivation and targets have also been proposed.

In chapter 2, a novel discharge/charge mechanism allowing the ultralow charge potential is realized by constructing a MnO_2 and Ru nanoparticles supported Super P carbon composite cathode. In the DMSO-based electrolyte with 120 ppm of H_2O, the charge potential can be reduced to be as low as about 3.2 V. Long cycle life (200 cycles at 500 mA g^{-1}) is achieved.

In chapter 3, tetraglyme-based electrolyte with varied H_2O content (11 ppm, 78 ppm, 1700 ppm and 4600 ppm) instead of the volatile DMSO-based electrolyte is employed in Li-O_2 battery. The H_2O content is proved to have influence on the composition and morphology of discharge products. In the presence of 4600 ppm of H_2O, the charge potential can be optimized to about 3.2 V and the rate capability can be improved. At a high current density of 1000 mAh g^{-1}, the battery can run for 50 cycles, suggesting the stable cycling performance.

In chapter 4, in order to contribute to the practical application of Li-air battery, the Li-O_2 battery operated in humid O_2 atmosphere is developed by introducing a hydrophobic ionic liquid-based electrolyte. In varied relative humidity (dry O_2, 21%, 51% and 74%), the battery shows different charge ability and the discharge products have different compositions and morphologies. It is realized that the battery is well operated for 200 cycles with low overpotentials at a relative humidity of 51%.

Chapter 5 focuses on the protection of Li metal anode from H_2O/moisture attack in the Li-O_2 battery operated in humid O_2 atmosphere. A super-hydrophobic quasi-solid electrolyte composed SiO_2 nanoparticles, polymer binder and ionic liquid is designed. The electrolyte has high thermal stability, ion conductivity, electrochemical stability, and especially efficient resistibility towards H_2O penetration. Thus, the Li metal anode can retain intact in Li-O_2 battery operated in humid O_2 atmosphere and 150 discharge-charge cycles are achieved.

Chapter 6 is the general conclusion and proposed implications for future work of this research.

1.5 Reference

[1] F. Mwasilu, J. J. Justo, E. K. Kim, T. D. Do, J. W. Jung, Electric vehicles and smart grid interaction: A review on vehicle to grid and renewable energy sources integration, *Renew Sust Energ Rev* **2014**, *34*, 501.

[2] B. Dunn, H. Kamath, J. M. Tarascon, Electrical Energy Storage for the Grid: A Battery of Choices, *Science* **2011**, *334*, 928.

[3] J. Lu, L. Li, J. B. Park, Y. K. Sun, F. Wu, K. Amine, Aprotic and Aqueous Li-O_2 Batteries, *Chem. Rev.* **2014**, *114*, 5611.

[4] A. S. Thielmann, A.; Isenmann, R.; Wietschel, M., Fraunhofer Institute for Systems and Innovation Research ISI (Karlsruhe) (Hrsg.): Technology roadmap energy storage for electric mobility 2030, *Karlsruhe: Fraunhofer ISI* **2012**.

[5] K. M. Abraham, Z. Jiang, A polymer electrolyte-based rechargeable lithium/oxygen battery, *J. Electrochem. Soc.* **1996**, *143*, 1.

[6] F. J. Li, H. Kitaura, H. S. Zhou, The pursuit of rechargeable solid-state Li-air batteries, *Energy Environ. Sci.* **2013**, *6*, 2302.

[7] Y. G. Wang, H. S. Zhou, A lithium-air battery with a potential to continuously reduce O_2 from air for delivering energy, *J. Power Sources* **2010**, *195*, 358.

[8] B. Kumar, J. Kumar, Cathodes for Solid-State Lithium-Oxygen Cells: Roles of Nasicon Glass-Ceramics, *J. Electrochem. Soc.* **2010**, *157*, A611.

[9] J.-S. Lee, S. T. Kim, R. Cao, N.-S. Choi, M. Liu, K. T. Lee, J. Cho, Metal-Air Batteries with High Energy Density: Li-Air versus Zn-Air, *Adv. Energy Mater.* **2011**, *1*, 34.

[10] M. M. O. Thotiyl, S. A. Freunberger, Z. Peng, P. G. Bruce, The carbon electrode in nonaqueous Li-O_2 Cells, *J. Am. Chem. Soc.* **2013**, *135*, 494.

[11] H.-D. Lim, K.-Y. Park, H. Song, E. Y. Jang, H. Gwon, J. Kim, Y. H. Kim, M. D. Lima, R. O. Robles, X. Lepro, R. H. Baughman, K. Kang, Enhanced Power and Rechargeability of a Li-O_2 Battery Based on a Hierarchical-Fibril CNT Electrode, *Adv. Mater.* **2013**, *25*, 1348.

[12] Y.-C. Lu, B. M. Gallant, D. G. Kwabi, J. R. Harding, R. R. Mitchell, M. S. Whittingham, Y. Shao-Horn, Lithium-oxygen batteries: bridging mechanistic understanding and battery performance, *Energy Environ. Sci.* **2013**, *6*, 750.

[13] A. C. Luntz, B. D. McCloskey, Nonaqueous Li-Air Batteries: A Status Report, *Chem. Rev.* **2014**, *114*, 11721.

[14] J. Wang, Y. Li, X. Sun, Challenges and opportunities of nanostructured materials for aprotic rechargeable lithium-air batteries, *Nano Energy* **2013**, *2*, 443.

[15] Z. Q. Peng, S. A. Freunberger, L. J. Hardwick, Y. H. Chen, V. Giordani, F. Barde, P. Novak, D. Graham, J. M. Tarascon, P. G. Bruce, Oxygen Reactions in a Non-Aqueous Li^+ Electrolyte, *Angew. Chem. Int. Ed.* **2011**, *50*, 6351.

[16] L. Johnson, C. M. Li, Z. Liu, Y. H. Chen, S. A. Freunberger, P. C. Ashok, B. B. Praveen, K. Dholakia, J. M. Tarascon, P. G. Bruce, The role of LiO_2 solubility in O_2 reduction in aprotic solvents and its consequences for Li-O_2 batteries, *Nature Chem.* **2014**, *6*.

[17] J. B. Yang, D. Y. Zhai, H. H. Wang, K. C. Lau, J. A. Schlueter, P. Du, D. J. Myers, Y. K. Sun, L. A. Curtiss, K. Amine, Evidence for lithium superoxide-like species in the discharge product of a Li-O_2 battery, *Phys. Chem. Chem. Phys.* **2013**, *15*, 3764.

[18] D. Y. Zhai, H. H. Wang, K. C. Lau, J. Gao, P. C. Redfern, F. Y. Kang, B. H. Li, E. Indacochea, U. Das, H. H. Sun, H. J. Sun, K. Amine, L. A. Curtiss, Raman Evidence for Late Stage Disproportionation in a Li-O_2 Battery, *J. Phys. Chem. Lett.* **2014**, *5*, 2705.

[19] S. A. Freunberger, Y. H. Chen, N. E. Drewett, L. J. Hardwick, F. Barde, P. G. Bruce, The Lithium-Oxygen Battery with Ether-Based Electrolytes, *Angew. Chem. Int. Ed.* **2011**, *50*, 8609.

[20] M. M. O. Thotiyl, S. A. Freunberger, Z. Q. Peng, P. G. Bruce, The Carbon Electrode in Nonaqueous Li-O_2 Cells, *J. Am. Chem. Soc.* **2013**, *135*, 494.

[21] B. D. McCloskey, A. Speidel, R. Scheffler, D. C. Miller, V. Viswanathan, J. S. Hummelshoj, J. K. Norskov, A. C. Luntz, Twin Problems of Interfacial

Carbonate Formation in Nonaqueous Li-O_2 Batteries, *J. Phys. Chem. Lett.* **2012**, *3*, 997.

[22] Y.-C. Lu, H. A. Gasteiger, M. C. Parent, V. Chiloyan, Y. Shao-Horn, The Influence of Catalysts on Discharge and Charge Voltages of Rechargeable Li-Oxygen Batteries, *Electrochem. Solid-State Lett.* **2010**, *13*, A69.

[23] Y.-C. Lu, Z. Xu, H. A. Gasteiger, S. Chen, K. Hamad-Schifferli, Y. Shao-Horn, Platinum-Gold Nanoparticles: A Highly Active Bifunctional Electrocatalyst for Rechargeable Lithium-Air Batteries, *J. Am. Chem. Soc.* **2010**, *132*, 12170.

[24] A. K. Thapa, K. Saimen, T. Ishihara, Pd/MnO_2 Air Electrode Catalyst for Rechargeable Lithium/Air Battery, *Electrochem. Solid-State Lett.* **2010**, *13*, A165.

[25] Z. Peng, S. A. Freunberger, Y. Chen, P. G. Bruce, A Reversible and Higher-Rate Li-O_2 Battery, *Science* **2012**, *337*, 563.

[26] H.-G. Jung, Y. S. Jeong, J.-B. Park, Y.-K. Sun, B. Scrosati, Y. J. Lee, Ruthenium-Based Electrocatalysts Supported on Reduced Graphene Oxide for Lithium-Air Batteries, *ACS Nano* **2013**, *7*, 3532.

[27] F. Li, D.-M. Tang, Y. Chen, D. Golberg, H. Kitaura, T. Zhang, A. Yamada, H. Zhou, Ru/ITO: A Carbon-Free Cathode for Nonaqueous Li-O_2 Battery, *Nano Lett.* **2013**, *13*, 4702.

[28] E. Yilmaz, C. Yogi, K. Yamanaka, T. Ohta, H. R. Byon, Promoting Formation of Noncrystalline Li_2O_2 in the Li-O_2 Battery with RuO_2 Nanoparticles, *Nano Lett.* **2013**, *13*, 4679.

[29] Z. Guo, D. Zhou, H. Liu, X. Dong, S. Yuan, A. Yu, Y. Wang, Y. Xia, Synthesis of ruthenium oxide coated ordered mesoporous carbon nanofiber arrays as a catalyst for lithium oxygen battery, *J. Power Sources* **2015**, *276*, 181.

[30] J. Lu, Y. Lei, K. C. Lau, X. Luo, P. Du, J. Wen, R. S. Assary, U. Das, D. J. Miller, J. W. Elam, H. M. Albishri, D. Abd El-Hady, Y.-K. Sun, L. A. Curtiss, K. Amine, A nanostructured cathode architecture for low charge overpotential in lithium-oxygen batteries, *Nat. Commun.* **2013**, *4*.

[31] D. Zhang, Z. Fu, Z. Wei, T. Huang, A. Yu, Polarization of Oxygen Electrode in

Rechargeable Lithium Oxygen Batteries, *J. Electrochem. Soc.* **2010**, *157*, A362.

[32] S. Dong, X. Chen, K. Zhang, L. Gu, L. Zhang, X. Zhou, L. Li, Z. Liu, P. Han, H. Xu, J. Yao, C. Zhang, X. Zhang, C. Shang, G. Cui, L. Chen, Molybdenum nitride based hybrid cathode for rechargeable lithium-O_2 batteries, *Chem. Commun.* **2011**, *47*, 11291.

[33] A. K. Thapa, T. Ishihara, Mesoporous alpha-MnO_2/Pd catalyst air electrode for rechargeable lithium-air battery, *J. Power Sources* **2011**, *196*, 7016.

[34] L. Wang, X. Zhao, Y. Lu, M. Xu, D. Zhang, R. S. Ruoff, K. J. Stevenson, J. B. Goodenough, $CoMn_2O_4$ Spinel Nanoparticles Grown on Graphene as Bifunctional Catalyst for Lithium-Air Batteries, *J. Electrochem. Soc.* **2011**, *158*, A1379.

[35] J.-L. Shui, N. K. Karan, M. Balasubramanian, S.-Y. Li, D.-J. Liu, Fe/N/C Composite in Li-O_2 Battery: Studies of Catalytic Structure and Activity toward Oxygen Evolution Reaction, *J. Am. Chem. Soc.* **2012**, *134*, 16654.

[36] F. Li, R. Ohnishi, Y. Yamada, J. Kubota, K. Domen, A. Yamada, H. Zhou, Carbon supported TiN nanoparticles: an efficient bifunctional catalyst for non-aqueous Li-O_2 batteries, *Chem. Commun.* **2013**, *49*, 1175.

[37] C. S. Park, K. S. Kim, Y. J. Park, Carbon-sphere/Co_3O_4 nanocomposite catalysts for effective air electrode in Li/air batteries, *J. Power Sources* **2013**, *244*, 72.

[38] J. Tang, S. Wu, T. Wang, H. Gong, H. Zhang, S. M. Alshehri, T. Ahamad, H. Zhou, Y. Yamauchi, Cage-Type Highly Graphitic Porous Carbon-Co_3O_4 Polyhedron as the Cathode of Lithium Oxygen Batteries, *ACS Appl. Mater. Interfaces* **2016**, *8*, 2796.

[39] W.-J. Kwak, K. C. Lau, C.-D. Shin, K. Amine, L. A. Curtiss, Y.-K. Sun, A Mo_2C/Carbon Nanotube Composite Cathode for Lithium-Oxygen Batteries with High Energy Efficiency and Long Cycle Life, *ACS Nano* **2015**, *9*, 4129.

[40] J.-J. Xu, D. Xu, Z.-L. Wang, H.-G. Wang, L.-L. Zhang, X.-B. Zhang, Synthesis of Perovskite-Based Porous $La_{0.75}Sr_{0.25}MnO_3$ Nanotubes as a Highly Efficient

Electrocatalyst for Rechargeable LithiumOxygen Batteries, *Angew. Chem. Int. Ed.* **2013**, *52*, 3887.

[41] L. Wang, M. Ara, K. Wadumesthrige, S. Salley, K. Y. S. Ng, Graphene nanosheet supported bifunctional catalyst for high cycle life Li-air batteries, *J. Power Sources* **2013**, *234*, 8.

[42] S. H. Oh, R. Black, E. Pomerantseva, J.-H. Lee, L. F. Nazar, Synthesis of a metallic mesoporous pyrochlore as a catalyst for lithium-O_2 batteries, *Nature Chem.* **2012**, *4*, 1004.

[43] N. N. Feng, P. He, H. S. Zhou, Enabling Catalytic Oxidation of Li_2O_2 at the Liquid-Solid Interface: The Evolution of an Aprotic Li-O_2 Battery, *ChemSusChem* **2015**, *8*, 600.

[44] Y. Chen, S. A. Freunberger, Z. Peng, O. Fontaine, P. G. Bruce, Charging a Li-O_2 battery using a redox mediator, *Nature Chem.* **2013**, *5*, 489.

[45] W. R. Torres, S. E. Herrera, A. Y. Tesio, M. del Pozo, E. J. Calvo, Soluble TTF catalyst for the oxidation of cathode products in Li-Oxygen battery: A chemical scavenger, *Electrochim. Acta* **2015**, *182*, 1118.

[46] H. Yang, Q. Wang, R. Zhang, B. D. Trimm, M. S. Whittingham, The electrochemical behaviour of TTF in Li-O_2 batteries using a TEGDME-based electrolyte, *Chem. Commun.* **2016**, *52*, 7580.

[47] B. J. Bergner, A. Schuermann, K. Peppler, A. Garsuch, J. Janek, TEMPO: A Mobile Catalyst for Rechargeable Li-O_2 Batteries, *J. Am. Chem. Soc.* **2014**, *136*, 15054.

[48] B. J. Bergner, M. R. Busche, R. Pinedo, B. B. Berkes, D. Schroeder, J. Janek, How To Improve Capacity and Cycling Stability for Next Generation Li-O_2 Batteries: Approach with a Solid Electrolyte and Elevated Redox Mediator Concentrations, *ACS Appl. Mater. Interfaces* **2016**, *8*, 7756.

[49] B. Sun, X. Huang, S. Chen, J. Zhang, G. Wang, An optimized $LiNO_3$/DMSO electrolyte for high-performance rechargeable Li-O_2 batteries, *Rsc Advances* **2014**, *4*, 11115.

[50] D. Sharon, D. Hirsberg, M. Afri, F. Chesneau, R. Lavi, A. A. Frimer, Y.-K.

Sun, D. Aurbach, Catalytic Behavior of Lithium Nitrate in Li-O_2 Cells, *ACS Appl. Mater. Interfaces* **2015**, *7*, 16590.

[51] D. Sun, Y. Shen, W. Zhang, L. Yu, Z. Yi, W. Yin, D. Wang, Y. Huang, J. Wang, D. Wang, J. B. Goodenough, A Solution-Phase Bifunctional Catalyst for Lithium-Oxygen Batteries, *J. Am. Chem. Soc.* **2014**, *136*, 8941.

[52] B. J. Bergner, C. Hofmann, A. Schuermann, D. Schroeder, K. Peppler, P. R. Schreiner, J. Janek, Understanding the fundamentals of redox mediators in Li-O_2 batteries: a case study on nitroxides, *Phys. Chem. Chem. Phys.* **2015**, *17*, 31769.

[53] H. D. Lim, H. Song, J. Kim, H. Gwon, Y. Bae, K. Y. Park, J. Hong, H. Kim, T. Kim, Y. H. Kim, X. Lepro, R. Ovalle-Robles, R. H. Baughman, K. Kang, Superior Rechargeability and Efficiency of Lithium-Oxygen Batteries: Hierarchical Air Electrode Architecture Combined with a Soluble Catalyst, *Angew. Chem. Int. Ed.* **2014**, *53*, 3926.

[54] W.-J. Kwak, D. Hirshberg, D. Sharon, M. Afri, A. A. Frimer, H.-G. Jung, D. Aurbach, Y.-K. Sun, Li-O_2 cells with LiBr as an electrolyte and a redox mediator, *Energy Environ. Sci.* **2016**, *9*, 2334.

[55] Z. Liang, Y.-C. Lu, Critical Role of Redox Mediator in Suppressing Charging Instabilities of Lithium-Oxygen Batteries, *J. Am. Chem. Soc.* **2016**, *138*, 7574.

[56] C. K. Lee, Y. J. Park, CsI as Multifunctional Redox Mediator for Enhanced Li-Air Batteries, *ACS Appl. Mater. Interfaces* **2016**, *8*, 8561.

[57] K. P. C. Yao, J. T. Frith, S. Y. Sayed, F. Barde, J. R. Owen, Y. Shao-Horn, N. Garcia-Araez, Utilization of Cobalt Bis(terpyridine) Metal Complex as Soluble Redox Mediator in Li-O_2 Batteries, *J. Phys. Chem. C* **2016**, *120*, 16290.

[58] D. Kundu, R. Black, B. Adams, L. F. Nazar, A Highly Active Low Voltage Redox Mediator for Enhanced Rechargeability of Lithium-Oxygen Batteries, *ACS Cent Sci* **2015**, *1*, 510.

[59] R. Black, S. H. Oh, J.-H. Lee, T. Yim, B. Adams, L. F. Nazar, Screening for Superoxide Reactivity in Li-O_2 Batteries: Effect on Li_2O_2/LiOH

Crystallization, *J. Am. Chem. Soc.* **2012**, *134*, 2902.

[60] N. B. Aetukuri, B. D. McCloskey, J. M. Garcia, L. E. Krupp, V. Viswanathan, A. C. Luntz, Solvating additives drive solution-mediated electrochemistry and enhance toroid growth in non-aqueous Li-O_2 batteries, *Nature Chem.* **2015**, *7*, 50.

[61] M. H. Cho, J. Trottier, C. Gagnon, P. Hovington, D. Clement, A. Vijh, C. S. Kim, A. Guerfi, R. Black, L. Nazar, K. Zaghib, The effects of moisture contamination in the Li-O_2 battery, *J. Power Sources* **2014**, *268*, 565.

[62] K. U. Schwenke, M. Metzger, T. Restle, M. Piana, H. A. Gasteiger, The Influence of Water and Protons on Li_2O_2 Crystal Growth in Aprotic Li-O_2 Cells, *J. Electrochem. Soc.* **2015**, *162*, A573.

[63] S. Meini, M. Piana, N. Tsiouvaras, A. Garsuch, H. A. Gasteiger, The Effect of Water on the Discharge Capacity of a Non-Catalyzed Carbon Cathode for Li-O_2 Batteries, *Electrochem. Solid-State Lett.* **2012**, *15*, A45.

[64] Z. Y. Guo, X. L. Dong, S. Y. Yuan, Y. G. Wang, Y. Y. Xia, Humidity effect on electrochemical performance of Li-O_2 batteries, *J. Power Sources* **2014**, *264*, 1.

Chapter 2. Water-driven low charge potentials by designing air cathodes of Li-O_2 batteries in dimethyl sulfoxide (DMSO)-based electrolyte

2.1 Introduction

The success of deploying Li-O_2 battery in the future will be crucially dependent on how small the overpotentials at the cathode side can be reduced and how many cycles they can work reversibly.[1-3] Currently, two strategies have been widely applied for these issues. One is to use carbon-free or carbon-alternative cathodes, like nanoporous gold,[4] TiC[5] and conductive metal oxide supported Ru,[6-7] which can circumvent side reactions involving carbon. The charge overpotentials ensuring the decomposition of Li_2O_2 are reduced to ~0.54 V, corresponding to charge potentials of ~3.50 V. This direct electrochemical oxidation of Li_2O_2 was revealed to involve multiple processes, in which the initial delithiation occurring at an overpotential of 0.44 V, possibly suggests the theoretical limit.[8-9] Alternatively, redox mediators have been introduced to chemically oxidize Li_2O_2 and the apparent charge potentials are typically determined by the mediators. For instance, tetrathiafulvalene (TTF) and lithium iodide (LiI) reduce the charge potential to ~3.50 V, equal to a charge overpotential of 0.54 V.[10-12] In principle, Li_2O_2 can be oxidized by mediators possessing higher redox potentials than its equilibrium potential; however, practical mediators are very limited. A more efficient and compatible one for further potential reduction is still lacking. By either the direct or indirect (mediators) Li_2O_2 oxidation strategy, it will be a great challenge to reduce the charge potentials to feasible values. Exploring new reaction mechanisms at the oxygen cathodes to significantly improve the round-trip efficiency and cycling stability is essential and urgently necessary for the development of Li–O_2 batteries.

Water in electrolytes has been found to affect the morphologies of discharge products and increase the discharge capacity,[13-15] but its presence in electrolytes or

O_2 atmosphere resulted in rapid charge potential increase and hence battery death after several cycles.[15-17] In addition to the main discharge product Li_2O_2, a byproduct LiOH was also detected.[16] We found that the decomposition of LiOH is strongly related to the applied catalysts, such as Ru nanoparticles supported on Super P (Ru/SP). To reduce the charge overpotentials of Li–O_2 batteries, a trace amount of water in electrolytes and electrolytic manganese oxide (MnO_2) nanoparticles are both utilized to favour the transformation of the discharge product from Li_2O_2 to LiOH and its following decomposition on charging. The MnO_2 incorporated in Ru/SP (Ru/MnO_2/SP) also allows for the water regeneration at the cathode during the discharge/charge cycles. This enables the Li–O_2 battery to operate with a small discharge/charge potential gap and superior cycling stability. A reaction mechanism by converting Li_2O_2 to LiOH in the presence of both water and Ru/MnO_2/SP is proposed.

2.2 Experimental and Characterization

2.2.1 Preparation of Ru/MnO_2/SP

Electrolytic MnO_2 (MnO_2) was received from TOSOH, Japan and ball-milled to nanometer scale. Ru/SP was synthesized as follows: 85 mg of SP was stirred into a solution of ethylene glycol (EG, purity of ~99.5%, Wako Chemicals) containing 7.5 mg of Ru in $RuCl_3 \cdot xH_2O$ (purity of 36 - 42 wt% based on Ru, Wako Chemicals), and its pH was adjusted to 13 with 0.1 M of NaOH in EG. The suspension was then heated to 160 ^oC for 3 h with flowing N_2. After cooling to 80 ^oC, its pH was adjusted to 3 using 0.1 M HCl and the resulting mixture was further stirred for 12 h. The final product Ru/SP was centrifuged, washed with de-ionized water until the solution pH reached ~7 and dried at 80 ^oC in a vacuum oven for 12 h. For the preparation of Ru/MnO_2/SP, the as-synthesized Ru/SP and MnO_2 nanoparticles with a weight ratio Ru/MnO_2/SP = 7.5:7.5:85 were sonicated into an ethanol aqueous solution for 3 h and

stirred overnight. Then, the product Ru/MnO_2/SP was collected and dried at 80 ^oC under vacuum for 12 h.

2.2.2 Preparation of electrolyte

Dimethyl sulfone (DMSO) is reported to be relatively in Li-O_2 battery and is used as electrolyte solvent in this chapter. DMSO was firstly dried over 4 Å molecular sieves and then using Li metal. The Li salt of $LiClO_4$ was used as received from Wako Chemicals. The water in the prepared electrolytes was from the Li salt. The water content was measured on a desk-top Karl–Fisher Titration instrument and the value was determined to be ~120 ppm.

2.2.3 Fabrication of batteries and electrochemical test

The electrode film composed of Ru/MnO_2/SP or Ru/SP and PTFE (A dispersion of 60 wt%, Du Pont-Mitsui Fluorochemicals Co. Ltd.) with a ratio of 85:15 wt% was rolled with a glass rod. The mass loading of Ru/MnO_2/SP or Ru/SP is ~0.5 mg cm^{-2}. The electrode film was pressed onto a hydrophobic carbon paper (SIGRACET Gas Diffusion Media, Type GDL 35BA) to work as a cathode. The anode was consisted of $LiFePO_4$ (Sumitomo Osaka Cement), SP and PTFE (70/20/10) pressed on an Al mesh. The amount of DMSO-based electrolytes in a coin cell was 100 ml. The employed separator was a glass microfibre filter paper (GF/A, Whatman). The Li–O_2 battery assembly in 2032 coin cells was conducted in an Ar-filled glove box that has a dew point of around - 90 ^oC (~0.1 ppm of H_2O) and O_2 content below 5 ppm. The cells stored in a glass chamber with a volume capacity of 650 ml were purged with O_2 (99.999%) before electrochemical tests (see Fig. 2.1). Galvanostatic discharge/charge was conducted on a Hokuto discharging/charging system. All the electrochemical measurements were conducted at 25 ^oC. The specific capacities and currents are based on the mass of Ru/MnO_2/SP or Ru/SP in cathodes.

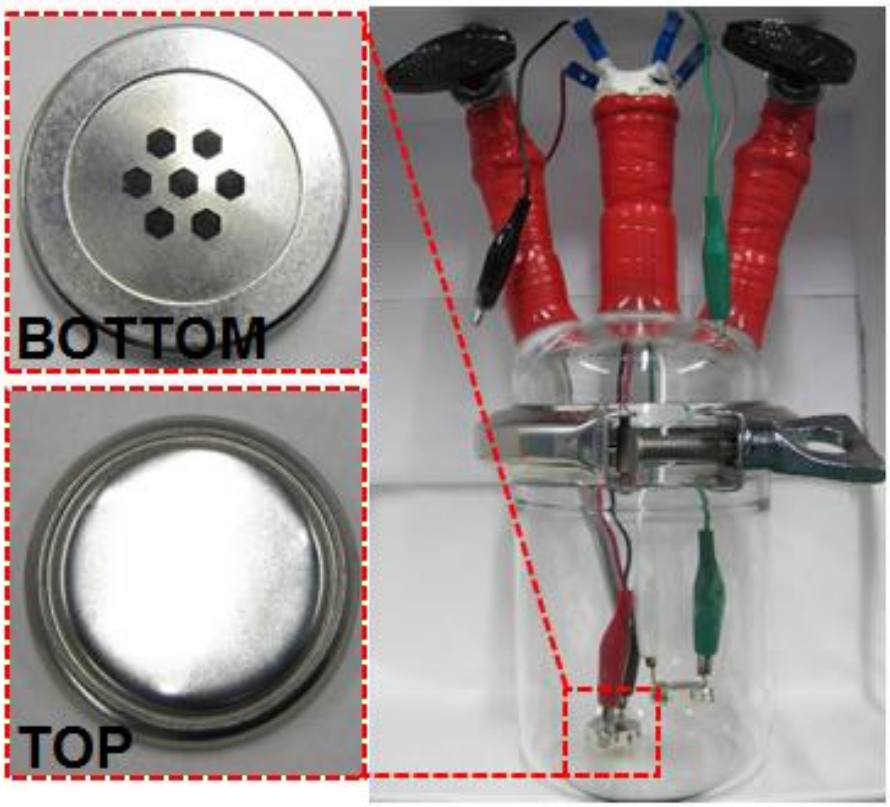

Fig. 2.1. The photo of a fabricated Li-O_2 battery. The bottle is filled with O_2 gas. There are several pores on the bottom of a coin cell, allowing O_2 gas diffusion.

2.2.4 Characterization

The contact angles of electrolytes on the cathode were examined on AST Products with a model of Optima. The discharged and charged cathodes were extracted in the glove box and washed with dried dimethoxyethane (DME). XRD was performed on a Bruker D8 Advanced diffractometer with Cu Kα (λ = 1.5406 Å) radiation with a scan rate of 0.016° per s. SEM was obtained on Hitachi S4800. The Ru/MnO_2/SP was mixed with KBr and then pressed to a pellet for Fourier transform infrared spectroscope (FTIR) characterization on a JASCO instrument of FT/IR-6200 from 2000 to 400 cm^{-1} with a resolution of 2 cm^{-1}. The electrolytes during cycles were collected by washing the glass fibre filter separators with acetone-d_6, and subjected to ^{1}H NMR (Bruker, 500 MHz).

Titration of LiOH and Li_2O_2 in a discharged Ru/SP cathode. The titration contains

two steps: (i) titration of LiOH and (ii) titration of I_2:

(i) The Ru/SP cathode was extracted from a discharged coin cell in an Ar-filled glove box, washed with dried DME and dried under vacuum. The cathode was taken out of the glove box, and put into a conical flask with 20 ml of de-ionized water immediately. The flask was vigorously shaken to promote the complete reaction of Li_2O_2 with H_2O. The alkaline solution was titrated with a standard 5 mmol L^{-1} of HCl, and the end point was indicated by 0.1 mL of phenolphthalein in isopropanol.

Involved reaction:

$$Li_2O_{2(s)} + 2H_2O_{(l)} \rightarrow H_2O_{2(l)} + 2LiOH_{(aq)} \quad (1)$$

(ii) After the alkaline titration was finished, three reagents were added into the existing solution in sequence: 0.5 mL of 2 wt% KI in H_2O, 0.1 mL of 60 wt% H_2SO_4, and 25 µL of a molybdate based catalyst solution. The catalyst solution was prepared by dissolving 0.5 g ammonium molybdate in 5 mL of 30 wt% ammonia aqueous solution, followed by adding 1.5 g of ammonium nitrate and diluting the solution to 25 mL total using de-ionized water. The resultant solution turns yellow upon reagent addition due to I_2 formation, and the I_2 was immediately titrated to a pale yellow color using 1 mmol L^{-1} of $Na_2S_2O_3$ solution. At this point, 0.1 mL of 5 wt% starch indicator was added, which turned blue, and the titration was continued until the color disappeared.

Involved reactions:

$$H_2O_2 + 2KI + H_2SO_4 \rightarrow I_2 + K_2SO_4 + 2H_2O \quad (2)$$

$$I_2 + 2Na_2S_2O_3 \rightarrow Na_2S_4O_6 + 2NaI \quad (3)$$

2.2.5 Estimation of charge potentials

The reactions occurring at a cathode and an anode and the potentials's dependence are described below:

Total: $LiOH \rightarrow Li + 1/2H_2O + 1/4O_2$

(+) $LiOH \rightarrow Li+ + 1/2H_2O + 1/4O_2 + e^-$

$\varphi_+ = \varphi_{O_2/LiOH}^o + 0.059\lg\alpha_{Li+} + 0.059 * 1/2\lg\alpha_{H_2O}$

(-) $Li^+ + e^- \rightarrow Li$

$\varphi_- = \varphi_{Li+/Li}^o + 0.059\lg\alpha_{Li+}$

Charge potential: $\varphi = \varphi_+ - \varphi_- = (\varphi_{O_2/LiOH}^o - \varphi_{Li+/Li}^o) + 0.059 * 1/2\lg\alpha_{H_2O}$

Standard potential estimation based on Gibbs free energy

$LiOH \rightarrow Li + 1/4O_2 + ½\ H_2O$

Go -438.96 -237.14 kJ/mol

$E^o = -\Delta G^o/F = 3.32$ V

$E = E^o + 0.059 * 1/2\lg\alpha_{H_2O}$

For example, $[H_2O] = 10 \sim 100$ ppm

$E \approx 3.17 \sim 3.20$ V

In the estimation process, the concentration of O_2 dissolved in electrolyte is not considered. The initial concentration of H_2O in the electrolyte is used to estimate the equilibrium potential of LiOH in the charging process, without considering that H_2O has been completely or practically converted to LiOH in the discharging process.

2.3 Results and Discussion

2.3.1 Low overpotentials at Ru/MnO_2/SP cathode

The Li–O_2 batteries were constructed with Ru/MnO_2/SP pressed onto a carbon paper as cathodes, 0.5 M $LiClO_4$ in DMSO containing 120 ppm of H_2O as electrolytes and $LiFePO_4$ in replacement of Li anodes. The $LiFePO_4$ is not a practical anode, but is able to avoid the reaction of Li metal and the trace amount of H_2O and any

contamination from formation of the solid electrolyte interface layer on the Li anode.[10] It has a stable potential of ~3.45 V vs Li^+/Li regardless of the state of charge and favours the investigation on the discharge/charge behaviour in the presence of H_2O and the underlying reaction mechanism specifically at the oxygen cathode. The discharge/charge potentials at the oxygen cathode of the Li–O_2 batteries are converted to against Li for discussion.

The Li–O_2 battery with Ru/MnO_2/SP as cathode and the DMSO-based electrolyte containing ppm-leveled H_2O is discharged and charged at 500 mA g^{-1}. From Fig. 2.2a, a charge potential plateau as low as ~3.20 V, corresponding to an overpotential of ~0.24 V, can be clearly observed. Its corresponding dQ/dV curve in Fig. 2.2b shows sharp oxygen reduction reaction and oxygen evolution reaction peaks in the discharging and charging process, respectively, which are consistent with the flat discharge and charge plateaus. In addition, a small plateau at ~3.60 V is also obtained in the charge profile in Fig. 2.2a. It could be resulted from the affinity of DMSO with the Ru/MnO_2/SP cathode that has a large contact angle of 62° (Fig. 2.2c). This may enable the oxygen evolved in a charging process to accumulate in the voids between the residual discharge product and the cathode. It would induce slow diffusion of electrolytes into the voids for the decomposition of the remaining discharge products

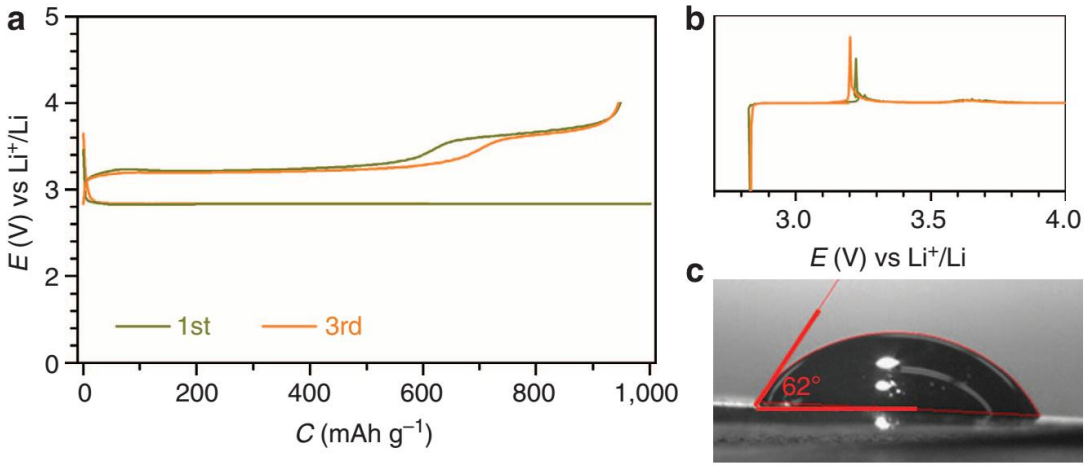

Fig. 2.2. (a) Discharge/charge profiles of the Li–O_2 batteries with a configuration of (Ru/MnO_2/SP)/electrolyte/$LiFePO_4$. (b,c) The corresponding dQ/dV curves and the contact angle of the electrolyte on the cathode.

and result in the relatively large overpotential at ~3.60 V. The trace amount of H_2O in electrolytes is demonstrated to play a crucial role on reducing charge overpotentials of Li–O_2 batteries in all the widely used electrolytes, which was empirically considered as a negative factor in a Li-ion battery.[18]

2.3.2 Product analysis on the discharge/charged cathode

The discharged and charged Ru/MnO_2/SP cathodes in the DMSO-based electrolyte containing water have been characterized by X-ray diffraction (XRD). As shown in Fig. 2.3a, the discharge products are identified as a mixture of LiOH and Li_2O_2, referring to the standard powder diffraction files of 01-085-0777 and 00-009-0355, respectively, suggesting LiOH converted from Li_2O_2. To avoid the effect of MnO_2, quantification of LiOH and Li_2O_2 was conducted on the Ru/SP cathode with the same discharge capacity as in Fig. 2.2a via iodometric titration. The discharge product Li_2O_2 reacts with H_2O via $Li_2O_{2(s)} + 2H_2O_{(l)} \rightleftarrows H_2O_{2(l)} + 2LiOH_{(aq)}$,[19-20] where H_2O_2 further oxidizes iodide to iodine, the titrated target. The LiOH and Li_2O_2 in the discharged cathode were titrated via two steps and estimated to 16.02 and 1.48 mmol, respectively, which are in agreement with the XRD patterns of the discharged cathode in Fig. 2.3a. The majority of LiOH formed at a discharged cathode is revealed by the characteristic absorbance peak in the infrared (FTIR) spectra in Fig. 2.3b. Based on the electrons passing through the cathode and the oxygen derived from the discharge products of LiOH and Li_2O_2 by iodometric titration, the discharging process is a 1.97e^-/O_2 process, quite close to the theoretical value of 2.00e^-/O_2. This suggests that LiOH is converted from Li_2O_2 via a chemical, not an electrochemical, process in the discharging processes.

After charge, the discharge products LiOH and Li_2O_2 were decomposed, as evidenced by the disappearance of their characteristic diffraction peaks in Fig. 2.3a, b. Further, the discharge products were directly observed by scanning electron microscope (SEM) in Fig. 2.3c. All the products are toroidal particles with obvious layering. These are quite similar to the toroidal aggregates in a Li_2O_2-only discharged

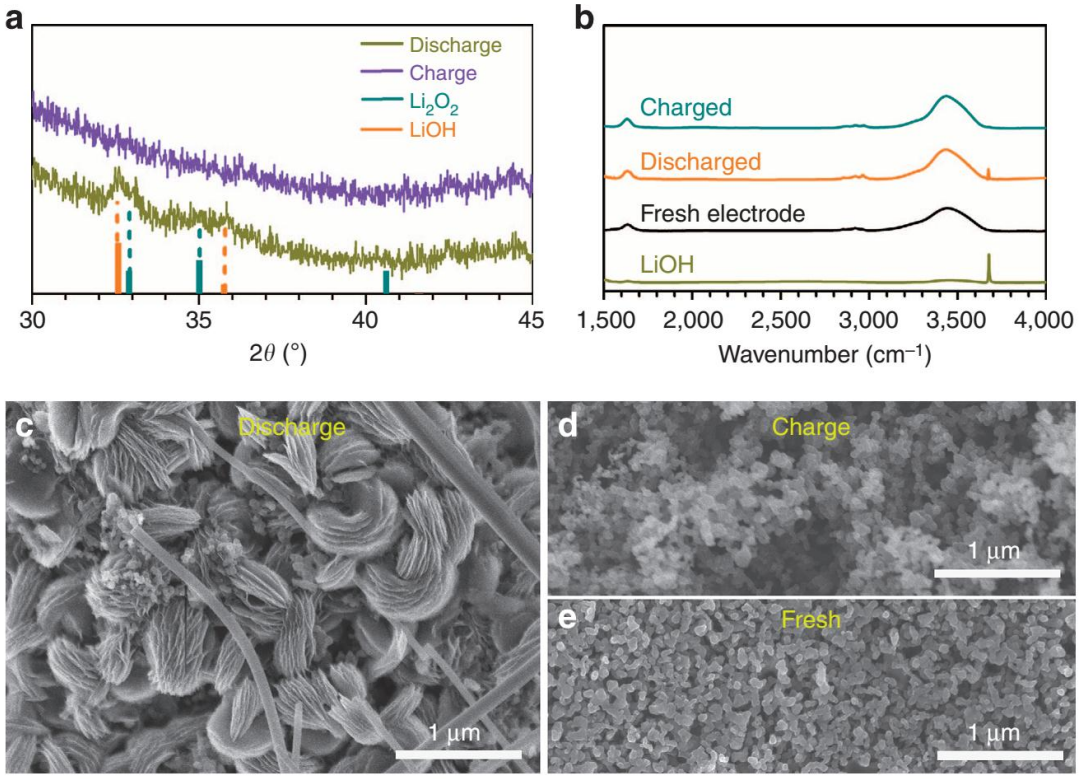

Fig. 2.3. Characterization of the discharged/charged cathodes. (a) Ex situ XRD patterns of the discharged and charged Ru/MnO_2/SP cathodes in DMSO-based electrolyte with 120 ppm H_2O. (b) FTIR spectra of the charged and discharge cathodes. (c,d) SEM images of the discharged and charged cathodes, in comparison to the fresh cathode (e).

cathode,[21-22] which may suggest that the LiOH was derived from Li_2O_2 in the presence of H_2O in electrolytes by persisting the similar shape. The charged cathode becomes more porous after decomposition of the discharge products in Fig. 2.3d in comparison to the fresh cathode in Fig. 2.3e. These results indicate that the low charge overpotentials demonstrated in Fig. 2.2a resulted from the electrochemical decomposition of LiOH.

2.3.3 Rate capability and cycling stability

The Li–O_2 battery with Ru/MnO_2/SP and the DMSO-based electrolyte containing

ppm-leveled H_2O was examined at varied current densities, as shown in Fig. 2.4a. The polarization is obviously increased with the current density from 250 to 500 and 1000 mA g^{-1}. The overpotential in the discharging and charging process at 250 mA g^{-1} is 0.11 V and 0.21 V, respectively, leading to a small discharge/charge potential gap of 0.32 V. The Li–O_2 battery was continuously discharged and charged at 500 mA g^{-1} for 200 cycles and ~800 h, and the selected runs of discharge and charge are shown in Fig. 2.4b. The discharge and charge curves during the first 150 cycles are almost overlapped except the first charge. A slight charge potential increase beyond the 150 cycles can also be observed, which could be related to the electrolyte instability during many cycles.[23-24] The discharge and charge capacities in the 200 cycles are almost constant, and the corresponding coulombic efficiency in each run is approaching 98% (Fig. 2.4c), indicative of good reversibility. This may be partially

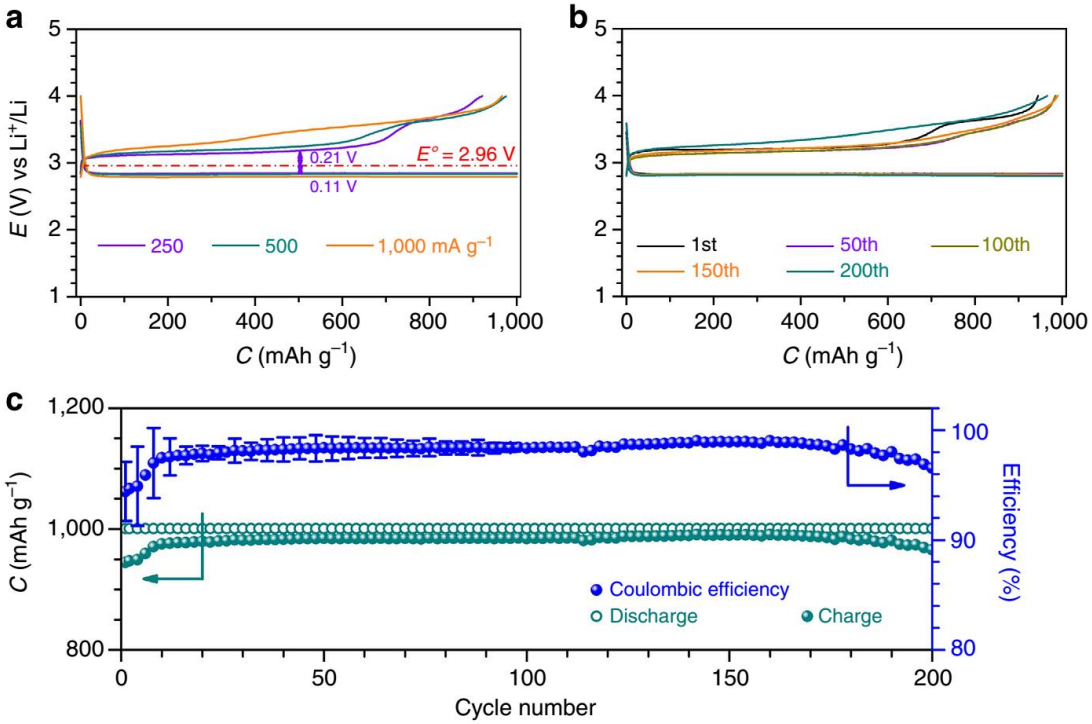

Fig. 2.4. Rate capability and cycling performance of the Li–O_2 batteries with Ru/MnO_2/SP. (a) Discharge/charge profiles of the tenth run at varied current densities from 250 to 500 and 1000 mA g^{-1}. (b) Discharge/charge profiles of the selected runs over the 200 cycles at 500 mA g^{-1}. (c) Plot of discharge/charge capacities and the corresponding coulombic efficiencies against cycle number and error bars (s.e.m.) in the first 100 cycles.

benefited from the conversion of chemically active Li_2O_2 to LiOH. The low charge potentials sustained for so many cycles, to the best of our knowledge, have never been achieved before. The small discharge/charge potential gap and good cycling stability of the Li–O_2 battery are rewarded by the 'water catalysis' at the Ru/MnO_2/SP cathode.

2.3.4 Reaction mechanism

The equilibrium potential of LiOH in an aqueous solution is estimated to be ~3.42 V vs Li^+/Li based on Nernst equation.[25-26] However, in this studied electrolyte system the trace amount of H_2O and $LiClO_4$ are both the solutes and DMSO is the solvent. The equilibrium potential of LiOH is dependent on the concentration of H_2O, and it can be roughly estimated to be ~3.20 V, considering a concentration of 100 ppm of H_2O in the electrolyte (see the estimation process in Experimental section 2.2.5). This is in good agreement with the observed low charge potential plateaus in all the widely employed electrolytes DMSO-based electrolytes for Li–O_2 batteries in Figs 2.1a. Based on the above results, a mechanism for the discharging and charging process of the battery with Ru/MnO_2/SP and the electrolyte containing a trace amount of H_2O can be proposed and schematically described in Fig. 2.5a. On discharging, O_2 accepts electrons via the external circuit and is reduced to generate the primary discharge product Li_2O_2.[27-29] At the same time, the Li_2O_2 reacts with H_2O from the electrolyte and is converted to LiOH via Steps (i and ii). Although Step (i) is an equilibrium,[15] it can be largely promoted to move forward by the conversion of one of the products H_2O_2 to H_2O over MnO_2 via Step (ii).[30] The two Steps (i and ii) occur sequentially, and quickly transform Li_2O_2 to LiOH as long as H_2O remains in the electrolyte. This has been confirmed by the presence of substantial LiOH in discharged cathodes as revealed by both of the XRD patterns and the IR spectra in Fig. 2.3. This is consistent with the observations of Aetukuri et al.,[14] and Schwenke et al.,[15] where the H_2O in electrolytes is possibly consumed by the employed Li anode or saturated by the product LiOH, and the lack of a promoter like MnO_2 for

Step (ii) made the equilibrium reaction in Step (i) to move backward and result in the major discharge product Li_2O_2 as detected.

In the following charging process, the resultant LiOH can be directly oxidized via Step (iii) to regenerate H_2O at low charge potentials, by which the residual Li_2O_2 is then converted to LiOH via Steps (i and ii) and oxidized. To demonstrate the feasibility of Step (iii), commercial LiOH was ball-milled and then thoroughly mixed with Ru/SP with a ratio of 30:70 (wt/wt). The electrodes of Ru/SP with and without LiOH under Ar atmosphere were subjected to linear scanning voltammetry (LSV) at a low scan rate of 0.01 mV s^{-1} as depicted in Fig. 2.5b. The Ru/SP electrode incorporated with LiOH presents significant oxidation currents and an oxidation onset potential of ~3.27 V in Fig. 2.5b, which is in sharp contrast with no oxidation response on the electrode without LiOH. At a carbon electrode pre-filled with LiOH, a high charge potential of ~4.0 V was reported.[31] This suggests that over Ru/SP LiOH

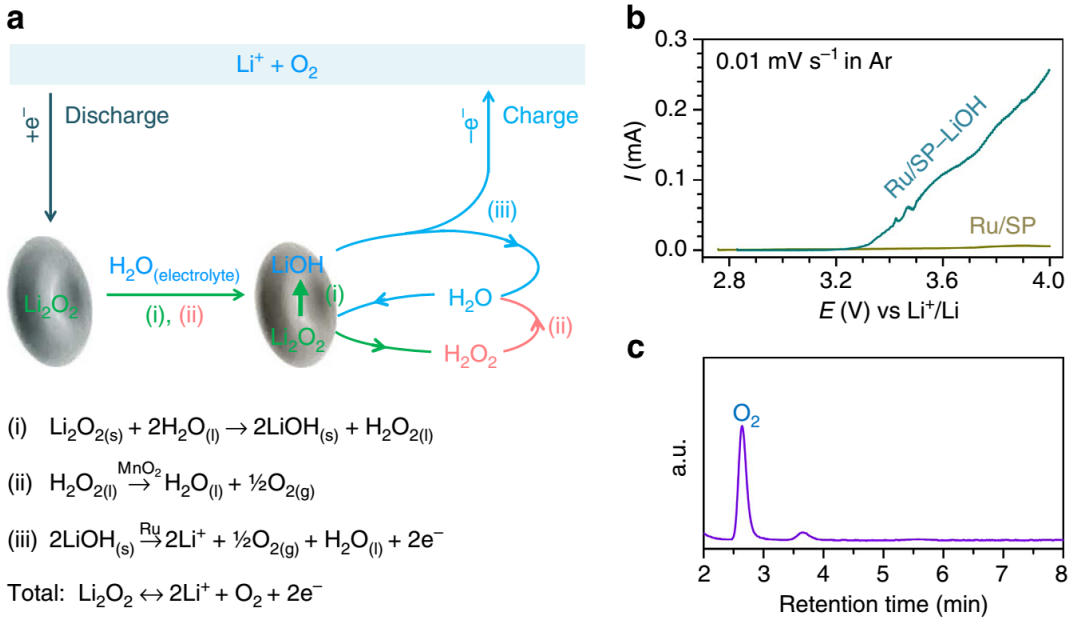

Fig. 2.5. Proposed reaction mechanism, LSV and gas analysis. (a) (i) is a spontaneous process; (ii) is promoted over MnO_2 nanoparticles in Ru/MnO_2/SP; and oxidation of LiOH in (iii) occurs at low charge overpotentials over Ru nanoparticles. (b) Linear scanning voltammetry (LSV) curves of the Ru/SP electrodes with and without LiOH under Ar atmosphere. (c) Gas chromatography (GC) analysis on the gas evolved in a charging process.

was oxidized at low potentials, though it may be dependent on its morphology and facet orientation and the catalyst. The gas evolved in a charging process can be identified as O_2 by a gas chromatography (GC) mounted with a thermal conductivity detector, as evidenced by the sharp GC signal of O_2 in Fig. 2.5c. As shown in the whole discharging and charging process in Fig. 2.5a, H_2O is not consumed and can be circulated to behave like a catalyst. The total electrochemical reaction occurring at the oxygen cathode is $2Li^+ + O_2 + 2e^- \rightleftarrows Li_2O_2$, consistent with the Li–O_2 battery chemistry.

2.4 Conclusions

The 'water catalysis' at the oxygen cathode side has been demonstrated to reduce the charge overpotentials to ~0.24 V, corresponding to ~3.20 V vs Li^+/Li and provides a possible solution to the current challenges of Li–O_2 batteries. With the Ru/MnO_2/SP cathode and the DMSO-based electrolyte containing ppm-leveled H_2O, the Li–O_2 battery presents a small discharge/charge potential gap of 0.32 V and superior cycling stability of 200 cycles ~800 h. These have not been achieved before, and are rewarded by the proposed reaction mechanism. Although the $LiFePO_4$ applied in batteries is not a practical anode of Li–O_2 batteries, the reaction mechanism at the oxygen cathode may be extended to a practical Li–O_2 battery by using a Li ion-conducting ceramic membrane to separate the electrolyte with water and the Li anode. This could also alleviate the carbon-related side reactions by converting the chemically active Li_2O_2 to LiOH, and it will make the cheap and lightweight carbon possible as cathodes in Li–O_2 batteries, which has been suggested to avoid. This investigation will enable the battery to operate in ambient air by eliminating CO_2 and advance the Li–O_2/air battery technology.

2.5 References

[1] J. Lu, L. Li, J.-B. Park, Y.-K. Sun, F. Wu, K. Amine, Aprotic and Aqueous Li-O_2 Batteries, *Chem. Rev.* **2014**, *114*, 5611.

[2] F. Li, T. Zhang, H. Zhou, Challenges of non-aqueous Li-O_2 batteries: electrolytes, catalysts, and anodes, *Energy Environ. Sci.* **2013**, *6*, 1125.

[3] Y. Shao, F. Ding, J. Xiao, J. Zhang, W. Xu, S. Park, J.-G. Zhang, Y. Wang, J. Liu, Making Li-Air Batteries Rechargeable: Material Challenges, *Adv. Funct. Mater.* **2013**, *23*, 987.

[4] Z. Peng, S. A. Freunberger, Y. Chen, P. G. Bruce, A Reversible and Higher-Rate Li-O_2 Battery, *Science* **2012**, *337*, 563.

[5] M. M. O. Thotiyl, S. A. Freunberger, Z. Peng, Y. Chen, Z. Liu, P. G. Bruce, A stable cathode for the aprotic Li-O_2 battery, *Nature Mater.* **2013**, *12*, 1049.

[6] F. Li, D.-M. Tang, Y. Chen, D. Golberg, H. Kitaura, T. Zhang, A. Yamada, H. Zhou, Ru/ITO: A Carbon-Free Cathode for Nonaqueous Li-O_2 Battery, *Nano Lett.* **2013**, *13*, 4702.

[7] F. Li, D.-M. Tang, Z. Jian, D. Liu, D. Golberg, A. Yamada, H. Zhou, Li-O_2 Battery Based on Highly Efficient Sb-Doped Tin Oxide Supported Ru Nanoparticles, *Adv. Mater.* **2014**, *26*, 4659.

[8] Y.-C. Lu, Y. Shao-Horn, Probing the Reaction Kinetics of the Charge Reactions of Nonaqueous Li-O_2 Batteries, *J. Phys. Chem. Lett.* **2013**, *4*, 93.

[9] W. Fan, Q. Zhang, W. Deng, Y. Wang, Niobic Acid Nanosheets Synthesized by a Simple Hydrothermal Method as Efficient Bronsted Acid Catalysts, *Chem. Mater.* **2013**, *25*, 3277.

[10] Y. Chen, S. A. Freunberger, Z. Peng, O. Fontaine, P. G. Bruce, Charging a Li-O_2 battery using a redox mediator, *Nature Chem.* **2013**, *5*, 489.

[11] H.-D. Lim, H. Song, J. Kim, H. Gwon, Y. Bae, K.-Y. Park, J. Hong, H. Kim, T. Kim, Y. H. Kim, X. Lepro, R. Ovalle-Robles, R. H. Baughman, K. Kang, Superior Rechargeability and Efficiency of Lithium-Oxygen Batteries: Hierarchical Air Electrode Architecture Combined with a Soluble Catalyst,

Angew. Chem. Int. Ed. **2014**, *53*, 3926.

[12] S. Meini, S. Solchenbach, M. Piana, H. A. Gasteiger, The Role of Electrolyte Solvent Stability and Electrolyte Impurities in the Electrooxidation of Li_2O_2 in Li-O_2 Batteries, *J. Electrochem. Soc.* **2014**, *161*, A1306.

[13] S. Meini, M. Piana, N. Tsiouvaras, A. Garsuch, H. A. Gasteiger, The Effect of Water on the Discharge Capacity of a Non-Catalyzed Carbon Cathode for Li-O_2 Batteries, *Electrochem. Solid-State Lett.* **2012**, *15*, A45.

[14] N. B. Aetukuri, B. D. McCloskey, J. M. Garcia, L. E. Krupp, V. Viswanathan, A. C. Luntz, Solvating additives drive solution-mediated electrochemistry and enhance toroid growth in non-aqueous Li-O_2 batteries, *Nature Chem.* **2015**, *7*, 50.

[15] K. U. Schwenke, M. Metzger, T. Restle, M. Piana, H. A. Gasteiger, The Influence of Water and Protons on Li_2O_2 Crystal Growth in Aprotic Li-O_2 Cells, *J. Electrochem. Soc.* **2015**, *162*, A573.

[16] Z. Guo, X. Dong, S. Yuan, Y. Wang, Y. Xia, Humidity effect on electrochemical performance of Li-O_2 batteries, *J. Power Sources* **2014**, *264*, 1.

[17] M. H. Cho, J. Trottier, C. Gagnon, P. Hovington, D. Clement, A. Vijh, C. S. Kim, A. Guerfi, R. Black, L. Nazar, K. Zaghib, The effects of moisture contamination in the Li-O_2 battery, *J. Power Sources* **2014**, *268*, 565.

[18] V. Aravindan, J. Gnanaraj, S. Madhavi, H.-K. Liu, Lithium-Ion Conducting Electrolyte Salts for Lithium Batteries, *Chem. Eur. J.* **2011**, *17*, 14326.

[19] R. Black, S. H. Oh, J.-H. Lee, T. Yim, B. Adams, L. F. Nazar, Screening for Superoxide Reactivity in Li-O_2 Batteries: Effect on Li_2O_2/LiOH Crystallization, *J. Am. Chem. Soc.* **2012**, *134*, 2902.

[20] B. D. McCloskey, A. Valery, A. C. Luntz, S. R. Gowda, G. M. Wallraff, J. M. Garcia, T. Mori, L. E. Krupp, Combining Accurate O_2 and Li_2O_2 Assays to Separate Discharge and Charge Stability Limitations in Nonaqueous Li-O_2 Batteries, *J. Phys. Chem. Lett.* **2013**, *4*, 2989.

[21] S. H. Oh, R. Black, E. Pomerantseva, J.-H. Lee, L. F. Nazar, Synthesis of a

metallic mesoporous pyrochlore as a catalyst for lithium-O_2 batteries, *Nature Chem.* **2012**, *4*, 1004.

[22] R. R. Mitchell, B. M. Gallant, Y. Shao-Horn, C. V. Thompson, Mechanisms of Morphological Evolution of Li_2O_2 Particles during Electrochemical Growth, *J. Phys. Chem. Lett.* **2013**, *4*, 1060.

[23] M. J. Trahan, S. Mukerjee, E. J. Plichta, M. A. Hendrickson, K. M. Abraham, Studies of Li-Air Cells Utilizing Dimethyl Sulfoxide-Based Electrolyte, *J. Electrochem. Soc.* **2013**, *160*, A259.

[24] D. Sharon, M. Afri, M. Noked, A. Garsuch, A. A. Frimer, D. Aurbach, Oxidation of Dimethyl Sulfoxide Solutions by Electrochemical Reduction of Oxygen, *J. Phys. Chem. Lett.* **2013**, *4*, 3115.

[25] F. Cheng, J. Chen, Metal-air batteries: from oxygen reduction electrochemistry to cathode catalysts, *Chem. Soc. Rev.* **2012**, *41*, 2172.

[26] A. Manthiram, L. Li, Hybrid and Aqueous Lithium-Air Batteries, *Adv. Energy Mater.* **2015**, *5*.

[27] C. O. Laoire, S. Mukerjee, K. M. Abraham, E. J. Plichta, M. A. Hendrickson, Elucidating the Mechanism of Oxygen Reduction for Lithium-Air Battery Applications, *J. Phys. Chem. C* **2009**, *113*, 20127.

[28] B. D. McCloskey, R. Scheffler, A. Speidel, G. Girishkumar, A. C. Luntz, On the Mechanism of Nonaqueous Li-O_2 Electrochemistry on C and Its Kinetic Overpotentials: Some Implications for Li-Air Batteries, *J. Phys. Chem. C* **2012**, *116*, 23897.

[29] L. Johnson, C. Li, Z. Liu, Y. Chen, S. A. Freunberger, P. C. Ashok, B. B. Praveen, K. Dholakia, J.-M. Tarascon, P. G. Bruce, The role of LiO_2 solubility in O_2 reduction in aprotic solvents and its consequences for Li-O_2 batteries, *Nature Chem.* **2014**, *6*, 1091.

[30] V. Giordani, S. A. Freunberger, P. G. Bruce, J. M. Tarascon, D. Larcher, H_2O_2 Decomposition Reaction as Selecting Tool for Catalysts in Li-O_2 Cells, *Electrochem. Solid-State Lett.* **2010**, *13*, A180.

[31] S. Meini, N. Tsiouvaras, K. U. Schwenke, M. Piana, H. Beyer, L. Lange, H. A.

Gasteiger, Rechargeability of Li-air cathodes pre-filled with discharge products using an ether-based electrolyte solution: implications for cycle-life of Li-air cells, *Phys. Chem. Chem. Phys.* **2013**, *15*, 11478.

Chapter 3. Advanced information of water function in Li-O_2 batteries with tetraglyme-based electrolyte

3.1 Introduction

Water in dimethylethane (DME) based electrolytes or moisture was recently found to enhance the discharge capacity by Aetukuri *et al.*[1] and Meini *et al.*,[2] respectively, but no cycling behavior of such batteries was reported. Guo *et al.* applied a tetraglyme (G4) based electrolyte and a carbon black cathode without a catalyst in a Li-O_2 battery under humidified O_2 atmosphere and found a mixed discharge product of LiOH and Li_2O_2,[3] but the charge potentials increased rapidly to above 4.0 V beyond the second cycle and the performance deteriorated during cycles.[3-7] Li *et al.* proposed to convert the discharge product Li_2O_2 to LiOH and subsequently achieved low charge potentials and excellent cycling performance over the combinatory catalyst of electrolytic MnO_2 (MnO_2) and Ru supported on Super P (Ru/MnO_2/SP) with the presence of limited amount of water in the dimethyl sulfoxide (DMSO) based electrolyte.[8] However, the high volatility and strong stink smell of DMSO will prevent its use in the future practical, open Li-air batteries.

In this chapter, tetraglyme (G4) with an ultralow vapour pressure of 0.009 mmHg at 25 °C[9-10] is employed as an electrolyte solvent together with limited amount of water, and Ru and MnO_2 are applied as cathode catalysts to improve the charge efficiency and cycling performance of Li-O_2 batteries, respectively. The charge overpotentials and the morphologies of discharge products were revealed to depend on the H_2O concentration in the G4 based electrolyte.

3.2 Experimental and Characterization

3.2.1 Preparation of Ru/SP, Ru/MnO_2/SP, MnO_2/SP and LiOH/Ru/SP

Ru nanoparticles supported on Super P (Ru/SP) were synthesized as following: 15 mg of Ru in $RuCl_3 \cdot xH_2O$ was added to ethylene glycol (EG) containing 170 mg of SP. After stirring overnight, NaOH in EG was slowly added to adjust the pH to 13. The suspension was heated to 160 °C for 3 hrs with flowing N_2 and then its pH was adjusted to 3 with 0.1 M HCl. The resultant suspension was filtered and washed with deionized water until the pH reached about 7. The obtained Ru/SP was dried at 80 °C in a vacuum oven for 12 hrs. For the preparation of MnO_2 and Ru nanoparticles supported on Super P (Ru/MnO_2/SP), MnO_2 ball-milled to nanometer scale and Ru/SP were firstly dispered in aqueous solution with a weight ratio of MnO_2 : Ru : SP = 7.5 : 7.5 : 85. After sonicated for 30 min and then stirred for 2 hrs, the suspension was filtered and the product Ru/MnO_2/SP was dried at 80 °C under vacuum for 12 hrs. MnO_2/SP with a weight ratio of MnO_2 : SP = 7.5 : 92.5 was prepared by a similar way. MnO_2 nanoparticles and SP were firstly sonicated in aqueous solution for 30 min and further stirred for 2 hrs. The product MnO_2/SP was obtained after filtered and dired at 80 °C in a vacuum oven for 12 hrs. For the preparation of LiOH/Ru/SP, LiOH powder was firstly ball-milled and then mixed with Ru/SP with a weight ratio of LiOH : Ru/SP = 30 : 70.

3.2.2 Preparation of electrolyte

Tetraglyme (G4) was dried over 4 Å molecular sieves. $LiClO_4$ was dried at 80 °C in a vacuum oven overnight. The dry electrolyte with 0.5 M $LiClO_4$ in G4 was stored in a glove box under Ar atmosphere. The water concentration in the dry electrolyte measured by Karl-Fischer titration is about 11 ppm. Ultrapure deionized water (18.2 MΩ-cm, Millipore) was used for preparing electrolytes with water concentrations of 78 ppm, 1700 ppm and 4600 ppm.

3.2.3 Preparation of cathode and anode

Cathodes: The electrode films composed of Ru/MnO_2/SP and PTFE with a ratio of 85 : 15wt% were prepared by rolling the paste of Ru/MnO_2/SP and PTFE solution.

Then, the electrode films were pressed onto hydrophobic carbon paper as the cathodes for Li-O_2 batteries. The mass loading of Ru/MnO_2/SP is about 0.5-1.0 mg cm^{-2}.

The Ru/SP cathodes (Ru/SP : PTFE = 85 : 15 wt%), MnO_2/SP (Ru/SP : PTFE = 85 : 15 wt%) cathodes and LiOH/Ru/SP cathodes were prepared by the similar way to Ru/MnO_2/SP cathodes.

Anodes: To avoid any contamination from reactions between a Li metal anode and H_2O, $LiFePO_4$ was employed as the anode. The potential of $LiFePO_4$ is invariant with the state of charge at ~3.45 V. The anode was prepared by rolling the paste consisting of $LiFePO_4$, Super P and PTFE (80 : 15 : 5 wt%), and then the film was pressed onto an Al mesh. The mass loading of $LiFePO_4$ is above 10 mg cm^{-2} to provide excess Li^+. All potentials are reported to against Li/Li^+.

3.2.4 Fabrication of batteries and electrochemical test

The amount of electrolytes in a coin cell was 40 μL. Glassy fiber filter paper was employed as separator. The battery assembly was conducted in a 2032 coin cell with holes on the top in an Ar filled glove box (< 0.1 ppm of H_2O and 5 ppm of O_2). The Li-O_2 battery stored in a sealed glass chamber with a volume capacity of 650 mL was purged with O_2 (99.999%) before electrochemical tests.

3.2.5 Measurements and characterization

All the electrochemical measurements were conducted at 25 °C. Galvanostatic discharge/charge was conducted on a Hokuto discharging/charging system. Cyclic voltammograms were carried out on a Solartron system. The specific capacities and currents are based on the mass of Ru/MnO_2/SP in cathodes. For *ex-situ* X-ray diffraction (XRD) and scanning electron microscopy (SEM) measurements of the discharged cathodes, discharged batteries were transferred to an argon-filled glove box and the cathodes were extracted and placed in a glass vial. The cathodes were rinsed with DME to wash off the electrolyte salt and then dried in a vacuum chamber for 5 min. The dried cathodes were placed in a home-built X-ray cell sealed with a

kapton® polyimide film. XRD measurements were performed on a Bruker D8 Advanced diffractometer with Cu Kα (λ = 1.5406 Å) radiation with a scan rate of 0.016 °/s. SEM was performed on Hitachi S8000. The dried cathodes were taken to the SEM sample loading chamber in a sealed glass bottle. The time from opening the glass bottle to finishing sample loading into the SEM machine was < 10 seconds.

3.3 Results and Discussion

3.3.1 Discharge and charge ability of Li-O_2 battery with electrolyte containing varied H_2O contents

The Li-O_2 batteries were assembled with $LiFePO_4$ in replacement of Li anodes to avoid reactions of Li metal and H_2O.[8, 11] All the discharge/charge potentials have been converted to against Li/Li^+. Fig. 3.1a shows the first discharge and charge profiles of Li-O_2 batteries with the Ru/MnO_2/SP cathode and G4 based electrolytes containing varied concentrations of H_2O. The Li-O_2 batteries were operated with a limited specific capacity of 1000 mAh g^{-1} and a cut-off voltage window from 2.3 V to 4.15 V. In the dry electrolyte (~11 ppm), the charge potential is around 4.0 V. When H_2O is added into the electrolyte, the charge overpotentials are obviously reduced and dependent on its concentrations. As the H_2O concentration is increased to 4600 ppm, it typically presents a charge plateau at as low as 3.2 V, equal to an overpotential of 0.24 V. It is much lower than 4.0 V of the Li-O_2 battery with the dry electrolyte. This suggests an important role of H_2O in electrolytes in charge overpotential reduction for Li-O_2 batteries. The difference in H_2O concentrations inducing low charge potentials in the DMSO[8] and G4 based electrolytes could be related to the viscosity, solvating ability and diffusion coefficient.[12]

Cyclic voltammogram (CV) was also conducted on the Li-O_2 batteries with the dry electrolyte and the electrolyte containing 4600 ppm of H_2O, as shown in Fig. 3.1b.

With the dry electrolyte, the Li-O_2 battery shows one cathodic peak E_{pc} at around 2.5 V, corresponding to reduction of O_2 to Li_2O_2. In the anodic scan, a weak peak at around 3.8 V is ascribed to oxidation of Li_2O_2. Comparatively, the Li-O_2 battery with 4600 ppm of H_2O in the electrolyte presents two cathodic peaks E_{pc1} and E_{pc2} at around 2.7 and 2.6 V, respectively. The peak E_{pc1} representing reduction of O_2 to LiO_2 is induced by the prolonged life time of LiO_2 in the presence of H_2O with high acceptor number (AN).[1] The other E_{pc2} is due to the sequential reduction of LiO_2 to Li_2O_2.[13-14] In the anodic scan, the chemical reaction between Li_2O_2 and H_2O enables a significant oxidation peak at around 3.3 V, which is in sharp contrast to that with the dry electrolyte. They are consistent with the discharge and charge plateaus in Fig. 3.1a.

3.3.2 Product analysis of discharged and charged cathodes by XRD and SEM

The discharged and charged Ru/MnO_2/SP cathodes in both of the dry and H_2O containing electrolytes were characterized by *ex-situ* X-ray diffraction (XRD). As shown in Fig. 3.2a, in the dry electrolyte, the discharge products on the Ru/MnO_2/SP

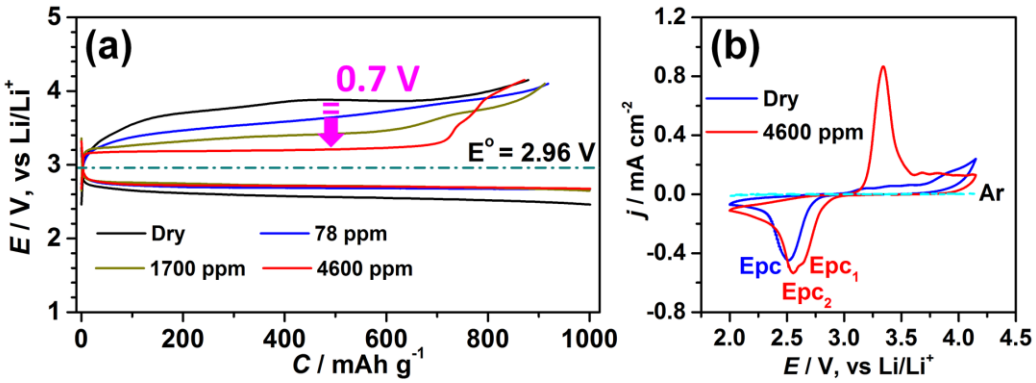

Fig. 3.1. (a) First discharge and charge profiles of Li-O_2 batteries with the Ru/MnO_2/SP cathode and electrolytes containing different concentrations of H_2O at 500 mA g^{-1}. (b) Cyclic voltammograms of Li-O_2 batteries with the dry electrolyte and electrolyte containing 4600 ppm of H_2O, respectively. Scan rate: 0.05 mV s^{-1}.

cathode are typically a mixture of Li_2O_2 and LiOH. While, in the electrolyte containing 4600 ppm of H_2O, only LiOH can be detected. This suggests that MnO_2 in cathodes greatly promotes the formation of LiOH from the equilibrium reaction $Li_2O_2(s) + H_2O(l) \leftrightarrow LiOH(s) + H_2O_2(l)$ by catalyzing H_2O_2 disproportionation. On the SP and Ru/SP cathodes of Li-O_2 batteries with dry electrolytes, the discharge product can be identified as Li_2O_2, consistent with the previous reports.[15] After charge, the discharge products, either Li_2O_2 or LiOH, on the SP, Ru/SP and Ru/MnO_2/SP cathodes were all reversibly decomposed, as evidenced by disappearance of their characteristic diffraction peaks in Fig. 3.2b. These show that the charge plateau at 3.2 V in Fig. 3.1a and the significant oxidation current in Fig. 3.1b are induced by oxidation of LiOH on the Ru/MnO_2/SP cathode.

For a reference, the Li-O_2 batteries with MnO_2/SP as the cathodes and the water containing electrolyte were discharged and charged at 250 mA g^{-1} and showed charge potentials higher than 4.2 V in Fig. 3.3a. With the Ru/SP cathode and the same electrolyte the Li-O_2 battery presents low charge potentials of 3.2 V (Fig. 3.3b), similar to those in Fig. 3.1a, indicating that only Ru has good catalytic activity toward

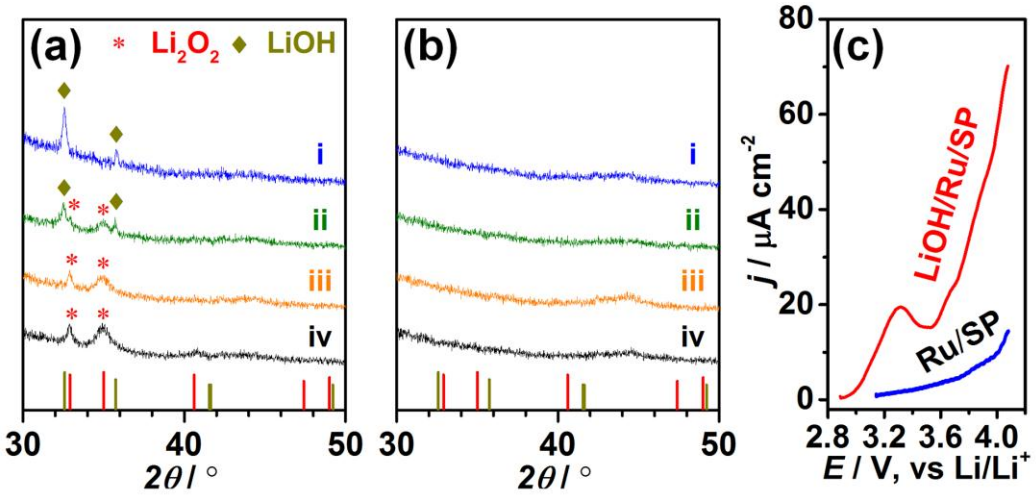

Fig. 3.2 *Ex-situ* XRD patterns of the cathodes after the first (a) discharge and (b) charge of the Li-O_2 batteries in the electrolyte with (i) 4600 ppm of H_2O on Ru/MnO_2/SP and in the dry electrolyte on (ii) Ru/MnO_2/SP, (iii) Ru/SP and (iv) SP cathodes. (c) Linear sweep voltammetry curves of LiOH/Ru/SP and Ru/SP, respectively. Scan rate: 0.05 mV s^{-1}.

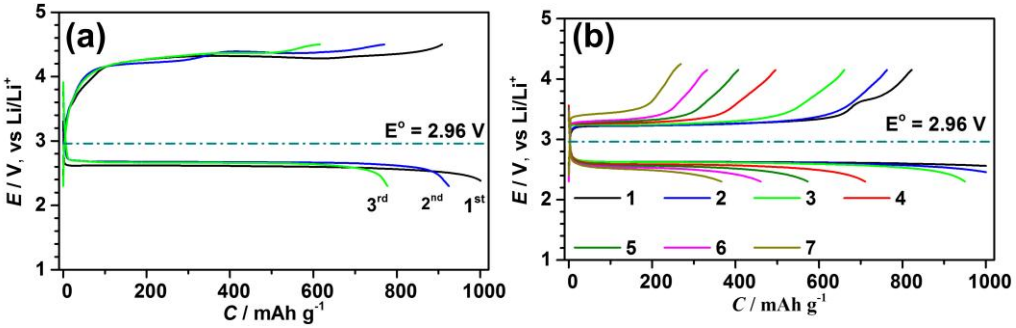

Fig. 3.3 The discharge-charge profiles of the Li-O_2 batteries with (a) MnO_2/SP and (b) Ru/SP cathodes and the electrolyte with 4600 ppm of H_2O.

LiOH oxidation in the combination of Ru, MnO_2, and SP. In order to verify oxidation of LiOH on Ru nanoparticles, commercially available LiOH after ball-milling was thoroughly mixed with Ru/SP and the resultant composite was assembled as the cathodes of Li-O_2 batteries. The Ru/SP cathodes with and without LiOH were subjected to linear sweep voltammetry (LSV). As shown in Fig. 3.2c, at around 3.3 V the oxidation peak can be assigned to oxidation of LiOH, which is consistent with the oxidation peak in Fig. 3.1b.

The discharge products on the Ru/MnO_2/SP cathodes were directly observed by scanning electron microscope (SEM). Fig. 3.4a shows the discharge products of Li_2O_2 and LiOH with a typically toroidal morphology in the dry electrolyte, and the particle size is around 300 nm. With the H_2O concentration increased to 78 ppm, the toroidal particles were evolved into larger particles with layering in Fig. 3.4b. The layered structures of the discharge product become more obvious in Fig. 3.4c and eventually develop into large sheets of LiOH in Fig. 3.4d, when the concentration of H_2O was increased to 1700 and 4600 ppm, respectively.[5] The morphology evolution process of the discharge products with various concentrations of H_2O in electrolytes is schematically illustrated in Fig. 3.4e. The small amount of H_2O in electrolytes can be completely converted to LiOH from Li_2O_2 with the promotion of MnO_2 in the cathode.[4, 8] The dissolution-deposition of LiOH at cathodes in electrolytes containing

varied concentrations of H_2O as shown in Fig. 3.4 governs the morphology evolution of the discharge products. After charge, all the discharge products were decomposed and disappeared, as shown in Fig. 3.5. This reversible behavior of formation and decomposition of discharge products LiOH and Li_2O_2 is consistent with the XRD patterns in Fig. 3.2b.

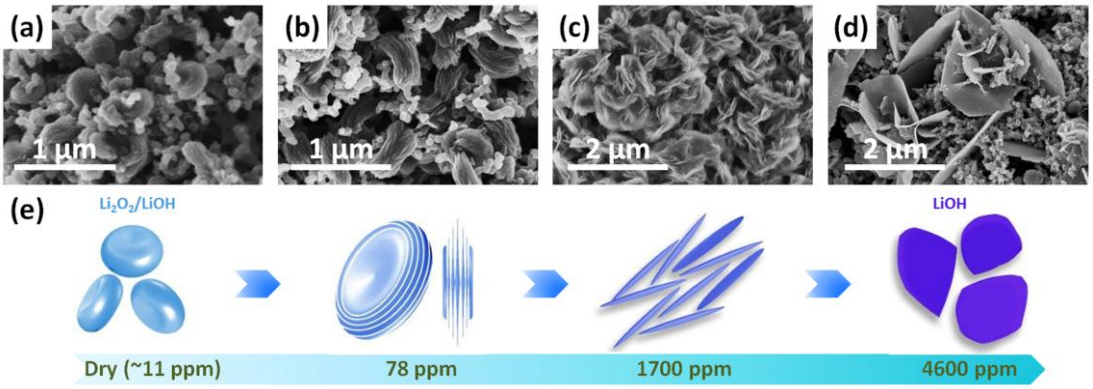

Fig. 3.4 SEM images of the Ru/MnO_2/SP cathodes after the first discharge of the Li-O_2 batteries with varied concentrations of H_2O: (a) dry electrolyte, (b) 78 ppm, (c) 1700 ppm and (d) 4600 ppm. (e) Morphology evolution of the discharge products in different H_2O containing electrolytes.

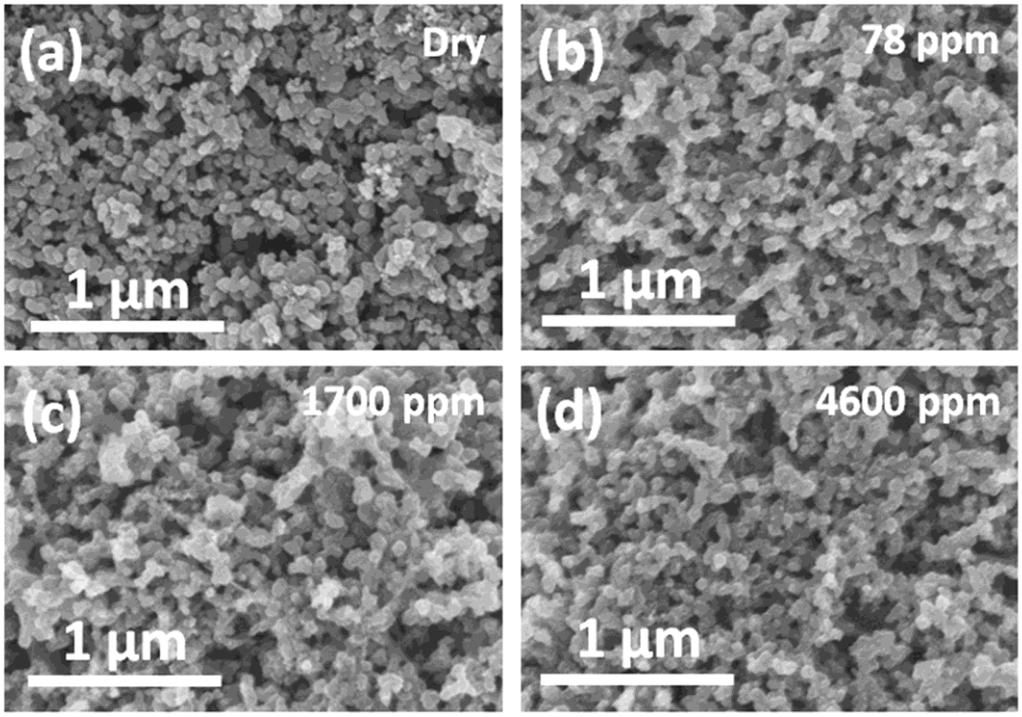

Fig. 3.5 SEM images of the Ru/MnO_2/SP cathode after charge in (a) dry electrolyte and in the electrolyte with H_2O of (b) 78 ppm, (c) 1700 ppm and (d) 4600 ppm.

3.3.3 Electrochemical performance

The rate capability of Li-O_2 batteries with the electrolyte containing 4600 ppm of H_2O was examined at varied current densities from 250 to 500, 1000 and 2000 mA g^{-1}, as shown in Fig. 3.6a. The overpotentials at 250 mA g^{-1} in the discharging and charging processes are 0.19 and 0.17 V, respectively. Even at a current density as high as 2000 mA g^{-1}, the Li-O_2 battery exhibits good discharge/charge performance, showing overpotentials of 0.38 and 0.36 V in the discharging and charging processes, respectively, as indicated in Fig. 3.6a. The high rate performance may be related to the kinetics of H_2O involved reactions at the Ru/MnO_2/SP cathode.

The cycling performance of the Li-O_2 battery was further investigated by discharging and charging at 1000 mA g^{-1} for 50 cycles, and the selected cycles are shown in Fig. 3.6b. The discharge and charge profiles of the Li-O_2 battery are almost stable during cycles except a slight charge potential increase beyond 30 cycles.

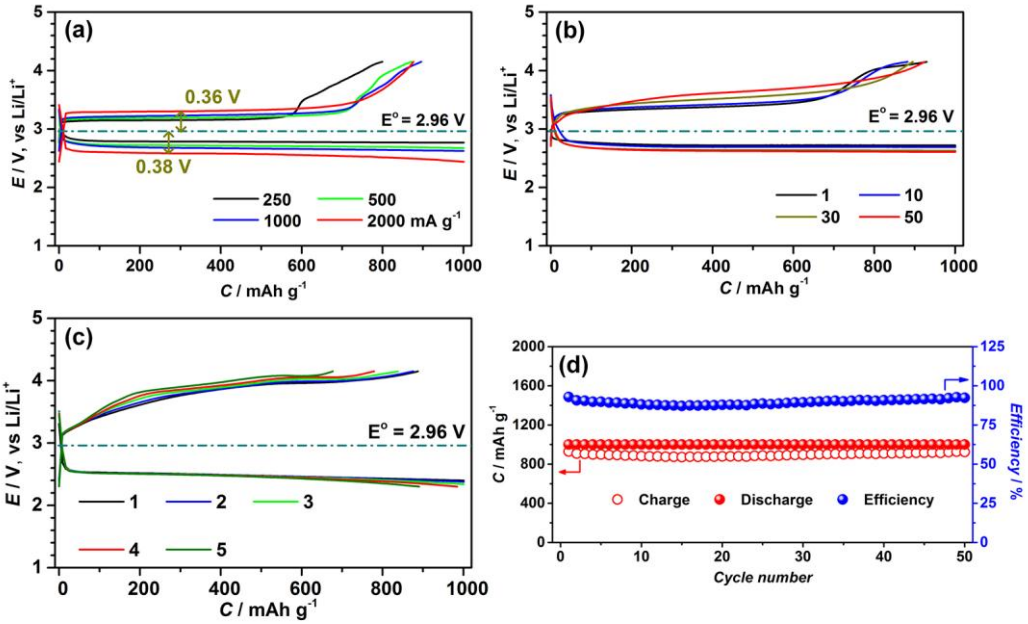

Fig. 3.6 (a) Rate capability and (b) discharge-charge profiles of the selected cycles in Li-O_2 batteries in the electrolyte containing 4600 ppm of H_2O at 1000 mA g^{-1}. (c) The discharge-charge profiles of Li-O_2 battery with the Ru/MnO_2/SP cathode and the dry electrolyte at 1000 mA g^{-1}. (d) Plot of discharge/charge capacities and the corresponding coulombic efficiencies against cycle number in the electrolyte containing 4600 ppm of H_2O at 1000 mA g^{-1}.

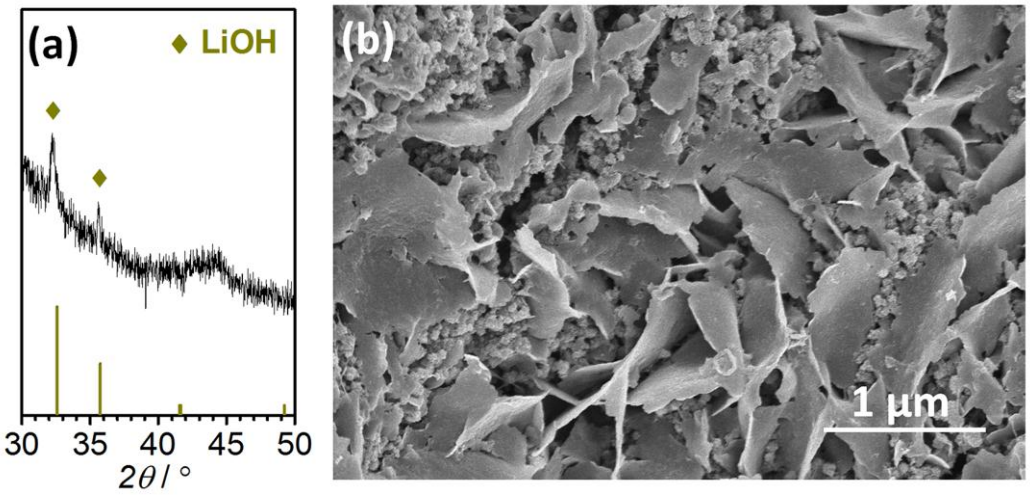

Fig. 3.7 (a) *Ex-situ* XRD pattern and (b) SEM image of the discharge products after 50 cycles in the Li-O_2 batteries with the Ru/MnO_2/SP cathode and the electrolyte containing 4600 ppm of H_2O.

The discharge and charge capacities change a little without decay during the 50 cycles, and the corresponding coulombic efficiency in each cycle is approaching 96% in Fig. 3.6d. After 50 cycles, the discharge product remains LiOH and it appears as sheets at the cathode in Fig. 3.7, consistent with Figs. 3.2a and 3.4d. The Li-O_2 battery with the dry electrolyte shows high charge potentials and poor cycling stability in Fig. 3.6c, which is contrasting to that with H_2O in electrolytes. The outstanding cycling performance with H_2O in electrolytes is benefited by the H_2O involved reactions at the Ru/MnO_2/SP cathode.

3.3.5 Proposed discharging and charging details

In conventional Li-O_2 batteries, O_2 accepts electrons and reacts with Li^+ to produce Li_2O_2 via multiple electrochemical and/or chemical reaction steps (Eq.(1-3)) as shown in Scheme 3.1. The intrinsic chemical and physical nature of Li_2O_2 leads to the high charge potentials of 4.0 V, as presented in dry electrolytes in Fig. 3.6c. For the reduced charge potentials as demonstrated, a mechanism for formation of LiOH and its following decomposition in discharging and charging processes is proposed,

respectively. In electrolytes with H_2O, the discharge product Li_2O_2 reacts with H_2O to form LiOH and H_2O_2 via an equilibrium Eq.(4) in Route 1 in Scheme 3.1.[1, 4-5, 8] Another possible mechanism for formation of LiOH is presented as Eq.(5-8) of Route 2 in Scheme 3.1: $O_2^{\bullet-}$ from O_2 reduction is followed by chemical protonation to produce perhydroxyl radicals ($HO_2^{\bullet}$) and LiOH;[5] and $HO_2^{\bullet}$ is immediately reduced and combines with Li^+ to generate LiOH and H_2O_2.[14, 16-18] In the discharging process via either Route 1 or Route 2, MnO_2 in the Ru/MnO_2/SP cathode greatly promotes LiOH formation by catalyzing H_2O_2 disproportionation via Eq.(9) in Scheme 3.1,[4, 8] as revealed by XRD in Fig. 3.2a. Simultaneously, MnO_2 ensures H_2O regeneration in cycles and improves cycling stability. For example, the accumulation of H_2O_2 during cycles makes the battery with Ru/SP without MnO_2 decay in Fig. 3.3b. In the following charging process, the discharge product LiOH can be decomposed at low potentials over Ru nanoparticles via Eq.(10) in Scheme 3.1.

Scheme 3.1 Proposed mechanism for the discharging and charging processes of the Li-O_2 battery with the Ru/MnO_2/SP cathode in the presence of H_2O in the electrolyte.

Discharging processes

Route 1

$$Li^+ + O_2 + e^- \rightarrow LiO_2 \qquad (E^0 = 3.0 \text{ V vs. } Li/Li^+) \qquad (1)$$

$$LiO_2 + Li^+ + e^- \rightarrow Li_2O_2 \qquad (E^0 = 2.96 \text{ V vs. } Li/Li^+) \qquad (2)$$

$$2LiO_2 \rightarrow Li_2O_2 + O_2 \qquad (3)$$

$$Li_2O_2 + 2H_2O \leftrightarrow 2LiOH + H_2O_2 \qquad (4)$$

Route 2

$$O_2 + e^- \rightarrow O_2^{\bullet-} \qquad (E^0 = 3.0 \text{ V vs. } Li/Li^+) \qquad (5)$$

$$O_2^{\bullet-} + H_2O + Li^+ \rightarrow HO_2^{\bullet} + LiOH \qquad (6)$$

$$HO_2^{\bullet} + O_2^{\bullet-} \rightarrow HO_2^- + O_2 \quad (7)$$

$$HO_2^- + H_2O + Li^+ \rightarrow H_2O_2 + LiOH \quad (8)$$

$$H_2O_2 \xrightarrow{MnO_2} H_2O + 1/2O_2 \quad (9)$$

Charging processes

$$2LiOH \rightarrow 2Li^+ + 1/2O_2 + H_2O + 2e^- \quad (E^0 = 3.32 \text{ V vs. } Li/Li^+) \quad (10)$$

3.4 Conclusions

We have constructed a Li-O_2 battery composed of Ru/MnO_2/SP cathodes and H_2O containing G4 based electrolytes. The Li-O_2 batteries demonstrated low charge potentials of 3.20 V, equal to overpotentials of 0.24 V, and good cycling stability. The discharge products and morphologies are strongly dependent on the concentrations of H_2O in electrolytes. In the Ru/MnO_2/SP cathode, MnO_2 facilitates formation of LiOH in the discharging processes and favors cycling stability, and Ru efficiently catalyzes its decomposition at low charge potentials. This may be able to circumvent carbon related side reactions by converting the chemically active Li_2O_2 to LiOH. The results will encourage more studies on Li-O_2 batteries with H_2O containing electrolytes and provide hints on the design and construction of rechargeable Li-O_2 batteries. To protect Li anodes from H_2O containing electrolytes by developing Li^+ conducting membranes will be essential for practical Li-O_2/air batteries.

3.5 Reference

[1] N. B. Aetukuri, B. D. McCloskey, J. M. Garcia, L. E. Krupp, V. Viswanathan, A. C. Luntz, Solvating additives drive solution-mediated electrochemistry and enhance toroid growth in non-aqueous Li-O_2 batteries, *Nature Chem.* **2015**, *7*, 50.

[2] S. Meini, M. Piana, N. Tsiouvaras, A. Garsuch, H. A. Gasteiger, The Effect of Water on the Discharge Capacity of a Non-Catalyzed Carbon Cathode for Li-O_2 Batteries, *Electrochem. Solid-State Lett.* **2012**, *15*, A45.

[3] Z. Guo, X. Dong, S. Yuan, Y. Wang, Y. Xia, Humidity effect on electrochemical performance of Li-O_2 batteries, *J. Power Sources* **2014**, *264*, 1.

[4] H. Geaney, C. O'Dwyer, Electrochemical investigation of the role of MnO_2 nanorod catalysts in water containing and anhydrous electrolytes for Li-O_2 battery applications, *Phys. Chem. Chem. Phys.* **2015**, *17*, 6748.

[5] K. U. Schwenke, M. Metzger, T. Restle, M. Piana, H. A. Gasteiger, The Influence of Water and Protons on Li_2O_2 Crystal Growth in Aprotic Li-O_2 Cells, *J. Electrochem. Soc.* **2015**, *162*, A573.

[6] K. U. Schwenke, S. Meini, X. Wu, H. A. Gasteiger, M. Piana, Stability of superoxide radicals in glyme solvents for non-aqueous Li-O_2 battery electrolytes, *Phys. Chem. Chem. Phys.* **2013**, *15*, 11830.

[7] S. Meini, S. Solchenbach, M. Piana, H. A. Gasteiger, The Role of Electrolyte Solvent Stability and Electrolyte Impurities in the Electrooxidation of Li_2O_2 in Li-O_2 Batteries, *J. Electrochem. Soc.* **2014**, *161*, A1306.

[8] F. J. Li, S. C. Wu, D. Li, T. Zhang, P. He, A. Yamada, H. S. Zhou, The water catalysis at oxygen cathodes of lithium-oxygen cells, *Nat. Commun.* **2015**, *6*, 7843.

[9] W. Xu, J. Xiao, J. Zhang, D. Wang, J.-G. Zhang, Optimization of Nonaqueous Electrolytes for Primary Lithium/Air Batteries Operated in Ambient Environment, *J. Electrochem. Soc.* **2009**, *156*, A773.

[10] S. A. Freunberger, Y. Chen, N. E. Drewett, L. J. Hardwick, F. Barde, P. G. Bruce, The Lithium-Oxygen Battery with Ether-Based Electrolytes, *Angew. Chem. Int. Ed.* **2011**, *50*, 8609.

[11] M. M. O. Thotiyl, S. A. Freunberger, Z. Peng, Y. Chen, Z. Liu, P. G. Bruce, A stable cathode for the aprotic Li-O_2 battery, *Nature Mater.* **2013**, *12*, 1049.

[12] C. O. Laoire, S. Mukerjee, K. M. Abraham, E. J. Plichta, M. A. Hendrickson, Influence of Nonaqueous Solvents on the Electrochemistry of Oxygen in the Rechargeable Lithium-Air Battery, *J. Phys. Chem. C* **2010**, *114*, 9178.

[13] C. J. Allen, J. Hwang, R. Kautz, S. Mukerjee, E. J. Plichta, M. A. Hendrickson, K. M. Abraham, Oxygen Reduction Reactions in Ionic Liquids and the Formulation of a General ORR Mechanism for Li-Air Batteries, *J. Phys. Chem. C* **2012**, *116*, 20755.

[14] C. Pozo-Gonzalo, A. A. J. Torriero, M. Forsyth, D. R. MacFarlane, P. C. Howlett, Redox Chemistry of the Superoxide Ion in a Phosphonium-Based Ionic Liquid in the Presence of Water, *J. Phys. Chem. Lett.* **2013**, *4*, 1834.

[15] F. Li, Y. Chen, D.-M. Tang, Z. Jian, C. Liu, D. Golberg, A. Yamada, H. Zhou, Performance-improved Li-O_2 battery with Ru nanoparticles supported on binder-free multi-walled carbon nanotube paper as cathode, *Energy Environ. Sci.* **2014**, *7*, 1648.

[16] M. Kar, T. J. Simons, M. Forsyth, D. R. MacFarlane, Ionic liquid electrolytes as a platform for rechargeable metal-air batteries: a perspective, *Phys. Chem. Chem. Phys.* **2014**, *16*, 18658.

[17] S. H. Lee, R. A. DeMayo, K. J. Takeuchi, E. S. Takeuchi, A. C. Marschilok, Progress toward Metal-Air Batteries: Mechanistic Investigation of the Effect of Water on the Oxygen Reduction Reaction at Carbon-Conductive Polymer-Silver Composite Air Electrodes, *J. Electrochem. Soc.* **2015**, *162*, A69.

[18] C. Pozo-Gonzalo, C. Virgilio, Y. Yan, P. C. Howlett, N. Byrne, D. R. MacFarlane, M. Forsyth, Enhanced performance of phosphonium based ionic liquids towards 4 electrons oxygen reduction reaction upon addition of a weak

proton source, *Electrochem. Commun.* **2014**, *38*, 24.

Chapter 4. Realizing high-performance Li-O_2 batteries in humid atmosphere by integrating a hydrophobic ionic liquid-based electrolyte

4.1 Introduction

For Li-air battery operated in ambient air, the thermodynamic instability of the ideal discharge products Li_2O_2 can initiate undesired reactions with the air components, especially moisture. The byproducts could further result in poor rechargeability. However, most of the present researches are conducted in pure O_2 atmosphere. Only limited publications have attempted to develop Li-O_2 battery in humidified atmosphere,[1-2] which is an inevitable step for the realization of practical Li-air battery. In a relative humidity (RH) of 15%, Guo *et al.* found the discharge capacity of the Li-O_2 battery with tetraglyme (G4) based electrolyte was enhanced by nearly two times compared to in dry O_2 atmosphere.[1] Similarly, Meini *et al.* reported a more than 5-fold increase of discharge capacity in a water vaporied Li-O_2 battery.[2] There are also works involving trace amount of H_2O in electrolytes.[3-6] However, in the cases where carbon black without an effective catalyst was applied as cathodes, the charge potential could be above 4.2 V,[1] resulting in electrolyte decomposition and deteriorated cycling performance (< 20 cycles). Therefore, moisture was considered to not benefit cycling stability and suggested to exclude from Li-O_2 battery.

Recently, by converting the discharge product to lithium hydroxide compound via reactions between Li_2O_2 and trace amount water in the DMSO and DME based electrolyte, Li *et al.* and Liu *et al.*, respectively, reported low charge potentials of ~3.2 V and 3.1 V together with good cycling stability.[7-8] The superior performance is realized through either constructing a composite cathode of electrolytic manganese dioxide and ruthenium supported on Super P or adding redox mediator LiI into electrolyte. However, DMSO and DME have high volatility, inferior to long time operation, which preclude their future usage in the practical, open Li-air battery.[9]

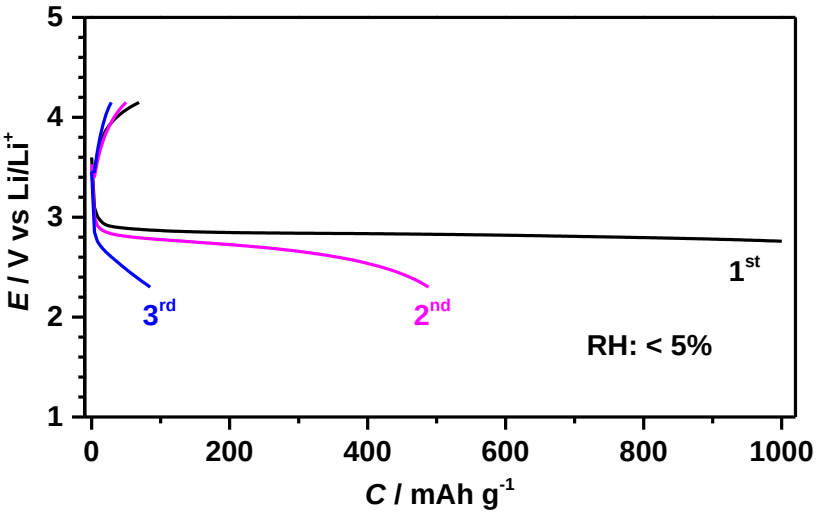

Fig. 4.1. The initial 3 cycles of discharge-charge profiles of the G4 based Li-O_2 battery at RH of < 5% at 500mA g^{-1}.

Alternatively, G4 having low vapor pressure and little volatility was attempted in Li-O_2 battery with H_2O containing electrolyte. This battery showed charge potential of ~3.2 V, but the cycling stability was poorer.[10] Additionally, the maximum H_2O concentration in the above mentioned electrolytes is limited to 4600 ppm for G4 based electrolyte. It is unknown whether these systems can sustain in humidified atmosphere at high RHs similar to that in air. In Fig. 4.1, at RH of < 5%, the G4 based Li-O_2 battery indicates bad rechargeability under 4.15 V, confirming G4 is not suitable for Li-air battery in humidified atmosphere. Therefore, the suitable electrolyte should be non-volatile and stable at the cathode in humidified atmosphere during discharge/charge.

Room temperature ionic liquids (ILs) show several merits, like good ionic conductivity, wide electrochemical windows, extremely low vapor pressure and nonflammability, to make them significantly attractive in the fields of lithium-ion battery, fuel cell, capacitor *etc*. ILs have also been considered as a potential electrolyte solvent for the non-aqueous Li-O_2/air batteries and showed charge potentials at ~4.0 V.[11-18] In this chapter, the hydrophobic IL (1-methyl-3-propylimidazolium bis (trifluoromethylsulfonyl)imide) dissolving LiTFSI (lithium bis

(trifluoromethanesulfonyl)imide) is employed as electrolyte and a composite of electrolytic manganese dioxide (MnO_2, 7.5 wt%) and RuO_2 (7.5 wt%) nanoparticles supported on Super P (RuO_2/MnO_2/SP) is used as the cathode to construct a synergistic system at cathode in humidified O_2 atmosphere for Li-O_2 battery. RuO_2 is found to be an effective catalyst for the electrochemical decomposition of lithium hydroxide compounds at low charge potential and is more moderate than noble metals and benefits electrolyte stability.[19-26] The MnO_2 and RuO_2 in the cathode function to improve the rechargeability and reduce the charge potentials, respectively. The novel system realizes low charge potential (3.34 V) and excellent cycling stability (218 cycles) at a RH of 51%. Also, a feasible design for a Li-O_2 battery in humidified atmosphere is proposed.

4.2 Experimental and Characterization

4.2.1 Preparation of RuO_2/MnO_2/SP

Super P (SP, 170 mg) was added into H_2O (200 mL) and the suspension was ultrasonicated for 30 min. After stirring for 2 hrs, Ru (11.4 mg) in $RuCl_3 \cdot xH_2O$ was added. The suspension was stirred overnight. Then, $NaHCO_3$ solution (0.1 M) was slowly added to adjust the pH to 10. After the suspension was continuously stirred for another 3 hrs, the resultant suspension was filtered and washed with deionized water until the pH reached about 7. The obtained sample was dried at 80 ^oC in a vacuum oven for 12 hrs and then calcined in air at 150 ^oC for 1hrs and 180 ^oC for 3 hrs to obtain RuO_2/SP. For the preparation of MnO_2 and RuO_2 nanoparticles supported on Super P (RuO_2/MnO_2/SP), MnO_2 ball-milled to nanometer scale and RuO_2/SP were firstly dispersed in an aqueous solution with a weight ratio of (MnO_2:RuO_2:SP=7.5:7.5:85). After sonicated for 30 min and then stirred for 2 hrs, the suspension was filtered and the product RuO_2/MnO_2/SP was dried at 80 ^oC under vacuum for 12 hrs.

4.2.2 Preparation of electrolyte

IL was used as received. Tetraglyme (G4) was dried over 4 Å molecular sieves. LiTFSI was dried at 80 ^{o}C in a vacuum oven overnight. The electrolytes with 0.5 M LiTFSI in IL and G4 were stored in a glove box under Ar atmosphere. The water concentrations in the IL based and G4 based electrolytes measured by Karl-Fischer titration are about 823 ppm and 11 ppm, respectively.

4.2.3 Preparation of cathode and anode

Cathodes: The electrode films composed of RuO_2/MnO_2/SP and PTFE with a ratio of 85:15 wt% were prepared by rolling the paste of RuO_2/MnO_2/SP sample and PTFE solution. After, the electrode films were pressed onto hydrophobic carbon paper as the cathodes for Li-O_2 batteries. The mass loading of RuO_2/MnO_2/SP is ~0.5 mg cm^{-2}.

Anodes: To avoid any contamination from reactions between a Li metal anode and H_2O, $LiFePO_4$ was employed as the anode material except as described. The anode was prepared by rolling the paste consisted of $LiFePO_4$, Super P and PTFE (80:15:5 wt%) and then pressed onto an Al mesh. The mass loading of $LiFePO_4$ is above 10 mg cm^{-2} to provide excessive Li^+. All potentials are reported to against Li/Li^+.

4.2.4 Fabrication of batteries and electrochemical test

The amount of electrolytes in a coin cell was 30 μL. Glassy fiber filter paper was employed as separator. The battery assembly was conducted in a 2032 coin cell with holes on the top in an Ar filled glove box (<0.1 ppm of H_2O and 1 ppm of O_2). The battery with Li metal as anode was assembled by using a LISICON membrane to separate anode from water contamination as described in previous work.[27] The Li-O_2 battery stored in a sealed glass chamber with a volume capacity of 650 mL was purged with O_2 (99.999%) before electrochemical tests. The different humidified atmospheres were controlled by adding proper amount of H_2O into the sealed glass chamber and measured by a thermo-hygrometer.

4.2.5 Measurements and characterization

All the electrochemical measurements were conducted at a constant room temperature. Galvanostatic discharge/charge was conducted on a Hokuto discharging/charging system. The specific capacities and currents are based on the mass of RuO_2/MnO_2/SP in cathodes. For *ex-situ* X-ray diffraction (XRD) measurements and scanning electron microscopy (SEM) measurements of the discharged cathodes, discharged batteries were transferred to an argon glove box and the cathodes were extracted and placed in a glass vial. The cathodes were rinsed with dimethylethane (DME) to wash off the electrolyte salt and then dried in a vacuum chamber connected to the glove box for 5 min. The dried cathodes were placed in a customer-built X-ray cell sealed with a kapton polyimide film. XRD measurements were performed on a Bruker D8 Advanced diffractometer with Cu Kα (λ = 1.5406 Å) radiation with a scan rate of 0.016 °/s. SEM was performed on Hitachi S8000. The dried cathodes were taken to the SEM sample loading chamber in a sealed glass bottle with a piece of lithium metal. The time from opening the glass bottle to finishing sample loading into the SEM machine was <10 seconds. In order to study the H_2O content in the electrolytes, 0.5 mL of electrolytes in dried glass bottles (1 mL) were putted into sealed battery chambers (650 mL) in the humidified atmosphere at RH of 51%. After rest for 1, 2, 4 and 7 days, the bottles were taken out in an Ar glove box and the H_2O content was measured by the Karl-Fischer titration.

4.3 Results and Discussion

4.3.1 Discharge and Charge Ability at Varied RHs

In order to avoid reactions between Li metal and moisture and to specifically explore the feasibility of the composite cathode and IL based electrolyte in humidified atmosphere, $LiFePO_4$ electrode is applied as the counter anode to construct the Li-O_2

battery.[8b,c] The discharge-charge profiles of IL based Li-O_2 batteries in O_2 atmospheres with varied RHs are shown in Fig 4.2. The Li-O_2 batteries are operated with a limited specific capacity of 1000 mAh g^{-1} and a cut-off voltage window from 2.3 V to 4.05 V. In the dry O_2 atmosphere, the discharge plateau is at ~2.68 V and in the charging process, the potential increases rapidly and reaches the cutoff of 4.05 V. The resultant potential gap is as high as 1.32 V. At the RHs of 21% and 51%, both of the discharge and charge overpotentials are reduced. In particular, at the RH of 51%, the discharge and charge plateaus are at ~2.94 V and 3.34 V, respectively. This results in a potential gap between discharge and charge as low as 0.4 V, indicating significantly promoted oxygen reduction reaction (ORR) and oxygen evolution reaction (OER) performance. Notably, the discharge plateau (2.94 V) is close to the equilibrium potential of Li_2O_2 (2.96 V). It may suggest a different ORR mechanism and will be discussed later. When the RH is 74%, the discharge plateau changes little, but the charge plateau increases, implying negative effect of excessive moisture in the O_2 atmosphere. These results indicate that the combination of the composite cathode and IL based electrolyte enables the Li-O_2 battery to operate at low overpotentials at the RH of 51%.

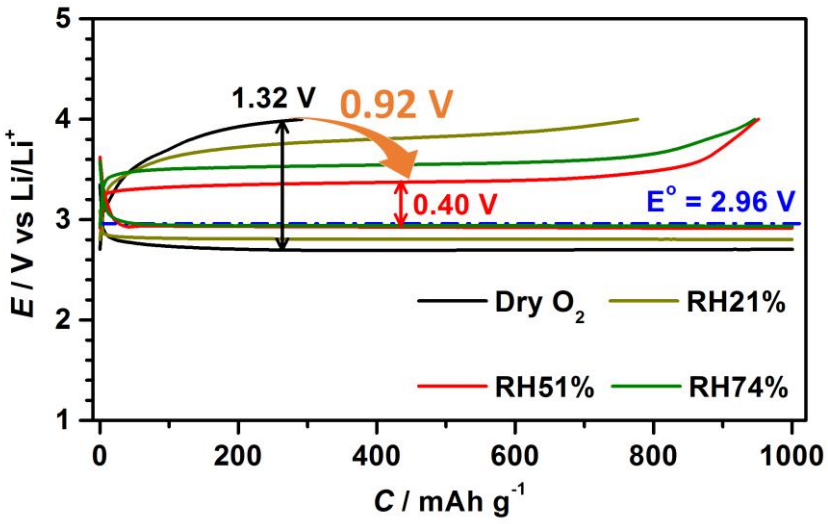

Fig. 4.2. Discharge-charge profiles of IL based Li-O_2 batteries in O_2 atmospheres with varied RHs at 500 mA g^{-1}.

4.3.2 Products Analysis after Discharge and Charge

The discharge/charge products at cathodes of the IL based Li-O_2 batteries at varied RHs were characterized by *ex-situ* X-ray diffraction (XRD) and the results are shown in Fig. 4.3. Due to the small sizes and low contents of MnO_2 and RuO_2, their diffraction peaks cannot be found at cathodes. As shown in Fig. 4.3a, in the dry O_2 atmosphere, the discharge products are a mixture of Li_2O_2 and LiOH. The formation of LiOH is resulted from the reaction between Li_2O_2 and H_2O in the electrolyte (~823 ppm H_2O). The mixture products result in high charge potentials in the following charging process. At the RH of 21%, the discharge products are identified as LiOH and the charge potential is ~3.8 V in Fig. 4.2. When the RHs are 51% and 74%, both of the discharge products are lithium hydroxide hydrate ($LiOH·H_2O$), but the charge potential is reduced to ~3.34 V at 51% and increased to 3.55 V at 74%. This is supposed to result from the solid $LiOH·H_2O$ dissolving in the excessive H_2O, evidenced by the decreased diffraction intensity of $LiOH·H_2O$ at the RH of 74% in Fig. 4.3a.[28] After fully charged, the diffraction peaks corresponding to Li_2O_2, LiOH or $LiOH·H_2O$ in the XRD patterns of Fig. 4.3b reversibly disappear, indicating oxidation decomposition of these products on the RuO_2/MnO_2/SP cathode.

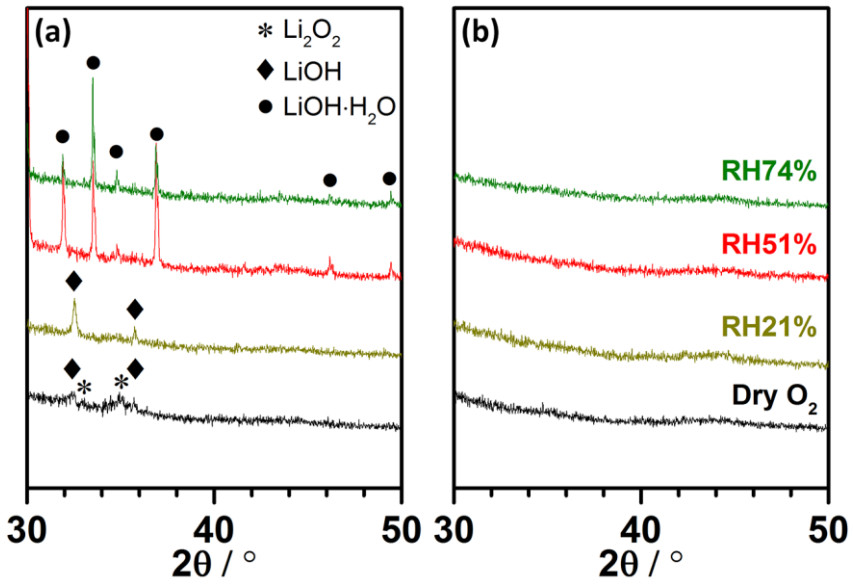

Fig. 4.3. *Ex-situ* XRD patterns of the cathodes after (a) discharge and (b) charge of IL based Li-O_2 batteries in various humidified atmospheres.

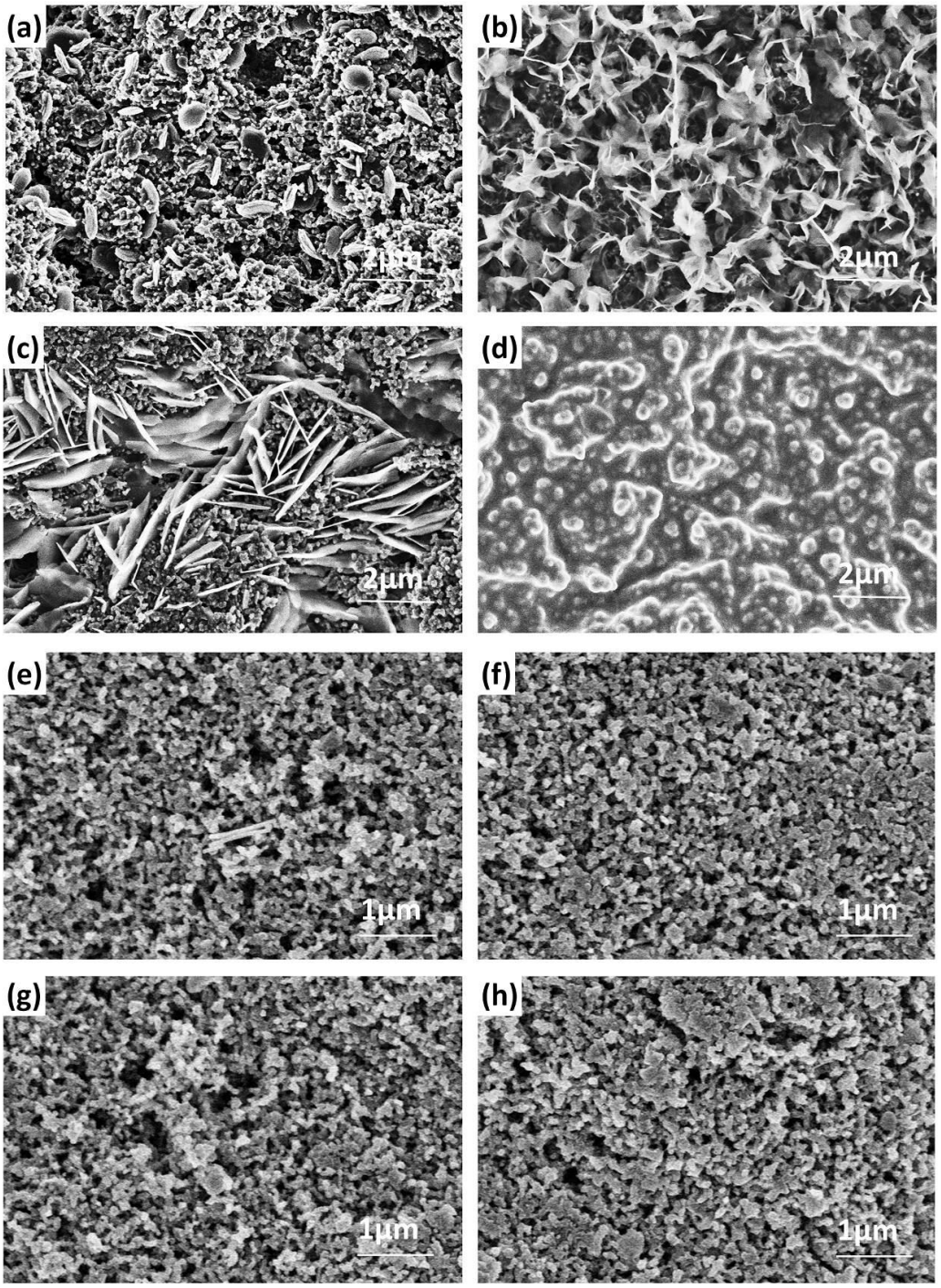

Fig. 4.4. SEM images of the cathodes after (a-d) discharge and (e-h) charge of IL based Li-O_2 batteries in (a, e) dry O_2 and in the atmospheres with RHs of (b, f) 21%, (c, g) 51% and (d, h) 74%, respectively.

Scanning electron microscope (SEM) was used to observe the morphologies of the discharge products at cathodes of the IL based Li-O_2 batteries in various

humidified O_2 atmospheres. Fig 4.4 records the morphology evolution processes of the discharge products from the typical toroid-like particles in the dry O_2 to small sheets at the RH of 21% and large flakes at the RH of 51% in Fig. 4.4a, b and c, respectively. When the RH is 74%, the $LiOH·H_2O$ flakes are converted to films covering on the surface of the cathode (Fig. 4.4d). Its formation is attributed to the dissolution-deposition of $LiOH·H_2O$ in the electrolyte and the highly humidified O_2 atmosphere. This may result in the different charge potential in Fig. 4.2. After fully charged, all the discharge products are decomposed and disappeared (Fig. 4.4e-h). This reversible behavior of formation and decomposition of the discharge products is consistent with the XRD results in Fig. 4.3.

4.3.3 Rate Capability and Cycling Performance

At the RH of 51%, the rate capability of the IL based Li-O_2 battery was examined (Fig. 4.5). The discharge/charge potential gaps at 250, 500 and 1000 mA g^{-1} are accordingly increased from 0.36 V to 0.40 and 0.50 V, suggesting the great kinetics of electrode reactions in the discharging and charging processes. The batteries were consecutively discharged and charged at 500 and 1000 mA g^{-1} (Fig. 4.6). The selected discharge and charge profiles over 218 cycles at 500 mA g^{-1} in Fig. 4.6a are almost overlapped and show no decay of the discharge/charge capacities. The corresponding coulombic efficiency maintains ~99%, indicative of superior rechargeability. Even at the high current density of 1000 mA g^{-1}, the battery can run for 95 cycles with a small increase in the discharge/charge potential gap in Fig. 4.6b, exhibiting excellent rate capability and rechargeability. It is notable that the IL based electrolyte applied in each Li-O_2 battery is only 30 μL and no more electrolyte was added during the long time operation. The excellent cycling stability and rate capability with low discharge/charge overpotentials of the Li-O_2 battery are attributed to the synergistic effect of the composite cathode of RuO_2/MnO_2/SP, IL based electrolyte and moisture in the O_2 atmosphere.

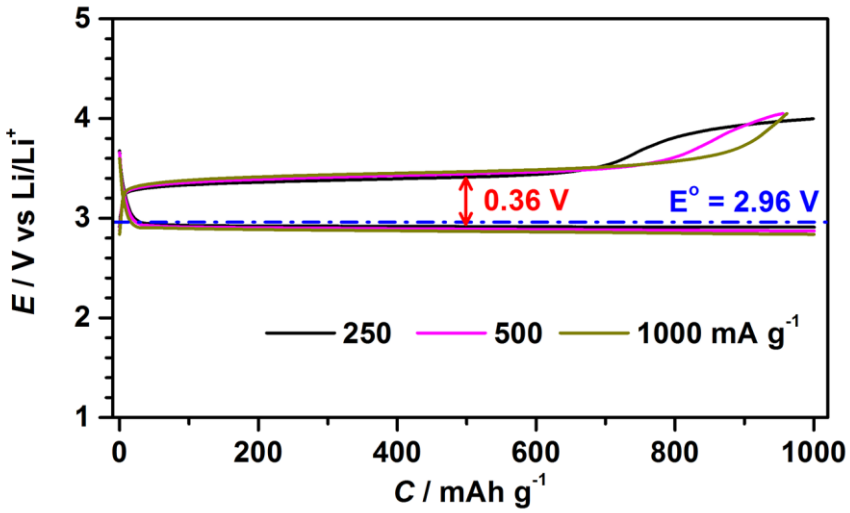

Fig. 4.5. Rate capability of IL based Li-O_2 battery at the RH of 51% in O_2 atmosphere.

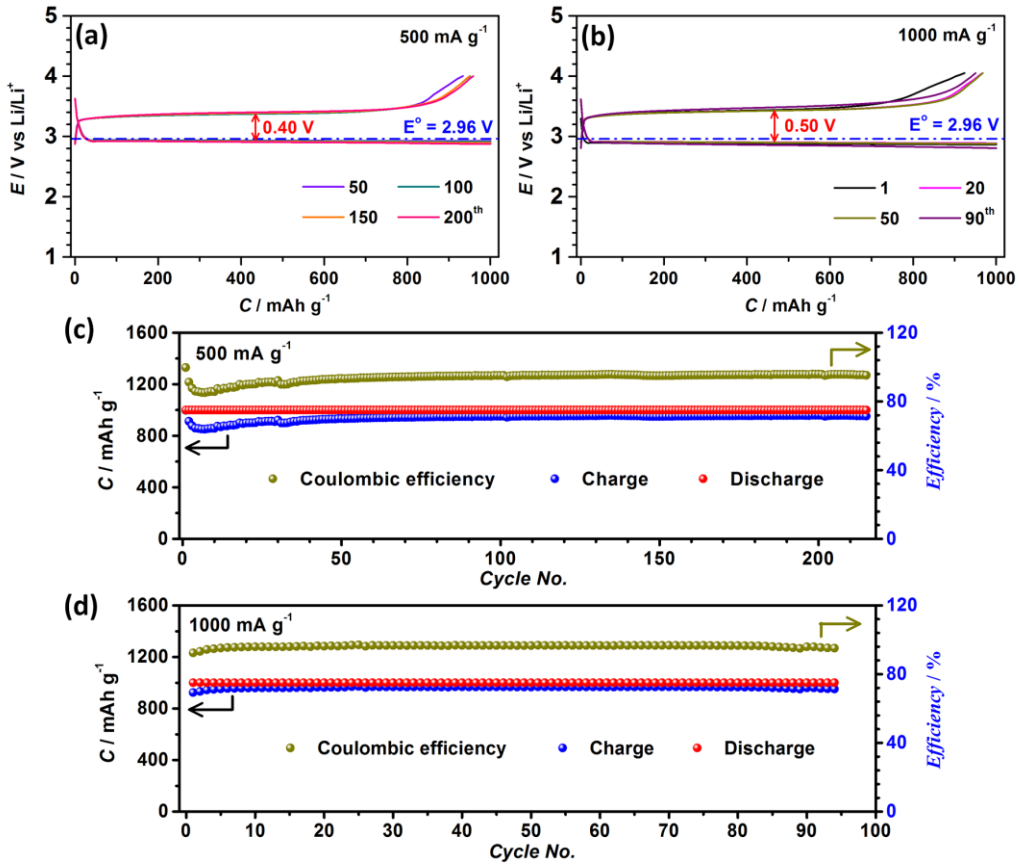

Fig. 4.6. Cycling performance of Li-O_2 batteries in O_2 atmosphere with a RH of 51%. Discharge-charge profiles of the selected cycles (a) at 500 mA g^{-1} and (b) at 1000 mA g^{-1}, and plots of discharge/charge capacities and the corresponding coulombic efficiencies against cycle number (c) at 500 mA g^{-1} and (d) at 1000 mA g^{-1}, respectively.

4.3.4 Discussion

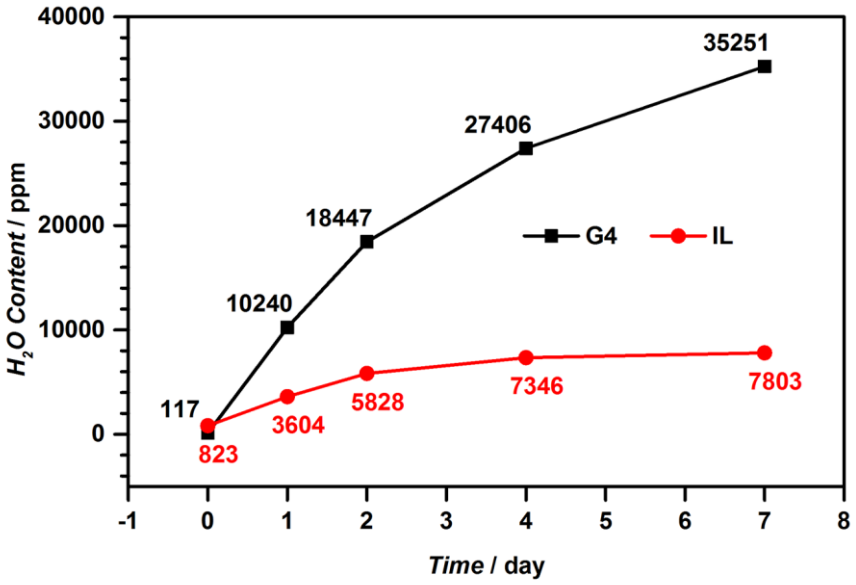

Fig. 4.7. H_2O contents of the G4 and IL based electrolyte after rest for 1, 2, 4 and 7 days in the humidified atmosphere at RH of 51%.

The unique properties of this IL enable it to be suitable for the superior Li-O_2 battery in humidified O_2 atmosphere: 1) The hydrophobic property of the IL is crucial for the construction of stable electrolyte/discharge product at cathodes/O_2 interfaces of the Li-O_2 battery in the humidified atmosphere.[29] Fig. 4.7 shows the H_2O content trends of G4 and IL based electrolytes after rest for 1, 2, 4 and 7 days in the humidified atmosphere at RH of 51%. The H_2O content of the G4 based electrolyte increases rapidly during 7 days. After 1 day, the H_2O content increases to as high as ~10000 ppm, and finally reaches to ~35000 ppm after 7 days. The excessive H_2O in the electrolyte results in solid $LiOH{\cdot}H_2O$ dissolving, leading to the poor charge ability (Fig. 4.1). Colm O'Dwyer and co-author also conducted the similar experiment and concluded the H_2O content for DMSO based electrolyte even increased much higher.[30] In contrast, the H_2O content of the hydrophobic IL based electrolyte increases much slowly. After 4 days, the value nearly reaches an equilibrium of ~7500 ppm and changes little after 7 days. The hydrophobic property allows the H_2O content

in the electrolyte stable and make sure the battery exhibits superior discharge-charge ability even after more than 200 cycles. 2) The IL based Li-O_2 battery exhibits strong ORR catalytic activity and remarkable discharge performance. As shown in Fig. 4.2, the discharge potentials are ~2.94 V at RHs of 51% and 74%. This value is approaching the theoretical equilibrium potential of Li_2O_2 (2.96 V), which is generally considered impossible in view of the inevitable polarization and therefore implies a different discharge mechanism. In a dry O_2 atmosphere, the discharge product is generated through an electrochemical reduction of O_2 to Li_2O_2 at a theoretical potential of 2.96 V (Route 1, Fig. 4.8). In this IL based Li-O_2 battery in humidified atmospheres, another possible discharge route is proposed (Route 2, Fig. 4.8). O_2 is firstly reduced to HO_2^- via E1 and then HO_2^- chemically reacts with Li^+ to produce LiOH and H_2O_2. In the presence of moisture in the atmosphere, LiOH is further converted to LiOH·H_2O. The equilibrium potential of E1 is ~3.1 V,[31] which is supposed to result in the high discharge potential. In the humidified atmospheres, both of the two reaction routes exist and compete. For Li-O_2 batteries with relatively low RHs, Route 1 dominates, resulting in lower discharge potentials. For Li-O_2 battery with high RHs, the moisture content is much higher, facilitating Route 2 and leading to high discharge potentials. The detailed intrinsical discharge (ORR) mechanism in this atmosphere should be further explored systematically. During charging process, LiOH·H_2O is decomposed at low potential over strong catalysis ability of RuO_2 and

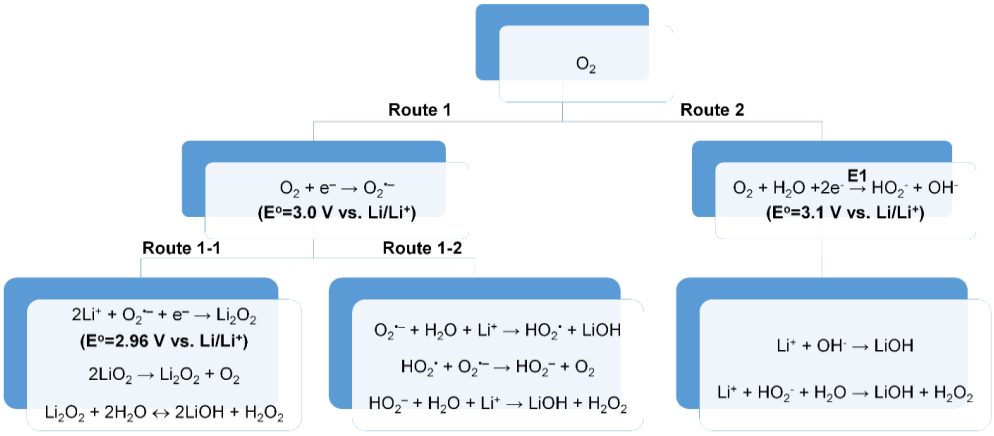

Fig. 4.8. Proposed discharge mechanism for Li-O_2 batteries with H_2O containing electrolyte and with moisture in the humidified atmosphere.

O_2 together with H_2O are regenerated. 3) The wide electrochemical window and high stability against strong oxidative intermediates ($O_2^{\bullet-}$, O_2^{2-}, HO_2^-, *etc*.) as well as non-volatility guarantee the IL based electrolyte function during the long time operation.[32] It enables the ILs based Li-O_2 battery to be consecutively discharged and charged for 218 cycles without overpotential increase at 500 mA g^{-1}.

4.3.5 An alternative solution towards protetion of Li metal anode in humid atmosphere

A feasible construction of the IL and RuO_2/MnO_2/SP based Li-O_2 battery with conventional Li metal anode was conceived as shown in Fig. 4.9. The Li metal anode is protected by a commercial lithium super ionic conductor (LISICON) film (Li_2O-Al_2O_3-SiO_2-P_2O_5-TiO_2-GeO_2) in a pouch cell, which selectively enables the transport of Li^+ ions and prevents the penetration of H_2O molecules. In the cathode side, the RuO_2/MnO_2/SP cathode and a glassy fiber filter paper incorporated with the IL based electrolyte are assembled together and pressed onto the opposite side of the LISICON film of the pouch cell. The whole pouch cells are put in glass chambers with dry O_2 and with humidified O_2 at a RH of 51%, respectively. The initial discharge/charge profiles at 250 mA g^{-1} are shown in Fig. 4.9. At RH of 51%, the battery exhibits flat discharge and charge plateaus at 2.94 V and 3.54 V, respectively.

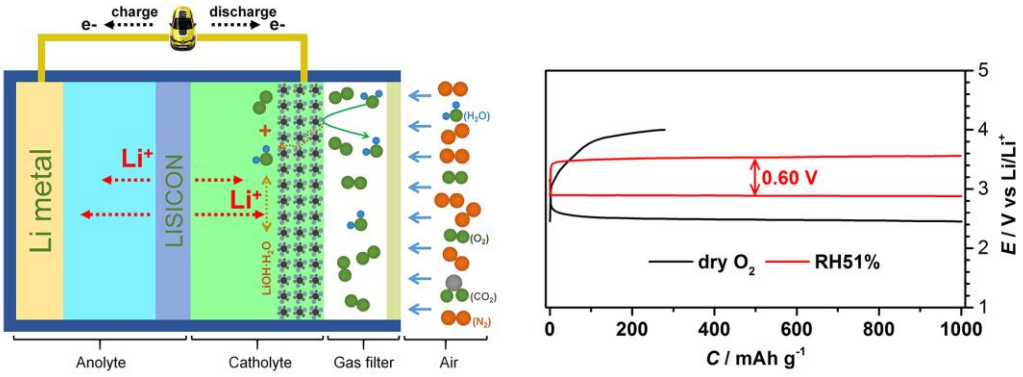

Fig. 4.9. Proposed discharge mechanism for Li-O_2 batteries with H_2O containing electrolyte and with

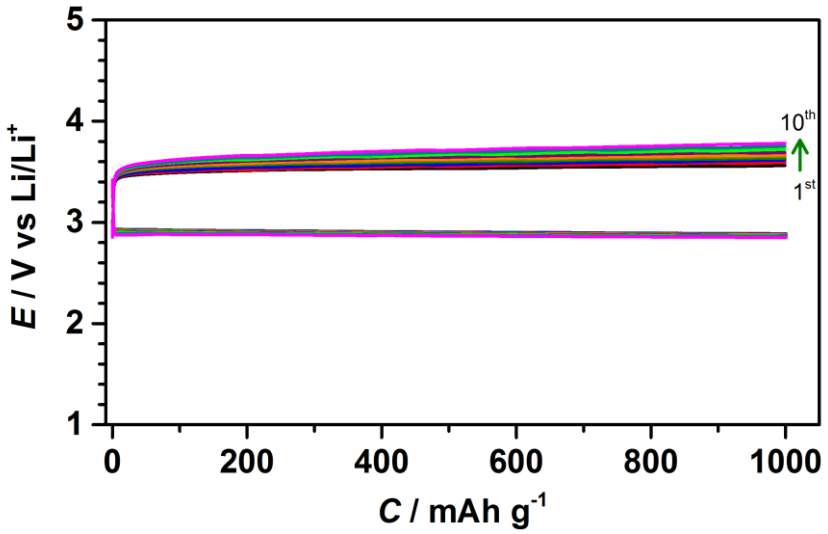

Fig. 4.10. The discharge-charge profiles of Li-O_2 batteries with LISICON as separator and Li metal as anode in humidified O_2 atmosphere at a RH of 51% at 250 mA g^{-1}.

Different from the increased potential at the end of charging process in Fig. 4.2, 4.5 and 4.6, the flat charge plateau in Fig. 4.9 is possibly due to the easier depositing for Li ions on the Li metal surface compared with Li ions inserting into $LiFePO_4$ electrodes. The discharge/charge potential gap is reduced from ~1.5 V in dry O_2 to only 0.6 V, which is quite small considering the large resistance of the LISICON film. During cycles, there is a small increase in the charge potentials (Fig. 4.10), which may result from the resistance increase of the LISICON film.[33]

4.4 Conclusion

A promising and rechargeable long-life system at cathode in humidified atmosphere at RH of 51% for Li-O_2 battery is realized by combining a hydrophobic ionic liquid and RuO_2/MnO_2/SP cathode. The discharge and charge potentials are optimized to 2.94 V and 3.34 V, leading to a small potential gap of 0.4 V. Such system can be consecutively discharged/charged for 218 cycles at 500 mA g^{-1} and 95 cycles at 1000 mA g^{-1}, indicating superior rechargeability and rate capability. The excellent

performance is benefited from the synergistic effect of the adopted hydrophobic ionic liquid, composite cathode of RuO_2/MnO_2/SP and moisture in the O_2 atmosphere. A prototype of a Li-O_2 battery operating in humidified O_2 atmosphere is built to present low discharge/charge potential gaps. It is the first time to obtain excellent cycling stability in the presence of moisture in O_2 atmosphere and will encourage more investigations on the construction of practical Li-air battery based on such system in air atmosphere.

4.5 References

[1] Z. Guo, X. Dong, S. Yuan, Y. Wang, Y. Xia, Humidity effect on electrochemical performance of Li-O_2 batteries, *J. Power Sources* **2014**, *264*, 1.

[2] S. Meini, M. Piana, N. Tsiouvaras, A. Garsuch, H. A. Gasteiger, The Effect of Water on the Discharge Capacity of a Non-Catalyzed Carbon Cathode for Li-O_2 Batteries, *Electrochem. Solid-State Lett.* **2012**, *15*, A45.

[3] K. U. Schwenke, M. Metzger, T. Restle, M. Piana, H. A. Gasteiger, The Influence of Water and Protons on Li_2O_2 Crystal Growth in Aprotic Li-O_2 Cells, *J. Electrochem. Soc.* **2015**, *162*, A573.

[4] K. U. Schwenke, S. Meini, X. Wu, H. A. Gasteiger, M. Piana, Stability of superoxide radicals in glyme solvents for non-aqueous Li-O_2 battery electrolytes, *Phys. Chem. Chem. Phys.* **2013**, *15*, 11830.

[5] N. B. Aetukuri, B. D. McCloskey, J. M. Garcia, L. E. Krupp, V. Viswanathan, A. C. Luntz, Solvating additives drive solution-mediated electrochemistry and enhance toroid growth in non-aqueous Li-O_2 batteries, *Nature Chem.* **2015**, *7*, 50.

[6] S. Meini, S. Solchenbach, M. Piana, H. A. Gasteiger, The Role of Electrolyte Solvent Stability and Electrolyte Impurities in the Electrooxidation of Li_2O_2 in Li-O_2 Batteries, *J. Electrochem. Soc.* **2014**, *161*, A1306.

[7] F. J. Li, S. C. Wu, D. Li, T. Zhang, P. He, A. Yamada, H. S. Zhou, The water catalysis at oxygen cathodes of lithium-oxygen cells, *Nat. Commun.* **2015**, *6*, 7843.

[8] T. Liu, M. Leskes, W. J. Yu, A. J. Moore, L. N. Zhou, P. M. Bayley, G. Kim, C. P. Grey, Cycling Li-O_2 batteries via LiOH formation and decomposition, *Science* **2015**, *350*, 530.

[9] D. G. Kwabi, T. P. Batcho, C. V. Amanchukwu, N. Ortiz-Vitoriano, P. Hammond, C. V. Thompson, Y. Shao-Horn, Chemical Instability of Dimethyl Sulfoxide in Lithium-Air Batteries, *J. Phys. Chem. Lett.* **2014**, *5*, 2850.

[10] S. C. Wu, J. Tang, F. J. Li, X. Z. Liu, H. S. Zhou, Low charge overpotentials in lithium-oxygen batteries based on tetraglyme electrolytes with a limited amount of water, *Chem. Commun.* **2015**, *51*, 16860.

[11] T. Kuboki, T. Okuyama, T. Ohsaki, N. Takami, Lithium-air batteries using hydrophobic room temperature ionic liquid electrolyte, *J. Power Sources* **2005**, *146*, 766.

[12] L. Cecchetto, M. Salomon, B. Scrosati, F. Croce, Study of a Li-air battery having an electrolyte solution formed by a mixture of an ether-based aprotic solvent and an ionic liquid, *J. Power Sources* **2012**, *213*, 233.

[13] S. Higashi, Y. Kato, K. Takechi, H. Nakamoto, F. Mizuno, H. Nishikoori, H. Iba, T. Asaoka, Evaluation and analysis of Li-air battery using ether-functionalized ionic liquid, *J. Power Sources* **2013**, *240*, 14.

[14] S. Monaco, F. Soavi, M. Mastragostino, Role of Oxygen Mass Transport in Rechargeable Li/O_2 Batteries Operating with Ionic Liquids, *J. Phys. Chem. Lett.* **2013**, *4*, 1379.

[15] G. A. Elia, J. Hassoun, W. J. Kwak, Y. K. Sun, B. Scrosati, F. Mueller, D. Bresser, S. Passerini, P. Oberhumer, N. Tsiouvaras, J. Reiter, An Advanced Lithium-Air Battery Exploiting an Ionic Liquid-Based Electrolyte, *Nano Lett.* **2014**, *14*, 6572.

[16] C. J. Allen, S. Mukerjee, E. J. Plichta, M. A. Hendrickson, K. M. Abraham, Oxygen Electrode Rechargeability in an Ionic Liquid for the Li-Air Battery, *J. Phys. Chem. Lett.* **2011**, *2*, 2420.

[17] T. Zhang, H. Zhou, A reversible long-life lithium-air battery in ambient air, *Nat. Commun.* **2013**, *4*.

[18] T. Zhang, H. Zhou, From Li-O_2 to Li-Air Batteries: Carbon Nanotubes/Ionic Liquid Gels with a Tricontinuous Passage of Electrons, Ions, and Oxygen, *Angew. Chem. Int. Ed.* **2012**, *51*, 11062.

[19] S. Trasatti, Electrocatalysis in the anodic evolution of oxygen and chlorine, *Electrochim. Acta* **1984**, *29*, 1503.

[20] J. Christensen, P. Albertus, R. S. Sanchez-Carrera, T. Lohmann, B. Kozinsky,

R. Liedtke, J. Ahmed, A. Kojic, A Critical Review of Li/Air Batteries, *J. Electrochem. Soc.* **2012**, *159*, R1.

[21] Z. Jian, P. Liu, F. Li, P. He, X. Guo, M. Chen, H. Zhou, Core-Shell-Structured CNT@RuO_2 Composite as a High-Performance Cathode Catalyst for Rechargeable Li-O_2 Batteries, *Angew. Chem. Int. Ed.* **2014**, *53*, 442.

[22] F. Li, D.-M. Tang, T. Zhang, K. Liao, P. He, D. Golberg, A. Yamada, H. Zhou, Superior Performance of a Li-O_2 Battery with Metallic RuO_2 Hollow Spheres as the Carbon-Free Cathode, *Adv. Energy Mater.* **2015**, *5*.

[23] K. Liao, X. Wang, Y. Sun, D. Tang, M. Han, P. He, X. Jiang, T. Zhang, H. Zhou, An oxygen cathode with stable full discharge-charge capability based on 2D conducting oxide, *Energy Environ. Sci.* **2015**, *8*, 1992.

[24] H.-G. Jung, Y. S. Jeong, J.-B. Park, Y.-K. Sun, B. Scrosati, Y. J. Lee, Ruthenium-Based Electrocatalysts Supported on Reduced Graphene Oxide for Lithium-Air Batteries, *ACS Nano* **2013**, *7*, 3532.

[25] E. Yilmaz, C. Yogi, K. Yamanaka, T. Ohta, H. R. Byon, Promoting Formation of Noncrystalline Li_2O_2 in the Li-O_2 Battery with RuO_2 Nanoparticles, *Nano Lett.* **2013**, *13*, 4679.

[26] P. Bhattacharya, E. N. Nasybulin, M. H. Engelhard, L. Kovarik, M. E. Bowden, X. S. Li, D. J. Gaspar, W. Xu, J.-G. Zhang, Dendrimer-Encapsulated Ruthenium Oxide Nanoparticles as Catalysts in Lithium-Oxygen Batteries, *Adv. Funct. Mater.* **2014**, *24*, 7510.

[27] Y. Wang, H. Zhou, A lithium-air battery with a potential to continuously reduce O_2 from air for delivering energy, *J. Power Sources* **2010**, *195*, 358.

[28] Q. Sun, H. Yadegari, M. N. Banis, J. Liu, B. Xiao, X. Li, C. Langford, R. Li, X. Sun, Toward a Sodium-"Air" Battery: Revealing the Critical Role of Humidity, *J. Phys. Chem. C* **2015**, *119*, 13433.

[29] D. Zhang, R. Li, T. Huang, A. Yu, Novel composite polymer electrolyte for lithium air batteries, *J. Power Sources* **2010**, *195*, 1202.

[30] H. Geaney, C. O'Dwyer, Examining the Role of Electrolyte and Binders in Determining Discharge Product Morphology and Cycling Performance of

Carbon Cathodes in Li-O_2 Batteries, *J. Electrochem. Soc.* **2016**, *163*, A43.

[31] M. Matsui, A. Wada, Y. Matsuda, O. Yamamoto, Y. Takeda, N. Imanishi, A novel aqueous lithium-oxygen cell based on the oxygen-peroxide redox couple, *Chem. Commun.* **2015**, *51*, 3189.

[32] M. Kar, T. J. Simons, M. Forsyth, D. R. MacFarlane, Ionic liquid electrolytes as a platform for rechargeable metal-air batteries: a perspective, *Phys. Chem. Chem. Phys.* **2014**, *16*, 18658.

[33] S. Hasegawa, N. Imanishi, T. Zhang, J. Xie, A. Hirano, Y. Takeda, O. Yamamoto, Study on lithium/air secondary batteries-Stability of NASICON-type lithium ion conducting glass-ceramics with water, *J. Power Sources* **2009**, *189*, 371.

Chapter 5. A water-impermeable solid-state electrolyte for Li-O_2 battery with improved safety and cycle life in humid atmosphere

5.1 Introduction

Recently, Li, *et al.* in our group reported a Li-O_2 battery based on the reversible formation and decomposition of LiOH with low overpotentials through water catalysis.[1] The battery was assembled with a dimethyl sulfoxide (DMSO)-based electrolyte containing hundred ppm of H_2O, a composite cathode (MnO_2 and Ru nanoparticles supported Super P carbon) and a $LiFePO_4$ counter anode. $LiFePO_4$ electrode with discharge/charge potential of ≈3.45 V (vs Li/Li^+) is not a practical anode, and has to be used to substitute the Li metal anode to avoid the reactions between Li metal and H_2O being added in the electrolyte. The system demonstrated a low charge potential (≈3.2 V vs Li/Li^+). In the case of using tetraglyme (G4)-based electrolyte, a higher content of H_2O (4600 ppm) has been introduced to achieve the low charge potential in the similar system.[2] Besides, in the dimethyl ether (DME)-based electrolyte, the low charge potential (≈3.1 V vs Li/Li^+) was presented through the water catalysis in Li-O_2 battery.[3] Very recently, Wu. et al. in our group developed a viable cathode-electrolyte system ($LiFePO_4$ electrodes substituted Li metal anode as the counter anodes) with low charge potential (≈3.3 V vs Li/Li^+) in the humid atmosphere with relative humidity (RH) of 51% by applying a hydrophobic ionic liquid (IL)-based electrolyte.[4] All of the results confirm that the conversion of discharge product to LiOH compound is an accessible way to promote the performance of Li-O_2 battery.

For anode, the Li metal is considered as the most promising candidate to ensure the attracting superiority of Li-air battery with paramount energy density, because it has much high specific capacity (3860 mAh g^{-1}). However, the application of Li metal anode is still prevented owing to the limited Coulombic efficiency and especially the

detrimental dendrite growth during Li plating/striping processes. The large Li dendrites can penetrate the common separator, lead to the batteries short-circuit and then significantly decrease the safety property of batteries. More importantly, for practical Li-air batteries operating in ambient air with the presence of moisture, the dramatic exothermal reactions between the reactive Li metal anode and H_2O crossover from air cathode will inevitably induce the deterioration of the Li metal and severe safety problems such as the burning of the combustible carbon-based cathode, the separator and the flammable organic liquid electrolytes, and even the explosion of battery, which may become a paradox and the key factor affecting the future application of Li-O_2 (air) battery.[5]

One available solution of the few is using the solid Li ion conducting glass-ceramic film (LiSICON, Li_2O-Al_2O_3-SiO_2-P_2O_5-TiO_2-GeO_2, Ohara Corporation), selectively allowing the transport of Li^+ and preventing the penetration of H_2O.[6-7] It was attempted to protect the Li metal anode in Li-O_2 battery in the RH of 51%.[4] Unfortunately, its instability in the alkaline condition and the increased electrochemical impedance during cycles resulted in the limited cycle life (10 cycles).[4] The poor mechanical flexibility and fragile property also hinder its application (Fig. 5.1). When the LiSICON film is bent or crushed, the cracks may result in the reduced resistibility towards H_2O permeation and the possible safety problems.

In this chapter, we proposed a potential solution for the development of a feasible Li-O_2 battery with Li metal anode in the humid atmosphere (RH of 45%) by constructing a super-hydrophobic H_2O-preventing quasi-solid electrolyte (SHQSE). Solid-state electrolytes are preferred because the utilization of solid-state electrolytes is widely accepted as an effective strategy to suppress the dendrite growth, subsequently improves the safety of rechargeable lithium batteries and they are considered as the promising candidate for their substitution of the flammable organic liquid electrolytes,[8-11] especially for SiO_2-based composite solid-state electrolyte with reliable safety, high ionic conductivity, stable electrochemical window, good

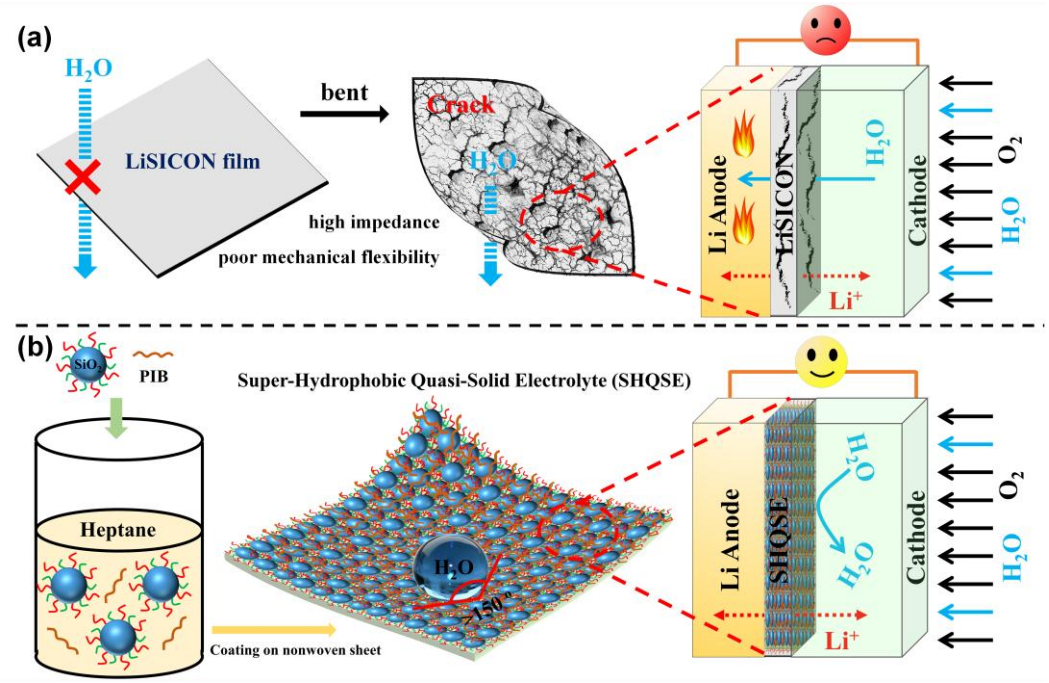

Fig. 5.1. (a) The schematic of Li-O_2 battery in humid atmosphere with LiSICON film to prevent H_2O crossover to Li metal anode. (b) Schematic of the proposed solid Li-O_2 battery in humid atmosphere based on the super-hydrophobic quasi-solid electrolyte (SHQSE).

thermal and mechanical stability.[12-14] Being used super-hydrophobic SiO_2 matric combined with Li^+-conducting IL as the solid electrolyte, our developed solid Li-ion configuration delivers stable mechanical strength, good thermal stability, high ionic conductivity, and wide voltage window, and more importantly, facilitates to suppress the H_2O crossover from cathode to Li metal anode. In order to take advantage of these remarkable properties, we incorporated this SHQSE into Li-O_2 battery, thus fabricating a new solid Li-O_2 battery operated in the RH of 45% and expecting to achieve long cycle life and good safety.

5.2 Experiment

5.2.1 Preparation of the super-hydrophobic quasi-solid electrolyte

Polyisobutylene (PIB) was used as the binder and added into heptane solvent to

form a homogeneous solution.[15-16] During stirring, the commercial super-hydrophobic silicon dioxide (SiO_2) treated with dimethyldichlorosilane (DDS) was added. The mass ratio between SiO_2 and PIB was set to 8:2. After stirring for 12h, the slurry was coated onto the non-woven fabrics to produce the SHQSE membrane through the doctor-blade technology. After drying the membranes in vacuum at 100 ^oC for 2 h, the obtained membranes were roll-pressed by a calender machine to ensure the quasi-solid electrolyte compact, and then continued to drying the membranes in vacuum at 100 ^oC for 12 h. The SHQSE was obtained by infiltrating the membrane with 0.5 M LiTFSI in 1-methyl-3-propylimidazolium bis(trifluoromethylsulfonyl) imide.

5.2.2 Permeation experiments

Permeation experiments are performed with a home-made reverse L-shaped device, which consist of two glass tubes and the SHQSE membrane or glass fiber membrane. These three components are assembled together by transparent instant adhesive. In a typical experiment, the H_2O solution dissolving $FeCl_3$ as the color indicator is slightly injected on the right side. The changes of the solution on two side are monitored and recorded by a digital camera.

5.2.3 Material characterization

The quasi-solid electrolyte membrane was characterized by X-ray diffraction (XRD, Bruker D8 Advanced diffractometer with Cu Kα (λ = 1.5406 Å). The thermogravimetric analysis (TGA) was conducted on BRUKER TG-DTA 2010SA-G4H. The H_2O contact angles on the solid electrolyte membrane were examined on AST Products with a model of Optima. The Fourier Transform Infrared Spectroscopy (FTIR) were carried out on the JASCO instrument of FT/IR-6200. The image of the solid electrolyte membrane was collected using scanning electron microscope (SEM, Hitachi S8000).

5.2.4 Electrochemical characterization

The ionic conductivity of SHQSE was investigated by the symmetrical cell stainless steel (SS)/SHQSE/SS using electrochemical impedance spectra (EIS) with AC amplitude of 5 mV from 10^6 to 0.1 Hz. The electrochemical stability of SHQSE was determined by the linear sweep voltammogram (LSV) at a scanning rate of 1.0 mV s^{-1}, where SHQSE was sandwiched between Li anode and SS. The Li plating/striping measurements were performed using the symmetrical Li/SHQSE/Li(Cu) cells employing a current density of 0.05 mA cm^{-2} per process and a plating/striping time of 30 min. The Li-O_2 batteries were assembled in 2032 coin cells with holes on the top in an Ar-filled glove box (< 0.1 ppm of H_2O and 5 ppm of O_2). The as-prepared SHQSE and RuO_2/MnO_2/SP were used as solid electrolyte and cathode, respectively. A Li metal (thickness of 0.5 mm, Honjo Metal) was used as the counter electrode. For comparision, the glassy fiber and 0.5 M LiTFSI in 1-methyl-3-propylimidazolium bis(trifluoromethylsulfonyl) imide were used as separator and liquid electrolyte. The coin cells were stored in a sealed glass chamber (≈650 mL) with a bottle of saturated K_2CO_3 solution. The relative humidity in this condition could keep ≈45%. Galvanostatic discharge/charge was conducted on a Hokuto discharging/charging system. The specific capacities and current densities were based on the mass of RuO_2/MnO_2/SP in cathode. The cycling performance was evaluated by discharging and charging with a limited specific capacity of 1000 mAh g^{-1} and a voltage range of 2.0 - 4.2 V at 500 mA g^{-1}.

5.3 Results and Discussion

5.3.1 Physical and chemical property

A general preparation process of the SHQSE membrane is illustrated in Fig. 5.1. After homogeneously mixing the super-hydrophobic silicon dioxide (SiO_2) and polyisobutylene (PIB) binder in heptane, the slurry was coated onto the non-woven fabrics to produce the as-prepared SHQSE membrane. Non-woven fabrics were used

as the porous substrate to assure the mechanical stability of the SHQSE membrane. The obtained membrane was dried under vacuum at 100 ^{o}C to evaporate the solvent and then roll-pressed by a calender machine. The calendaring process is important to ensure the SHQSE membrane compact. This process is similar to the commercial production of cathode and anode in Li-ion battery industry and it is simple for the large scale manufacture with low cost.

Fig. 5.2a shows a large piece of the as-prepared SHQSE membrane (thickness ≈ 30 µm). The morphology of the SHQSE membrane was characterized by scanning electron microscope (SEM) in Fig. 5.2c. It can be observed that the nanosilica particles are cross-link as a porous matrix with abundant networks and high open

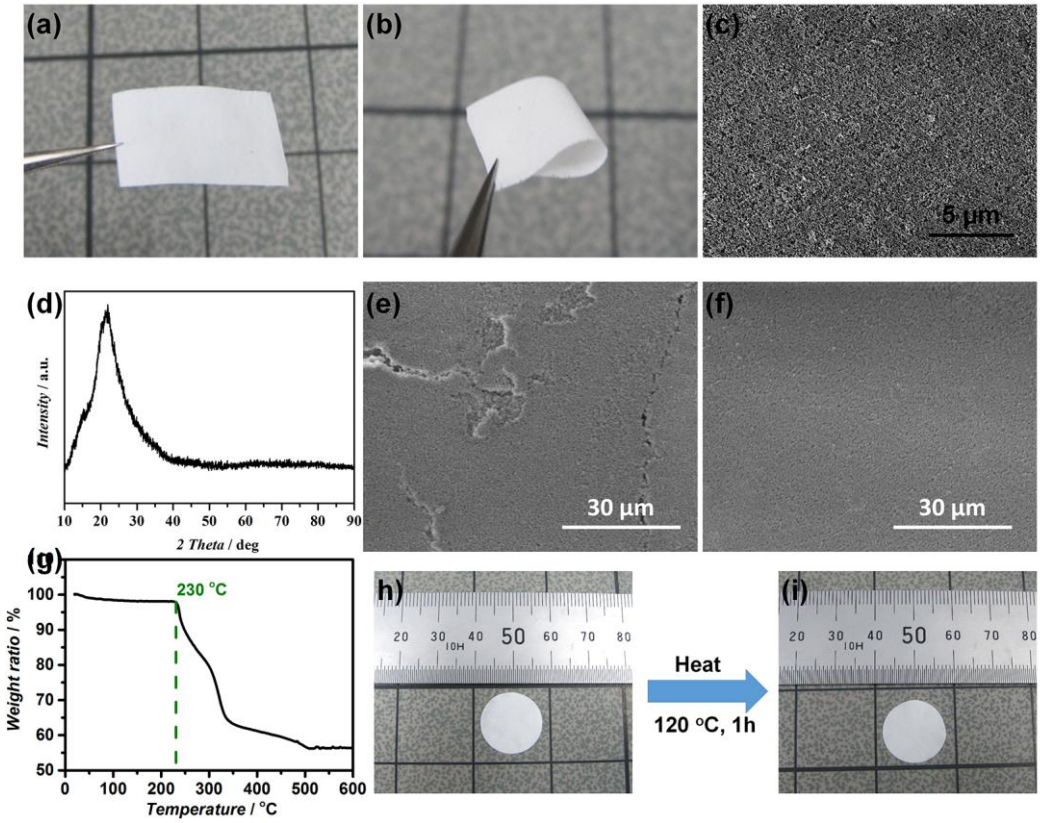

Fig. 5.2. (a, b) Photo images of the SHQSE membrane at flat and bend conditions. (c) SEM image of the SHQSE membrane. (d) The X-ray diffraction pattern of the solid electrolyte membrane. (e) SEM image of the as-prepared SHQSE without calendaring process after been bent. (f) SEM image of the as-prepared SHQSE with the calendaring process after been bent. (g) Thermogravimetric analysis (TGA) of the SHQSE membrane under a flow of air at 10 ^{o}C min^{-1}. (h, i) Photo images of the SHQSE membrane (e) before and (f) after the treatment at 120 ^{o}C for 1 h.

porosity. From the XRD pattern (Fig. 5.2d) of the SHQSE membrane, no obvious sharp peaks are observed, except a broad peak at 15° − 30°, indicating an amorphous form of SiO_2 particles. The SHQSE membrane can be bent at the large angle of 180 ° (Fig. 5.2b) without any crack (Fig. 5.2f), indicating the good flexibility. Whereas, the membrane without calendaring process showed exfoliation and fracture (Fig. 5.2e). This feature demonstrates the promising application for flexible energy storage devices. The thermal stability of the SHQSE membrane was evaluated from the result of thermogravimetric analysis (TGA) measurement (Fig. 5.2g). The SHQSE membrane presents nearly no weight loss until the temperature reaches about 230 °C, which is much higher than the commercial PE separator and implies a good thermal stability. After exposure to 120 °C for 1 h (Fig. 5.2i), no obvious shrinkage and degradation were observed (Fig. 5.2h). The outstanding thermal tolerance facilitates a large enhancement to the safety of Li-O_2 battery.

5.3.2 Super-hydrophobic test and resistibility towards H_2O permeation

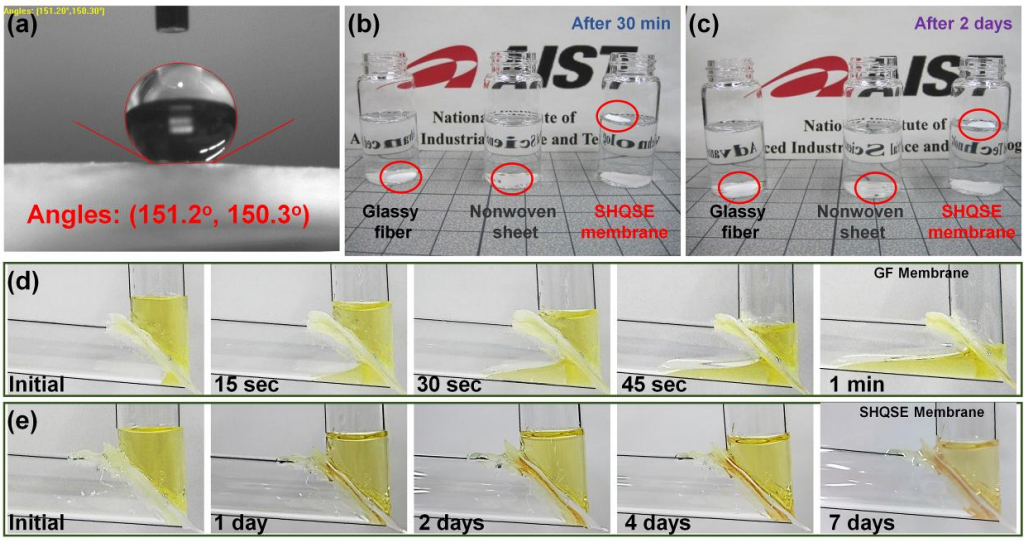

Fig. 5.3. (a) H_2O contact angles and the corresponding shape of H_2O droplets on the SHQSE membrane. (b, c) Hydrophobic tests of the glassy fiber (GF), nonwoven sheet, and SHQSE membranes. (d, e) Permeation experiments using 2 mL of H_2O with dissolved $FeCl_3$ as the color indicator: (d) GF membrane, (e) the SHQSE membrane.

The hydrophobic property of this SHQSE membrane is determined through the test of H_2O contact angle along with the behavior evolution in water and the home-designed H_2O penetration experiments (Fig. 5.3). The large H_2O contact angle (> 150 ^{o}) in Fig. 5.3a indicates the super-hydrophobic surface of the SHQSE membrane. When the membrane was put into H_2O, it can float on H_2O for a long term, in sharp contrast with glass fiber (GF) and the nonwoven fabric membranes. The GF and nonwoven fabric membranes immediately sink down under the H_2O (Fig. 5.3b, c). A permeation experiment was designed to evaluate the resistibility of the SHQSE membrane towards H_2O penetration. For the GF membrane (Fig. 5.3d), the H_2O solution quickly passes through the GF separator within 1 min, which shows hardly any resistance towards H_2O permeation. On the contrary, the SHQSE membrane with super-hydrophobic property effectively prevents the H_2O permeation, evidenced by the negligible H_2O passing through for at least 7 days (Fig 5.3e). These

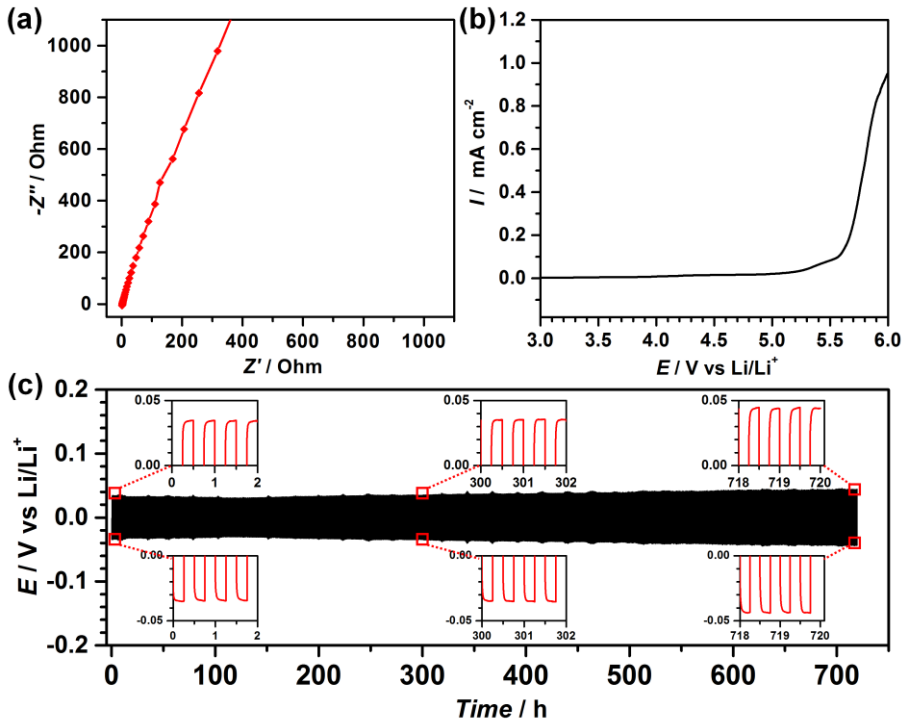

Fig. 5.4. (a) Nyquist plots of the SHQSE with the cell structure of stainless steel (SS)/SHQSE/SS. (b) LSV for the SHQSE at 1 mV s^{-1}. (c) Voltage-time curves of the Li plating/striping measurements using the symmetrical Li/SHQSE/Li cell at 0.05 mA cm^{-2} per process and a plating/striping time of 30 min.

results demonstrate the potential application of the SHQSE membrane on the prevention of H_2O crossover towards Li metal anode, which would become the key advantage of this SHQSE, especially for achieving Li-O_2 battery with long cycle life and good safety in humid atmosphere.

5.3.3 Electrochemical performance

5.3.3.1 Ion conductivity and electrochemical stability

With the aim of employing this super-hydrophobic SHQSE membrane to achieve the operation of Li-O_2 battery in humid atmosphere, a hydrophobic ionic liquid-based electrolyte (0.5 M LiTFSI dissovling in 1-methyl-3-propylimidazolium bis(trifluoromethylsulfonyl)imide) has been incorporated. The IL-based electrolyte would be physically entrapped within interconnected channels and pores rather than being chemically bound to the silica matrix, which suggests the high molecular mobility in the absence of forming high kinetic barriers and causing high activation energies to retard ion transfer.[17] The ionic conductivity of SHQSE was investigated through the electrochemical impedance measurement (EIS). From the Nyquist plot in Fig. 5.4a, the ionic conductivity σ can be calculated via the equation $\sigma=d/(R_bS)$,[9] where d is the thickness of the SHQSE, R_b is the resistance obtained from the Nyquist plot, and S is the surface area of the SHQSE. The calculated ionic conductivity is $\approx 0.91\times10^{-3}$ S cm^{-1}. The electrochemical stability under high potential is of great significance for the achievement of long-life solid Li-air batteries because the oxidative decomposition of electrolyte at high charge potential and the generated byproducts would result in the poor cycling performance of battery. To provide in-depth insight of the SHQSE, the linear sweep voltammogram (LSV) was performed. As shown in Fig. 5.4b, no obvious decomposition occurred before 5.5 V, demonstrating excellent electrochemical stability of this SHQSE.

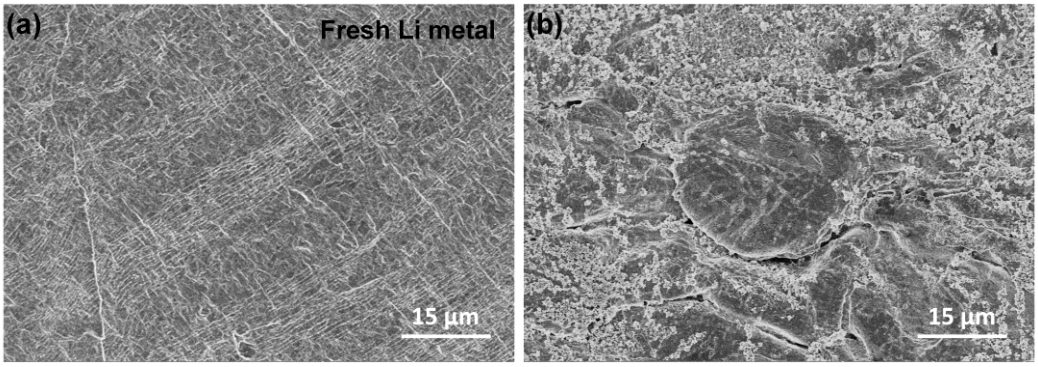

Fig. 5.5. SEM image of the fresh Li metal (a) and the Li metal (b) after plating/striping measurements using the symmetrical Li/SHQSE/Li cell.

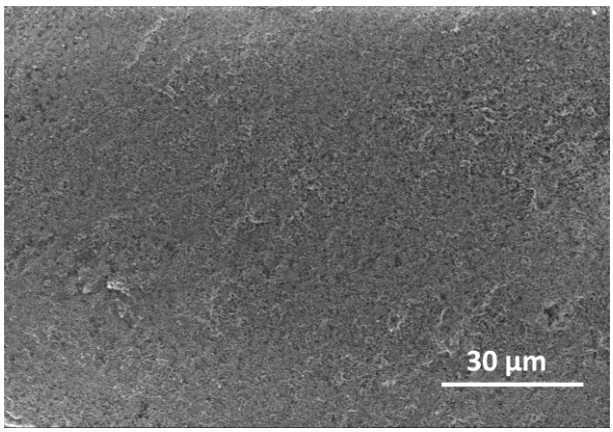

Fig. 5.6. SEM image of the SHQSE after plating/striping measurements using the symmetrical Li/SHQSE/Li cell for 1400 cycles (> 700 h).

The stability of Li plating/stripping processes in the SHQSE was investigated by galvanostatic cycling of symmetric lithium metal cells. The corresponding voltage-time curves in Fig. 5.4c, present that the voltages keep stable within 45 mV for more than 1400 cycles (> 700 h) without cell failure. After cycles, no formation of large Li dendrites was observed on the surface of Li metal (Fig. 5.5). The SHQSE analyzed by SEM (Fig. 5.6) remained well without crack and penetration. These results indicated that the formation of Li dendrites was efficiently mitigated by employing the SHQSE, which is derived from the high ionic conductivity of SHQSE and the good interfacial contact between SHQSE and Li electrodes.[12, 14]

5.3.3.2 Cycling performance

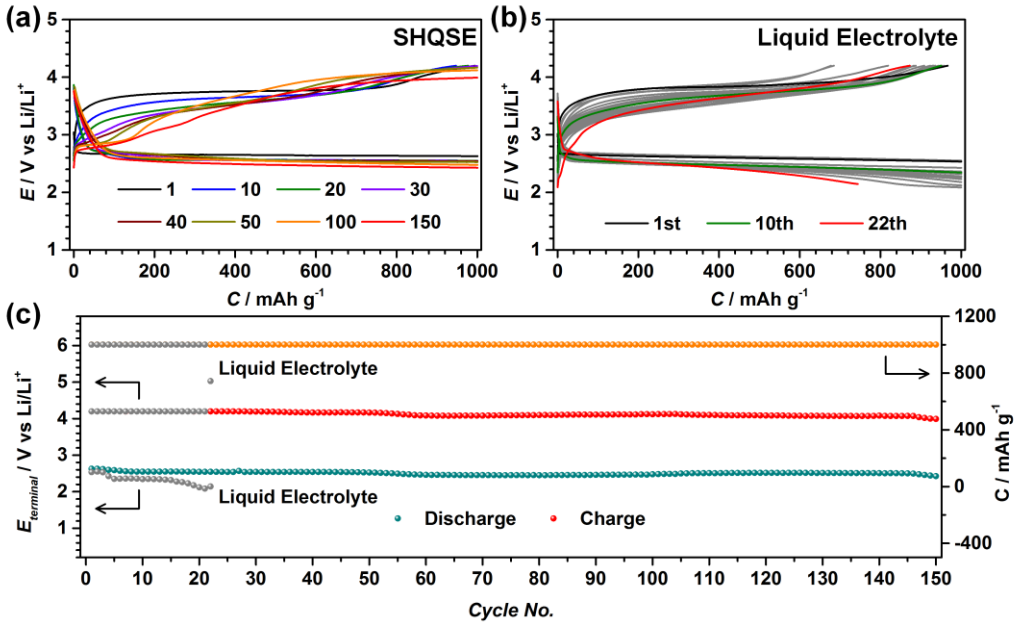

Fig. 5.7. The typical discharge-charge profiles of Li-O_2 batteries at RH of 45% assembled with: (a) SHQSE and (b) liquid electrolyte with GF. (c) The discharge and charge terminal voltage as well as the discharge capacity against cycle number. Current density: 500 mA g^{-1}.

In order to take advantages of the strong thermal tolerance, high ionic conductivity, good electrochemical stability at high potential and especially the super-hydrophobicity together with the strong resistibility towards H_2O permeation to Li metal anode, the SHQSE-based Li-O_2 batteries with Li metal anode, SHQSE and RuO_2/MnO_2/SP cathode were fabricated and expected to achieve superior cycling stability and solid safety property. The control Li-O_2 battery with GF membrane infiltrating with IL-LiTFSI electrolyte were also fabricated. The typical discharge and charge profiles during cycles were displayed in Fig. 5.7a. In the first cycle, the discharge and charge potentials are 2.65 V and 3.7 V, respectively, corresponding to the low overpotentials. Due to the demanding evolution of favorable ion transport pathways in SHQSE,[18-19] the charge potentials gradually decrease to 3.4 V until the 30th cycle. In the following, the battery reaches a relatively steady state, confirmed by the nearly overlap discharge curves from the 30th to150th cycles. The terminal voltages of discharge and charge processes remain constant for 150 cycles without

obvious increase of overpotentials in Fig. 5.7c. Accordingly, it can be concluded that the long-term operation of the Li-O_2 battery in the humid atmosphere (RH of 45%) is benefited from the SHQSE, which shows the strong resistibility towards H_2O crossover corrosion of Li metal anode. In a sharp contrast, the Li-O_2 battery with GF membrane infiltrating liquid electrolyte is unable to be sustained under the high moisture in the atmosphere. The poor capability of GF membrane for preventing H_2O permeation (Fig. 5.3d) results in the rapid corrosion of Li metal anode in the Li-O_2 battery. Subsequently, after 22 cycles, the terminal voltages gradually fall to the cut off voltage (2.0 V) with the discharge capacity decreasing to less than 800 mAh g^{-1}. The Li metal anode is seriously corroded, producing large amounts of LiOH on the surface (Fig. 5.8a) and leading to the poor cycling performance. In the case of SHQSE-based solid Li-O_2 battery, although little LiOH is formed (Fig. 5.8b), possibly due to the unsealed space on the edges of SHQSE and Li metal anode in a coin cell configuration, Li metal anode is effectively protected from H_2O corrosion and thus long cycle life can be achieved (150 discharge-charge cycles in Fig. 5.7a). The above results and discussions illustrate the crucial role of the SHQSE with super hydrophobicity for improving the cycling stability of Li-O_2 battery in the humid atmosphere.

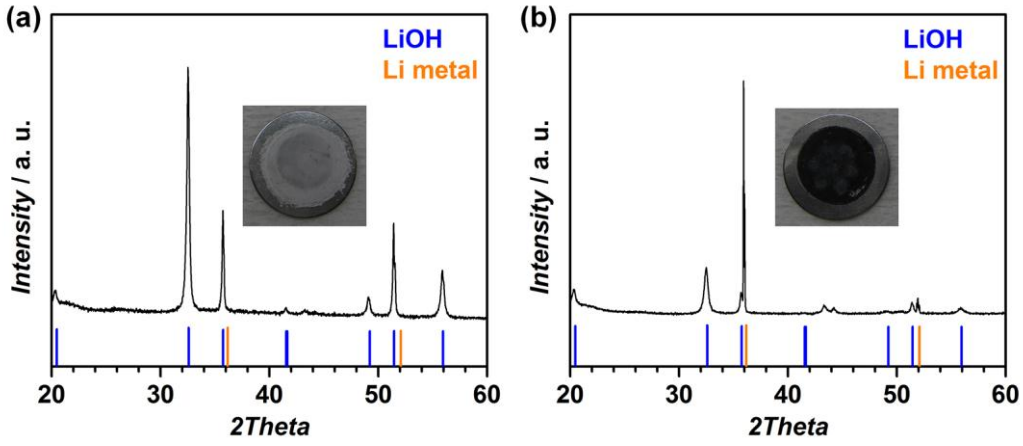

Fig. 5.8. XRD patterns of the Li metal anodes after cycles in Li-O_2 battery at RH of 45% assembled with (a) liquid electrolyte with GF and (b) SHQSE, respectively. The insets are the photos of corresponded Li metal anodes after cycles.

5.4 Conclusions

A quasi-solid electrolyte with super-hydrophobic property has been developed. The quasi-solid electrolyte manifests strong thermal tolerance (no obvious decomposition below 230 ^{o}C), high electrochemical stability (> 5.5 V), ionic conductivity (0.91×10^{-3} S cm^{-1}) and super hydrophobicity (contact angle > 150^{o}), enabling the achievement of a safe and long-life Li-O_2 battery in humid atmosphere. These results provide a new insight into how the super-hydrophobic property of solid-state electrolyte can hold back the H_2O crossover to the reactive Li metal anode, and suggest that the hydrophobic effects may play an important role in the achievement of safe and long-life Li-air battery. From our perspective, the primary purpose of this work underlines the importance of surface decoration for solid-state electrolyte with super-hydrophobic property in the future application of Li-air battery. Substantial efforts are still required before the practical application of Li-air battery as a power source for electric vehicle can be achieved.

5.5 References

[1] F. J. Li, S. C. Wu, D. Li, T. Zhang, P. He, A. Yamada, H. S. Zhou, The water catalysis at oxygen cathodes of lithium-oxygen cells, *Nat. Commun.* **2015**, *6*, 7843.

[2] S. C. Wu, J. Tang, F. J. Li, X. Z. Liu, H. S. Zhou, Low charge overpotentials in lithium-oxygen batteries based on tetraglyme electrolytes with a limited amount of water, *Chem. Commun.* **2015**, *51*, 16860.

[3] T. Liu, M. Leskes, W. J. Yu, A. J. Moore, L. N. Zhou, P. M. Bayley, G. Kim, C. P. Grey, Cycling Li-O_2 batteries via LiOH formation and decomposition, *Science* **2015**, *350*, 530.

[4] S. Wu, J. Tang, F. Li, X. Liu, Y. Yamauchi, M. Ishida, H. Zhou, A Synergistic System for Lithium–Oxygen Batteries in Humid Atmosphere Integrating a Composite Cathode and a Hydrophobic Ionic Liquid-Based Electrolyte, *Adv. Funct. Mater.* **2016**, *26*, 3291.

[5] L. Grande, E. Paillard, J. Hassoun, J.-B. Park, Y.-J. Lee, Y.-K. Sun, S. Passerini, B. Scrosati, The Lithium/Air Battery: Still an Emerging System or a Practical Reality?, *Adv. Mater.* **2015**, *27*, 784.

[6] K. U. Schwenke, M. Metzger, T. Restle, M. Piana, H. A. Gasteiger, The Influence of Water and Protons on Li_2O_2 Crystal Growth in Aprotic Li-O_2 Cells, *J. Electrochem. Soc.* **2015**, *162*, A573.

[7] T. Zhang, H. S. Zhou, A reversible long-life lithium-air battery in ambient air, *Nat. Commun.* **2013**, *4*, 1817.

[8] B. Kumar, J. Kumar, Cathodes for Solid-State Lithium-Oxygen Cells: Roles of Nasicon Glass-Ceramics, *J. Electrochem. Soc.* **2010**, *157*, A611.

[9] H. Kitaura, H. Zhou, Electrochemical performance and reaction mechanism of all-solid-state lithium-air batteries composed of lithium, $Li_{1+x}Al_yGe_{2-y}(PO_4)_{(3)}$ solid electrolyte and carbon nanotube air electrode, *Energy Environ. Sci.* **2012**, *5*, 9077.

[10] H. Kitaura, H. Zhou, Electrochemical Performance of Solid-State Lithium-Air

Batteries Using Carbon Nanotube Catalyst in the Air Electrode, *Adv. Energy Mater.* **2012**, *2*, 889.

[11] X. B. Zhu, T. S. Zhao, Z. H. Wei, P. Tan, L. An, A high-rate and long cycle life solid-state lithium-air battery, *Energy Environ. Sci.* **2015**, *8*, 3745.

[12] D. Zhou, R. Liu, Y.-B. He, F. Li, M. Liu, B. Li, Q.-H. Yang, Q. Cai, F. Kang, SiO_2 Hollow Nanosphere-Based Composite Solid Electrolyte for Lithium Metal Batteries to Suppress Lithium Dendrite Growth and Enhance Cycle Life, *Adv. Energy Mater.* **2016**, *6*.

[13] F. Wu, G. Q. Tan, R. J. Chen, L. Li, J. Xiang, Y. L. Zheng, Novel Solid-State Li/$LiFePO_4$ Battery Configuration with a Ternary Nanocomposite Electrolyte for Practical Applications, *Adv. Mater.* **2011**, *23*, 5081.

[14] J. Zhang, Y. Bai, X.-G. Sun, Y. Li, B. Guo, J. Chen, G. M. Veith, D. K. Hensley, M. P. Paranthaman, J. B. Goodenough, S. Dai, Superior Conductive Solid-like Electrolytes: Nanoconfining Liquids within the Hollow Structures, *Nano Lett.* **2015**, *15*, 3398.

[15] J. Heine, U. Rodehorst, J. P. Badillo, M. Winter, P. Bieker, Chemical Stability Investigations of Polyisobutylene as New Binder for Application in Lithium Air-Batteries, *Electrochim. Acta* **2015**, *155*, 110.

[16] J. Heine, U. Rodehorst, X. Qi, J. P. Badillo, C. Hartnig, U. Wietelmann, M. Winter, P. Bieker, Using Polyisobutylene as a Non-Fluorinated Binder for Coated Lithium Powder (CLiP) Electrodes, *Electrochim. Acta* **2014**, *138*, 288.

[17] Y. Y. Lu, S. K. Das, S. S. Moganty, L. A. Archer, Ionic Liquid-Nanoparticle Hybrid Electrolytes and their Application in Secondary Lithium-Metal Batteries, *Adv. Mater.* **2012**, *24*, 4430.

[18] E. Quartarone, P. Mustarelli, Electrolytes for solid-state lithium rechargeable batteries: recent advances and perspectives, *Chem. Soc. Rev.* **2011**, *40*, 2525.

[19] J. C. Bachman, S. Muy, A. Grimaud, H. H. Chang, N. Pour, S. F. Lux, O. Paschos, F. Maglia, S. Lupart, P. Lamp, L. Giordano, Y. Shao-Horn, Inorganic Solid-State Electrolytes for Lithium Batteries: Mechanisms and Properties Governing Ion Conduction, *Chem. Rev.* **2016**, *116*, 140.

Chapter 6 Conclusions

The realization of practical application for Li-air battery is retarded because of the high charge potential, low Coulombic efficiency, short cycle life and the contaminations in air especially moisture. In this research, in order to address the H_2O-related problems towards the practical Li-air battery operating in ambient air and take the advantages of H_2O for reported capacity promotion, we designed the cathode and the electrolyte to improve the battery performance in the presence of H_2O in electrolyte or moisture in O_2 gas. Main conclusions are presented as follows:

Chapter 2: LiOH was carefully designed as the discharge products to substitute the aggressive Li_2O_2 by building a composite cathode based on ruthenium (Ru) and electrolytic manganese oxide (MnO_2) nanoparticles supported Super P carbon (SP) and utilizing a trace amount of H_2O in the DMSO-based electrolyte. In conventional Li-O_2 batteries with H_2O-contaning electrolyte, on a basis of the reaction between Li_2O_2 and H_2O ($Li_2O_2 + 2H_2O \rightarrow 2LiOH + H_2O_2$), the forward process, producing LiOH and H_2O_2, is supposed to be inhibited because the accumulations of generated LiOH and H_2O_2 make the reaction reaches an equilibrium, resulting in the Li_2O_2 as the main products on cathode and small amount of LiOH together H_2O_2 dissolved in electrolyte. The resulting high charge potential for decomposing Li_2O_2 and the Li_2O_2-related side reactions are hard to be addressed. Once MnO_2 is introduced in our designed cathode, its catalysis decomposition towards H_2O_2 allows the reaction between Li_2O_2 and H_2O goes forward and the regenerated H_2O from H_2O_2 decomposition again participate in the reaction until all the Li_2O_2 is converted to be LiOH. Upon charge, the strong catalysis ability for oxidizing LiOH of Ru nanoparticles in cathode effectively reduces the charge potential. Several experiments were conducted to prove the proposed mechanism. LiOH as the discharge products can circumvent the Li_2O_2-related side reactions. In this case, an ultralow charge potential of about 3.20 V, corresponding to an overpotential of 0.24 V, was achieved.

This value is among the best reported. Besides, the Li-O_2 battery showed superior cycling stability (200 cycles).

Chapter 3: Since the high volatility and strong stink smell of DMSO will prevent its use in the future practical open Li-air batteries, tetraglyme (G4) with an ultralow vapour pressure is employed as an electrolyte solvent in the similar Li-O_2 battery system. Because of the different properties between DMSO and G4 on the viscosity, solvating ability and diffusion coefficient, more information was obtained. Varied amounts of H_2O (dry electrolyte (the remaining H_2O content of about 11 ppm), 78 ppm, 1700 ppm and 4600 ppm) in the electrolyte were introduced to investigate the H_2O function. As the H_2O content increases from 11 ppm to 4600 ppm, the charge potential correspondingly decreases from near 4.0 V to only 3.2 V. In DMSO-based electrolyte, only hundreds of ppm H_2O can reduce the potential to about 3.2 V. Besides, the discharge overpotentials showed reduction and this indicated more information about the mechanism. The composition of discharge products was also confirmed in these cases. With dry electrolyte, the discharge products were mainly Li_2O_2 and in the presence of 4600 ppm of H_2O, LiOH was the only detected products. The morphology of discharge products evolved from toroid-like particle (11 ppm) to large sheets (4600 ppm). The Li-O_2 battery showed excellent discharge/charge ability even at a high current density of 2000 mA g^{-1} in the presence of 4600 ppm H_2O in electrolyte. The cycling stability at 1000 mA g^{-1} was largely improved. Advanced information during discharge process was proposed.

Chapter 4: When operating Li-air batteries in ambient air condition, the excessive moisture can diffuse into the cathode and the electrolyte. The H_2O content in the hydrophilic G4-based electrolyte will be much higher than thousand ppm (more than 35000 ppm at RH of 51%) and the performance of Li-O_2 batteries will also be significantly influenced. Li-O_2 battery in the G4-based electrolyte at relative humidity (RH) of less than 5% showed poor discharge-charge ability. In order to promote the application in ambient air, a hydrophobic ionic liquid (IL)-based electrolyte was developed and the discharge-charge performance of Li-O_2 battery at varied RH

condition was studied. The H_2O content in the IL-based electrolyte at RH of 51% could reach a saturated state of about 7800 ppm, much lower than that in the G4-based electrolyte. This appropriate value allowed the realization of low charge potential (about 3.34 V) at RH of 51% and remarkable cycling stability (218 cycles at 500 mA g^{-1} and 92 cycles at 1000 mA g^{-1}). The discharge products at RH of 51% were identified to be a mixture of LiOH and $LiOH \cdot H_2O$ with flake-like morphology. The excellent results are attributed to the synergistic effect of the composite MnO_2/RuO_2/SP cathode, the IL-based electrolyte, and the moisture in the O_2 atmosphere. Furthermore, a Li metal anode-protected Li-O_2 battery in humid atmosphere was constructed by employing the H_2O-impermeable commercial lithium superionic conductor (LiSICON) film. The H_2O crossover towards Li metal anode was avoided to ensure the battery safety in humid atmosphere. The problem that lithium iron phosphate electrode had to be used in the previous experiments was solved.

Chapter 5: Although LiSICON can be used to realize the high-performance Li-O_2 battery in humid atmosphere, its instability in the alkaline condition and the increased electrochemical impedance during cycles resulted in the limited cycle life (10 cycles). The poor mechanical flexibility and fragile property also hinder its application. When the LiSICON film is bent or crushed, the cracks may result in the reduced resistibility towards H_2O permeation and the possible safety problems. Therefore, we further proposed a potential solution for the development of a feasible Li-O_2 battery with Li metal anode in the humid atmosphere (RH of 45%) by constructing a super-hydrophobic H_2O-preventing solid-state electrolyte (SHSSE). The SHSSE was prepared following a mixing and coating method, similar to the commercial production of cathode and anode in Li-ion battery industry and it is simple for the large scale manufacture with low cost. The permeation experiments confirmed the strong resistibility towards H_2O passing through. After keeping 7 days, no obvious H_2O passed through the SHSSE. Being used super-hydrophobic SiO_2 matric combined with Li^+-conducting IL as the solid-state electrolyte, our developed

solid-state Li-ion configuration delivers stable mechanical strength, favorable flexibility, good thermal stability (no decomposition below 230 ^{o}C), high ionic conductivity (0.91×10^{-3} S cm^{-1}), and wide voltage window (> 5.5 V), and more importantly, facilitates to suppress the H_2O crossover from cathode to Li metal anode. The SHSSE-based solid Li-O_2 battery operated in the RH of 45% achieved long cycle life and good safety. These results were believed to contribute to the realization of practical Li-air battery.

Although our research partially addressed the negative effect of H_2O in Li-O_2 battery and turned to manage the merit of H_2O for practical application of Li-O_2 battery by designing the cathode and electrolyte, much effort such as the exploration of solution towards CO_2-related problem should further be devoted to realize the practical Li-air battery.

List of Research Results

JOURNAL PAPER

First-author

[1] Shichao Wu, Jin Yi, Kai Zhu, Songyan Bai, Yang Liu, Yu Qiao, Masayoshi Ishida, Haoshen Zhou, A super-hydrophobic quasi-solid electrolyte for Li-O_2 battery with improved safety and cycle life in humid atmosphere, *Adv. Energy Mater.*, 2016, 1601759.

[2] Shichao Wu, Jing Tang, Fujun Li, Xizheng Liu, Yusuke Yamauchi, Masayoshi Ishida, Haoshen Zhou, A synergistic system for lithium–oxygen batteries in humid atmosphere integrating a composite cathode and a hydrophobic ionic liquid-based electrolyte, *Adv. Funct. Mater.*, 2016, 26, 3291.

[3] Shichao Wu, Jing Tang, Fujun Li, Xizheng Liu, Haoshen Zhou, Low charge overpotentials in lithium–oxygen batteries based on tetraglyme electrolytes with a limited amount of water, *Chem. Commun.*, 2015, 51, 16860.

[4] Shichao Wu, Kai Zhu, Jing Tang, Kaiming Liao, Songyan Bai, Jin Yi, Yusuke Yamauchi, Masayoshi Ishida, Haoshen Zhou, A long-life lithium ion oxygen battery based on commercial silicon particles as the anode, *Energy Environ. Sci.*, 2016, 9, 3263.

[5] Jing Tang[1], Shichao Wu[1], Tao Wang, Hao Gong, Huabin Zhang, M. Saad Alshehri, Tansir Ahamad, Haoshen Zhou, Yusuke Yamauchi, Cage-type highly graphitic porous carbon–Co_3O_4 polyhedron as the cathode of lithium–oxygen batteries, *ACS Appl. Mater. Interfaces*, 2016, 8, 2797.

Co-authored

[1] Fujun Li, Shichao Wu, Tao Zhang, Ping He, Atsuo Yamada, Haoshen Zhou, The water catalysis at oxygen cathodes of lithium–oxygen cells, *Nature Commun.*, 2015, 6, 7843.

[2] Jin Yi, Shichao Wu, Songyan Bai, Yang Liu, Na Li, Haoshen Zhou, Interfacial construction of Li_2O_2 for a performance-improved polymer Li-O_2 battery, *J. Mater. Chem. A*, 2016, 4 2403.

[3] Hairong Xue, Shichao Wu, Jing Tang, Hao Gong, Ping He, Jianping He, Haoshen Zhou, Hierarchical porous nickel cobaltate nanoneedle arrays as flexible carbon-protected cathodes for high-performance lithium-oxygen batteries, *ACS Appl. Mater. Interfaces*, 2016, 8, 8427.

[4] Yang Liu, Na Li, Shichao Wu, Kaiming Liao, Kai Zhu, Jin Yi, Haoshen Zhou, Reducing the charging voltage of a Li-O_2 battery to 1.9 V by incorporating a photocatalyst, *Energy Environ. Sci.*, 2015, 8, 2664.

[5] Songyan Bai, Xizheng Liu, Kai Zhu, Shichao Wu, Haoshen Zhou, Metal–organic framework-based separator for lithium–sulfur batteries, *Nature Energy*, 2016, 1, 16094.

PRESENTATIONS:

[1] Shichao Wu, Haoshen Zhou, A hydrophobic ionic liquid based Li-O_2 battery system in the humid atmosphere, 2016 International Conference on Green Energy and Applications, Singapore, March 23-24, 2016 (oral).

Acknowledgements

How time flies! Without knowing it, 3-year doctoral course is going to pass through. I feel a little excited every moment that I realize one of my dream being Dr. Wu will come true. At this special moment, I would like to give my sincere gratitude to everyone who has given me generous help on my way.

My deepest gratitude goes first and foremost to my supervisor, Prof. Haoshen Zhou (professor at University of Tsukuba and principle investigator at AIST). He provided me the opportunity to pursue Ph.D. at University of Tsukuba and to conduct my Ph.D. research at AIST. He let me learn to how to proceed scientific research with peace of mind to hold negative attitude. His research spirit of getting to the root of experimental phenomenon has benefited me a great deal. He always has many innovative ideas and inspired us to make better work. He is an extremely affable and approachable man and we can communicate with him like friends.

I also really pleased to acknowledge my vice-supervisors Prof. Masayoshi Ishida and Assistant Prof. Hanada at University of Tsukuba. When I first entered the university, they gave their selfless assistance in my daily life and work. They introduced two tutors (Mr. Aoishima and Mr. kajino) to help me. I also feel grateful to them. When they held parties, barbecue or other amusements, they often invite me. This provided me the chance to accommodate the life in Japan and I really had a happy time with them. From them, I know the importance of life as well as work.

My thanks would go to Dr. Tao Wang, senior fellow apprentice and Dr. Jing Tang, junior sister apprentice in my master course. They encouraged me to find the opportunity for pursuing the doctoral program in Japan and did me much favor to the success. They also provided their kindly help on SEM measurements and useful discussions.

I am greatly indebted to Dr. Fujun Li and Dr. Xizheng Liu. Dr. Fujun Li taught me how to study the previous articles, prepare electrodes for Li-O_2 battery, fabricate

Li-O_2 batteries, evaluate the battery performance and write the manuscript. I learned to many invaluable suggestions and experiences. This indeed laid a solid foundation in my future research. Dr. Xizheng Liu, like an elder brother, always provided useful information when I have some research difficulties. He often organized some tours and led me to appreciate the culture and natural scenery in Japan.

I wish to express my thanks to all the group members in Energy Interface Technology Research Group at AIST. Mr. J. Okagaki, Dr. H. Kitaura, Dr. E. Hosono, Dr. H. Matsuda and Dr. T. Saito gave their kindly help in daily research. Thanks to Dr. E. Yoo, for her good advice in the improvement of graduation presentation.

I also would like to express my appreciation to Dr. J. Yi, Dr. S. Guo, Dr. K. Liao, Dr. Haijun Yu, Dr. N. Li, Dr. D. Li, Dr. C. Zhang, Dr. T. Zhang, Dr. Z. Song, Dr. Y. Wang and Dr. Y(yarong). Wang, for their kindly help in my daily research and life. My heartfelt gratitude goes to my classmates, Mr. S. Bai and Ms. Q. Li. We went to AIST together every morning and went back every evening for more than two years. We and Dr. K. Zhu, Ms. Y. Liu always studied, discussed together about the research and achieved lots of improvements.

I would like to express my gratitude to the Japanese Government for the financial support (Monbusho Scholarship) during the doctoral course. It ensured that I could focus on the research work.

In particular, I am extremely grateful for my wife Xiujuan Zhang, my father Zhenmin Wu, my mother Wenqiao Lu and my little brother Shiyang Wu. Their ending support is my biggest motive power to encourage me becoming better and better. I will always do my best to realize better life and make you happy.